THE
PHYSICAL REVIEW
A Journal of Experimental and Theoretical Physics
VOL. 44, No. 10 NOVEMBER 15, 1933 SECOND SERIES

Changes in the X-Ray Diffraction Pattern of Nitrobenzene Produced by an Electric Field, Changes in Temperature and Circulation

F. C. TODD, *Ryerson Physical Laboratory, University of Chicago*
(Received July 17, 1933)

Comparable diffraction patterns of benzene and nitrobenzene were taken with Mo K radiation. Two balanced, krypton-filled ionization chambers were arranged to read the difference in the ionization current produced by the x-rays diffracted at the same angle from two similar scattering samples. By their use, the change in the intensity of the nitrobenzene diffraction pattern due to a field of 10 kv per cm was found to be less than 0.3 percent over the entire principal peak. An average of 35 readings on the peak gave a change in intensity of -0.02 ± 0.06 percent. These chambers were also used to measure the change in intensity of the diffraction pattern produced by (1) an increase in temperature from 16°C to 26°C, (2) an increase in temperature from 30°C to 42°C and (3) circulating the nitrobenzene past the point of illumination with x-rays at a velocity of 0.4 cm per second. These results were found to be in general agreement with the assumption that the nitrobenzene molecules associate in pairs and are dissociated by thermal or mechanical agitation.

INTRODUCTION

THE principal peak in the x-ray diffraction pattern of liquids is due to the interference between the separate molecules.[1] Any cause resulting in a more orderly arrangement of the molecules in the liquid will produce a sharpening of this peak and an increase in the maximum intensity of the peak. With a molecule having a permanent electric moment large in comparison with the moment induced by an electric field, such as nitrobenzene, an electric field will exert a force tending to cause the permanent electric moment of the molecule to line up in the direction of the field.[2] On the assumption of no interacting forces between the molecules, McFarlan[3] estimated that the change in intensity of the diffraction pattern due to any applicable electric field would, however, be too small to measure by ordinary methods. In checking his theory, McFarlan nevertheless found an increase in the intensity of the principal peak of the nitrobenzene diffraction pattern of 2.3 percent due to an electric field of 9 kv per cm. This contradiction of his simple theory led him to introduce a hypothesis concerning the motion of groups of molecules.

The purpose of this work was to investigate the basis for this hypothesis by determining the effect of an electric field on the entire nitrobenzene diffraction pattern. To complete the study, it was necessary to measure the effect of small changes in temperature and the effect of circulation on the nitrobenzene diffraction pattern. Some measurements on the effect of temperature have been previously reported.[4]

[1] P. Debye and H. Menke, Ergebnisse der Technischen Röntgenkunde **2**, 1 (1931).
[2] R. D. Bennett, J. Frank. Inst. **211**, 481 (1931).
[3] R. L. McFarlan, Phys. Rev. **35**, 1469–75 (1930).
[4] G. W. Stewart, Phys. Rev. **39**, 176A (1932).

The nitrobenzene molecule has a permanent electric moment of about 4.0×10^{-18} e.s. units. The permanent moment is not located in the NO_2 group alone; but this group is negative with respect to the benzene ring,[5] as shown by the structural chemical formula in Fig. 1A. Recent x-ray studies of crystalline benzene indicate that

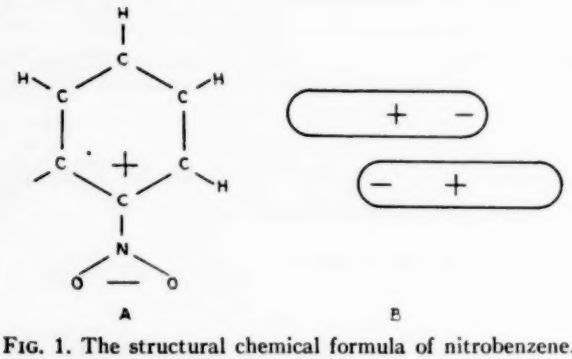

FIG. 1. The structural chemical formula of nitrobenzene.

the benzene molecule is flat[6] with all the carbon atoms in a single plane. Smyth[7] concludes from various evidence that the moment of the nitrobenzene molecule lies in the plane of the carbon atoms. This indicates that the nitrogen atom lies in the plane of the carbon atoms and that the oxygen atoms must be symmetrically placed with respect to this plane. Moreover, a comparison of the density and the atomic weights of nitrobenzene and benzene and a comparison of the x-ray diffraction patterns of these two liquids show that these are consistent with the hypothesis that the oxygen molecules also lie in the plane of the carbon atoms.

An explanation of the variation of the molar polarization of nitrobenzene with its concentration in a nonpolar solvent has been advanced which is based on the assumption that a certain fraction of the single molecules associate to form double molecules as shown in Fig. 1B.[8, 9] In this type of association, the dipoles of the single molecules oppose and cancel each other. It must be remembered that nitrobenzene is not an associated liquid[10] in the same sense as water since there are no electron linkages or coordinate links between the molecules. Malsch,[11] from a theoretical basis, and Pal,[8] by an empirical application, found that the number of dissociated molecules may be approximated by a relation of this type

$$N = N_0\epsilon^{-U(x,\ y,\ z,\ \theta,\ \phi)/kT},$$

where U signifies the potential energy of the dipole, while k and T have their usual significance. By this relation the number of dissociated molecules increases as the temperature is increased. The dipoles of the dissociated molecules are, however, no longer neutralized and these dipoles will interact with the neighboring molecules. This increases the intermolecular forces as is indicated by the increase in viscosity with temperature.[12]

DESCRIPTION OF APPARATUS

The source of x-rays was a water-cooled Coolidge molybdenum target tube operated at 30 m.a. and approximately 35 kv peak by a full wave rectifier. The radiation was filtered by a ZrO filter to produce a more monochromatic radiation. The spectrum of the radiation is shown in Fig. 5. The x-ray tube and the rectifier were oil-immersed in the same tank, described in detail elsewhere.[13] The electric circuit used was not the one there described, but will be explained in an early issue of *The Review of Scientific Instruments*. This circuit kept constant the intensity of the x-rays scattered at the principal peak of the benzene diffraction pattern, independently of changes in the line voltage. The circuit depends for its successful operation on the temperature of the x-ray tube filament changing as rapidly as the line voltage. Of course this is impossible; but this circuit does have a great advantage over those ordinarily employed. It was adjusted until a change of five percent in the line voltage produced a change of less than one percent in the intensity of the x-rays scattered at the benzene

[5] I. Estermann, Ergebnisse der Exakten Naturwissenschaften **8**, 303 (1929).

[6] E. G. Cox, Proc. Roy. Soc. (London) **A135**, 491–8 (1932).

[7] C. P. Smyth, *Dielectric Constant and Molecular Structure*, pp. 111–120.

[8] N. N. Pal, Phil. Mag. **10**, 265–80 (1930).

[9] C. P. Smyth, reference 7, pp. 171–3.

[10] N. V. Sidgwick, *The Electronic Theory of Valency*, p. 137.

[11] J. Malsch, Phys. Zeits. **33**, 383 (1932).

[12] A. van Iterbeck, Nature **130**, 399–400 (1932); Massy, Warren and Wolfenden, J. Chem. Soc. pp. 91–95 (1932).

[13] Bennett, Gingrich, and Pierce, Rev. Sci. Inst. **2**, 226 (1931).

peak. With this adjustment, the probable deviation of a single reading, as calculated from seventy readings, was 0.6 percent; and a plot of the deviations corresponded to an error curve. For the readings in this report, the line voltage was rechecked every few minutes to prevent its varying more than one percent from the mean. The points on the x-ray diffraction patterns for benzene and nitrobenzene in Fig. 6 indicate the steadiness of the circuit. All are single readings, except over the nitrobenzene peak where the points are averages of many readings. The curves approximate the average too closely to require correcting.

Although the probable deviation of the readings with this circuit is comparable with the best measurements on x-ray intensities, the accuracy is still insufficient to measure extremely small changes in intensity. To increase the accuracy, balanced ionization chambers were used, as shown schematically in Fig. 2. The vertical beam of x-rays from the tube was divided and passed through the two samples whose diffraction pat-

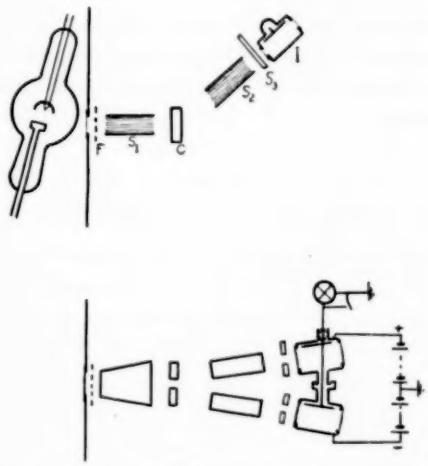

FIG. 2. Arrangement of apparatus for balanced readings of the ionization current. F is ZrO filter, S_1 and S_2 are Soller slits with slits 10 cm by 1 mm, C is scattering cell, S_3 is adjustable slit, I is the ionization chambers.

terns were to be compared. The two ionization chambers, mounted rigidly one above the other, were electrically connected to record the difference in ionization produced in the two chambers by the x-rays diffracted at the same angle from the two samples. This method has several advantages which increase the accuracy: (1) A change in the x-ray intensity produces only a secondary effect on the difference. (2) The difference between two balanced readings with the scattering samples interchanged gives twice the effect to be measured. The scattering cells were not interchanged but the condition of the liquid inside the cells was changed. (3) Since the difference in intensity is recorded, a much more sensitive measuring device may be employed. (4) The ionization produced by stray radiation is practically balanced out over a reading of long duration.

The ionization chambers were carefully constructed to minimize the errors inherent in the measurement of very small currents. Krypton gas at 72 cm pressure was used in a copper walled ionization chamber. The length of the absorbing path through the krypton gas was 6 cm. All the precautions outlined by Compton[14] for a similar chamber were carefully followed. The collecting electrodes are supported by two amber insulators, one in the electrometer and one in the ionization chambers. This reduces the chances for electrical leakage to a minimum, and the actually measured leakage was found to be very small. A Compton electrometer was used which had a sensitivity of 10,000 divisions per volt on a scale three meters distant.

The design of the circulating system for obtaining the effect of an electric field on the intensity of the diffraction pattern is shown in Fig. 3.

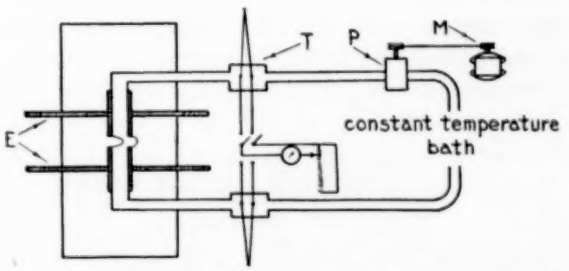

FIG. 3. Scattering cells and circulating system to determine effect of an electric field. E are the electrodes, T are thermocouples, P is the centrifugal pump and M is the synchronous motor.

The offset between the two cells produces the same state of turbulence in both. The thickness of the liquid in the scattering cell is 0.63 cm, approximately half the thickness for maximum

[14] A. H. Compton, Rev. Sci. Inst. 2, 365 (1931).

scattering. Air chambers on each side of the cell prevent the condensation of moisture on the mica windows. The power for applying the field to the cell and to the x-ray tube was supplied by the same phase of the distribution system but each high voltage unit was otherwise separate. This insured that the peak of the x-ray intensity occurred at the time of peak voltage on the scattering cell. The voltage applied to the scattering cell was read by an electrostatic voltmeter, while the rectifier was supplying power. The nitrobenzene was circulated at a velocity sufficient to prevent an average temperature rise of more than 0.5°C due to the electric field in the scattering cell. The liquid was recooled to its initial temperature by circulation through a long coil of copper tubing immersed in a constant temperature bath. This method was so effective that no increase in temperature at the entrance to the scattering cell could be detected during a reading. The circulation was produced by a centrifugal type pump driven by a synchronous motor to prevent any pulsations in the flowing liquid. The temperature of the nitrobenzene was read at the points shown in Fig. 3 by the thermocouples, which were calibrated to read to 0.1°C.

The scattering cell and arrangement of apparatus for the study of the effect of temperature and to determine the effect of circulation are shown in Fig. 4. The upper and the lower scattering cells are independent of each other and may be joined to either of the two independent circulating systems. By thus interchanging the temperature of the liquid in the scattering cells, the difference between two readings is twice the effect to be measured. The electrodes in the heating cell are connected to the same rectifier system as was used to find the effect of an electric field. By measuring the increase in temperature due to a given power input, the rate of circulation could be calculated from the specific heat of nitrobenzene, 0.34.[15]

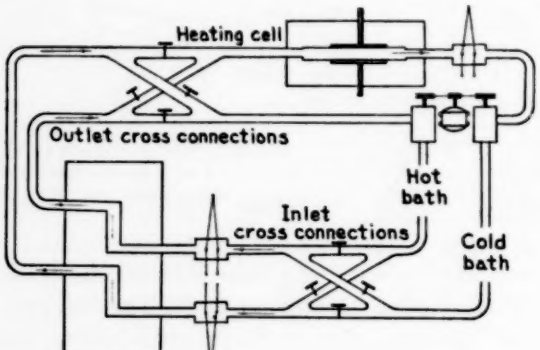

FIG. 4. Scattering cells and circulating system to study effect of temperature and circulation.

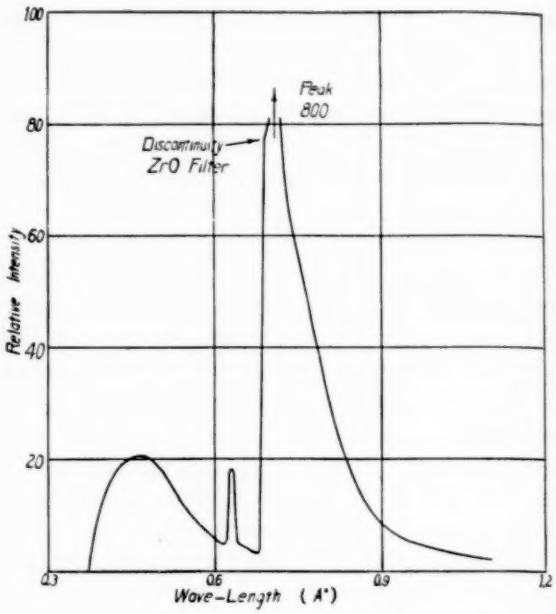

FIG. 5. Spectrum of radiation.

RESULTS

Fresh, commercial, c. p. nitrobenzene was used to obtain the diffraction pattern shown in Fig. 6. In the remaining tests, the nitrobenzene was used again several times as it discolored very slowly. It was kept in the circulating system only during the actual taking of data. While no precautions were taken to prevent contamination of the nitrobenzene with moisture from the atmosphere, all the materials with which the nitrobenzene came in contact were experimentally found to be dissolved inappreciably. In order partially to purify the nitrobenzene and to eliminate most of the anomalous conduction current, the nitrobenzene was circulated through the electric field for several minutes before each testing period.

The effect of an electric field of 10 kv per cm on the diffraction pattern is shown in Fig. 7. The readings for zero field were obtained to in-

[15] Handbuch der Physik, Vol. X, p. 349.

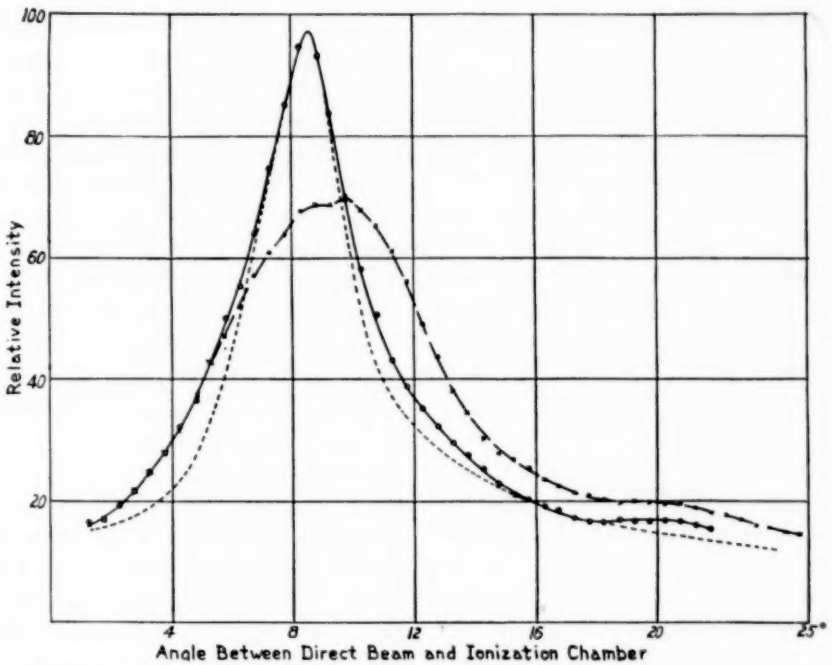

FIG. 6. X-ray diffraction patterns of liquids. Dotted curve is for benzene as given by Stewart, solid curve is for benzene, and dashed curve is for nitrobenzene.

sure that the circuit was not changing and when they varied too much the entire set was repeated. No corrections were made for the container scattering as the results apparently show no net effect. A group of 35 readings were taken at the angle of 8° 30′, each reading consisting of a drift rate with the field on the lower electrodes and another reading with the field on the upper electrodes. The average effect calculated from these readings was -0.02 ± 0.06 percent; that is, any effect due to the electric field is less than the precision of these experiments.

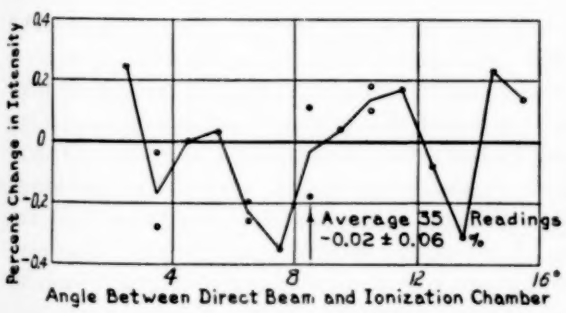

FIG. 7. Percent change in intensity of nitrobenzene diffraction pattern produced by an electric field. Strength of field 10 kv per cm, temperature of liquid 18°C and rate of circulation 0.5 cm per second.

The curves I and II in Fig. 8 show the effect of temperature on the nitrobenzene diffraction pattern. These curves give the change in intensity for several angles in percent of the total intensity diffracted at each angle. Curve I gives the increase in intensity produced by a 10°C increase in temperature from a reference temperature of 16°C. At still lower temperatures the readings were so irregular that a consistent group could not be obtained. Curve II similarly gives the increase in intensity produced by a 12°C increase in temperature from a reference temperature of 30°C. In this series of readings the nitrobenzene was not circulated while the readings were being taken; hence, no circulation effects are included. The dotted portions of the curves are not corrected for the container scattering. At these small angles, the fringing of the primary beam of x-rays plays an indeterminate rôle in the change of intensity. The readings showed a change in intensity of one x-ray beam relative to the other. This was traced to changing conditions in the oil surrounding the oil immersed x-ray tube and was partially eliminated. When the line voltage fluctuated rapidly, the readings were no longer so regular but varied over wide

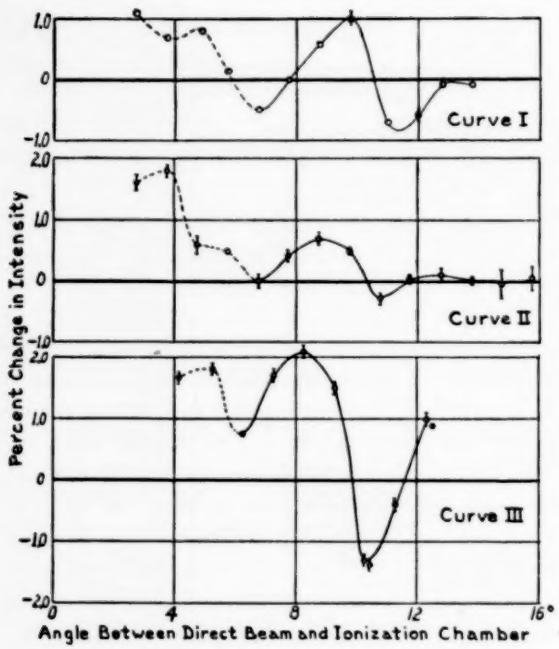

FIG. 8. Percent change in intensity of nitrobenzene diffraction pattern produced by temperature and circulation. Curve 1, increase in intensity produced by a 10°C increase in temperature from 16°C. Curve 2, increase in intensity produced by a 12°C increase in temperature from 30°C. Curve 3, change in intensity produced by circulating nitrobenzene at rate of 0.4 cm per second at a temperature of 23°C.

limits because of the characteristics of the circuit. To obtain the desired accuracy, readings were taken until a series of six, eight or more consecutive readings agreed. No points are given for which less than six readings were averaged.

Curve III in Fig. 8 presents the effect of circulating the nitrobenzene past the point of illumination by the x-rays at a velocity of 0.4 cm per second. The velocity was measured by the rise in temperature of the liquid for a given energy input as illustrated in Fig. 4. The existence of turbulence in the scattering cell was shown by the motion of air bubbles introduced into the circulating system. Turbulence was to be expected since the entrance and exit velocities of the liquid were three times that of the liquid in the cell. Nevertheless, the centrifugal pump circulated the liquid with sufficient steadiness to permit the reproducibility of the results shown in two readings, although these readings were taken several weeks apart.

DISCUSSION OF RESULTS

The readings in Fig. 7 to determine the effect of an electric field of 10 kv per cm on the x-ray diffraction pattern of nitrobenzene have no regularity that can be interpreted as a definite effect. Moreover, the average change in intensity at the peak of -0.02 ± 0.06 percent from 35 readings of 200 seconds duration is in direct contradiction to the average change of $+2.3\pm0.3$ percent from 100 readings of 50 seconds duration reported by McFarlan. The individual readings in Fig. 7 are equal to or smaller than McFarlan's calculated accuracy. The balanced ionization chambers and the special circuit are chiefly responsible for this increase in accuracy. In the scattering cell used by McFarlan, the nitrobenzene was cooled by natural circulation in a comparatively small container and became so hot, by his report, that he could not apply the electric field continuously. In the readings presented here, the temperature did not increase more than about a half degree and the effect due to circulation was cancelled out by the manner of taking the readings. The important question of whether the circulation destroyed any existing "cybotatic" state is difficult to answer; apparently it had no more effect on the diffraction pattern than did increase in temperature. It is the author's opinion that the entire effect measured by McFarlan was produced by the uncontrolled circulation and temperature. The rate of natural circulation and the temperature were higher in his cell while the electric field was being applied than while it was off.

Although the spectrum of the radiation is given in Fig. 5, a better comparison between the radiation used in this work and that used by others is given by the two benzene curves in Fig. 6. The difference between the benzene diffraction pattern given by Stewart[16] and the one given here is attributed to the use of a thicker scattering cell and of a less monochromatic beam of radiation to obtain the present curve. The thickness of the liquid in the scattering cell was 0.63 cm in all the tests included in this report. The secondary peak appearing at large angles agrees with the Debye[17] theory of intramolecular scattering.

[16] G. W. Stewart, Phys. Rev. **33**, 889 (1929).
[17] P. Debye, Phys. Zeits. **31**, 419 (1930).

It has previously been observed[18] for benzene and its presence explained. The benzene pattern is easily checked but it is impossible to check the intensity at the peak of the nitrobenzene diffraction pattern with the same accuracy. That this difference is not attributable to fluctuation in the x-rays is shown by the fact that the nitrobenzene diffraction pattern was taken several times between two benzene diffraction patterns during the continuous operation of the x-ray tube. The indefiniteness of the nitrobenzene peak becomes more pronounced as the temperature is lowered.

If the oxygen atoms in the nitrobenzene molecule lie in the plane of the carbon atoms and if association of the nitrobenzene molecules occurs as illustrated in Fig. 1B, the dipoles of the two associating molecules would practically cancel each other. The force exerted on the surrounding molecules by this associated pair would be very similar to the force exerted by the benzene molecule, which has no permanent moment. Consequently, the average separation of the nearest molecules in adjacent pairs should be approximately the same as for the benzene molecules. The average separation of molecules in the associated pairs should be less as a result of the greater intermolecular forces. The relation between the number of associated pairs of molecules and the total number of molecules is given by the equation presented in the introduction. The average separation between dissociated molecules should be intermediate to the other two spacings. The peak of the nitrobenzene diffraction pattern is much lower and broader than the benzene diffraction peak. This would not be expected, considering the similarity of the molecules, unless several spacings exist between the nitrobenzene molecules. Moreover, the effect of an increase in temperature is to decrease the intensity corresponding to the smaller spacings (larger angles) and to increase the intensity intermediate to the two extreme peaks of the diffraction pattern. The agitation induced by circulating the nitrobenzene produces the same type of effect as a temperature increase. The positions of maximum change in intensity occur at larger spacings (smaller angles) as the temperature is increased. This type of change is to be expected from the change in density with temperature, but not of this magnitude. The large change in the diffraction pattern of nitrobenzene, produced by small changes in temperature, should be compared with the change for benzene. The benzene peak decreases 1 percent in height for a change in temperature of about 51°C,[19] whereas the nitrobenzene peak increases 1 percent for about 17°C temperature rise.

The author feels deeply grateful to Dr. R. D. Bennett for suggesting the problem and to Professor W. C. Pierce for his helpful suggestions. He is especially indebted to Professor A. H. Compton for his interest and assistance in carrying through the project.

[18] E. Rumpf, Ann. d. Physik 9, 704 (1931).

[19] E. W. Skinner, Phys. Rev. 36, 1625 (1930).

Diffuse Scattering of X-Rays from Sodium Fluoride. II. Scattering at the Temperature of Liquid Air

G. E. M. JAUNCEY* AND P. S. WILLIAMS, *Department of Physics, Washington University*

(Received August 5, 1933)

The ratio of the intensity of x-rays diffusely scattered by a single crystal of NaF at 86°K to that of x-rays scattered by the crystal at 295°K has been determined at each of several angles ranging from 10° to 42°. The x-rays consisted of a continuous band of wave-lengths, of which the spectral distribution of intensity was known. From Shonka's value of 442°K for the characteristic temperature of NaF together with his f values for zero point energy, we have calculated the theoretical ratios for different angles. The experimental and theoretical ratios agree very well. The importance of being sure of the absence of Laue spots in this type of experiment is discussed. The experiment was performed by fixing the scattering angle ϕ and varying the crystal angle θ as in the original method of Jauncey and May. If θ is kept constant and ϕ varied there is no sure criterion for the absence of Laue spots. A formula for the ratio at zero scattering angle is given and at small angles the experimental ratio should approach this value. Curves showing the contrast in behavior of the Laue, diffuse and "total" (*see* Jauncey and Pennell) scattering from NaF and KCl with change of temperature from 295°K to 86°K are given.

I. INTRODUCTION

ACCORDING to the theory of Jauncey, Harvey and Woo[1, 2, 3, 4, 5] the intensity of the x-rays diffusely scattered from a crystal consisting of atoms of one kind is given by

$$S=S_1+S_2/(1+\alpha \text{ vers } \phi),^3 \qquad (1)$$

where $S_1=(f^2-F^2)/Z$ and $S_2=1-f''^2/Z^2$. There is some uncertainty as to the equality of f and f''. If, say, the K electrons are distinguishable from the L electrons in one and the same atom, then $f''>f$, but, if all the electrons form an electron gas about the nucleus and no electron can be distinguished as a K or an L electron, then $f''=f$. Recently, the senior author and Dr. G. G. Harvey had the opportunity of discussing with Dr. Ivar Waller of the University of Upsala the equality of f and f''. It appears that the f_0's used by James and Brindley[6] merely represent convenient steps in the calculation of the f values and are not to be considered as representing anything physical about particular electrons. According to this view, $f=f''$. Partly for convenience and partly for the reason just cited we shall in this paper assume $f=f''$.

II. EXPERIMENTAL METHOD

Jauncey, Claus and Harvey[7, 8, 9] have at various times measured the change of the intensity of the x-rays diffusely scattered from crystals of NaCl and KCl produced by a change in temperature and have found a qualitative but not quantitative agreement with theory. In these experiments, x-rays of an average wave-length as determined by absorption in aluminum were used. More recently, however, Harvey[10] has used monochromatic x-rays of wave-length 0.71A with sylvine at a temperature of 86°K (liquid air) and has found reasonably good quantitative agreement with theory. Jauncey and Pennell[11] have recently shown how a band

* The senior author was aided in part by a grant from the Rockefeller Foundation to Washington University for research in science.

[1] G. E. M. Jauncey, Phys. Rev. **37**, 1193 (1931).

[2] G. E. M. Jauncey and G. G. Harvey, Phys. Rev. **37**, 1203 (1931).

[3] G. E. M. Jauncey, Phys. Rev. **42**, 453 (1932).

[4] Y. H. Woo, Phys. Rev. **38**, 6 (1931).

[5] Y. H. Woo, Phys. Rev. **41**, 21 (1932).

[6] R. W. James and G. W. Brindley, Phil. Mag. **12**, 81 (1931).

[7] G. E. M. Jauncey, Phys. Rev. **20**, 421 (1922).

[8] W. D. Claus, Phys. Rev. **38**, 604 (1931).

[9] G. E. M. Jauncey and G. G. Harvey, Phys. Rev. **38**, 1925 (1931).

[10] G. G. Harvey, Phys. Rev. **43**, 707 (1933).

[11] G. E. M. Jauncey and Ford Pennell, Phys. Rev. **43**, 505 (1933).

of wave-lengths from the continuous radiation may be used in scattering experiments provided that the distribution of the intensity among the wave-lengths in the band is known. In this present research we have therefore used the band of wave-lengths whose intensity distribution is shown in Fig. 1.

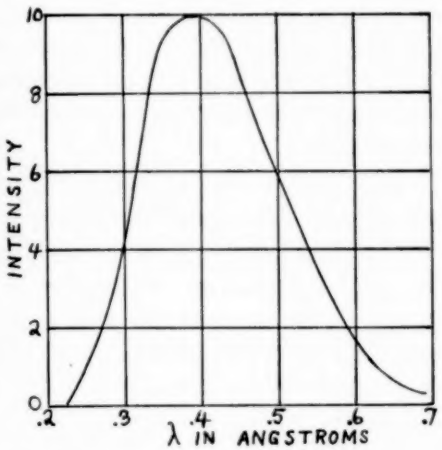

FIG. 1. Distribution of intensity in the continuous spectrum of x-rays.

However, in the present research we have found that the lack of good quantitative agreement with theory as cited above[7, 8, 9] is due not so much to the assumption of an average wave-length when a band of wave-lengths was used as to a fault in the experimental method. It is very necessary in experiments on the diffuse scattering of x-rays from crystals to be sure that Laue spots are not included in the radiation entering the window of the ionization chamber. The criterion for the absence of Laue spots is that the electrometer readings fall on a straight line when plotted against the crystal angle, which is measured between the normal to the crystal plate and the primary beam. An example of this is shown in Fig. 4 of a paper by Jauncey and May.[12] Applying this criterion much more carefully than heretofore we have found that the effect of the central Laue spot spreads out more than is to be expected from the geometry of the slit system. Hence at each angle of scattering we have taken a set of readings with the crystal angle increased by steps of 1 degree. This was first done at room temperature and then again at liquid air temperature. We thus obtained two curves similar to Jauncey and May's Fig. 4 for a given angle of scattering. The ratio of the ordinates of the two interpolated points gives the ratio of the scattering coefficients at the two temperatures.

In this research the cooling chamber was similar to that described by Williams,[13] with a modification to allow for varying the crystal angle during a run. A charcoal trap in liquid air provided the necessary vacuum in the cooling chamber.

III. Experimental Results

The experimental ratios are shown in the fourth column of Table I.

TABLE I. *Diffuse scattering of x-rays from NaF ratios: 86°K/295°K.*

	$\sin \frac{1}{2}\phi$	Theory	Experiment
0°	0.000	0.662	
10°	.087	.710	0.773
15°	.130	.756	.749
20°	.174	.813	.790
26°	.225	.858	.840
32°	.275	.898	.877
37°	.317	.921	.900
40°	.342	.934	.918
42°	.359	.939	.930
45°	.383	.947	

It should be mentioned here that there was considerable lapse of time between the readings at room temperature and those at liquid air temperature. In order to correct for any variation in the sensitivity of the electrometer each set of readings was compared with a set of readings obtained by scattering from a carbon slab held in the primary beam transmitted through the crystal and maintained throughout the experiment at room temperature.

IV. Comparison with Theory

S_1 of Eq. (1) is a function of F, the atom form factor with respect to a lattice point of the crystal. But F is a function of the temperature

[12] G. E. M. Jauncey and H. L. May, Phys. Rev. **23**, 128 (1924).

[13] P. S. Williams, Rev. Sci. Inst. **4**, 334 (1933).

according to the Debye-Waller[14, 15] formula

$$F=fe^{-Bx^2}, \tag{2}$$

where f is the atom form factor with respect to the center of the atom (the "true" atom form factor), $x\equiv(\sin\frac{1}{2}\phi)/\lambda$,

$$B=(6h^2/\mu k\Theta)\{\phi(z)/z+0.25\}, \tag{3}$$

μ is the mass of an atom of the crystal, h and k are Planck's and Boltzmann's constants, Θ is the characteristic temperature, $z=\Theta/T$, and $\phi(z)$ is a function evaluated by Debye. In the formula for B, Eq. (3), zero point energy is assumed.

Very fortunately for us a paper by Shonka[16] on the Laue or directed scattering of x-rays from NaF has appeared. The intensity of the Laue scattering corrected for extinction is proportional to F^2. From the intensities of the Laue scattering at room and liquid air temperatures, Shonka has obtained a characteristic temperature of 442°K. From Havighurst's F values for NaF at room temperature,[17] Shonka has then calculated the f values for this crystal on the assumption of zero point energy.

In our experiment the greatest angle of scattering was 42°. At values of ϕ no greater than 42° and for the wave-lengths used, the Breit-Dirac factor $1/(1+\alpha \text{ vers } \phi)^3$ is very nearly unity and for simplicity we have taken it as unity. Also in Eq. (17) of Jauncey and Pennell's paper[11] we may put $K_\phi=K_0$ and $T_\phi=1$. The theoretical ratio of the intensity of the diffuse scattering at 86°K to that at 295°K is therefore given by

$$R=\frac{\int\{Z^2-f^2+Zf^2(1-e^{-2B_1x^2})\}Id\lambda}{\int\{Z^2-f^2+Zf^2(1-e^{-2B_2x^2})\}Id\lambda}, \tag{4}$$

where $B_1=0.381$, $B_2=0.871$ (the values of B at 86°K and at 295°K, respectively), Z is the atomic number and I is the intensity distribution represented by Fig. 1. From Shonka's f values for zero point energy together with the spectral distribution shown in Fig. 1 we have evaluated each integral in Eq. (4) by quadrature and have then determined the theoretical ratios which are shown in the third column of Table I. The agreement between the theoretical values in the third column and the experimental values in the fourth column is good. With the exception of the experimental ratio at 10° our experimental ratios are all less but only slightly less than the theoretical ratios. Harvey[10] has also found for KCl that the experimental ratios are less than the theoretical ratios. We doubt, however, that the differences in the case of NaF represent any real discrepancy between the experimental and theoretical ratios.

V. Ratio at Zero Scattering Angle

By reference to Table I it is seen that a theoretical ratio is given for $\phi=0°$. At this angle the formula for R, Eq. (4), becomes indeterminate. However by differentiating the integrands of both numerator and denominator it can be shown that for each wave-length present the ratio approaches the value

$$R_{\phi=0°}=(-d^2f/dx^2+2B_1Z^2)/(-d^2f/dx^2+2B_2Z^2). \tag{5}$$

Wollan[18] has shown that at small values of $x\equiv(\sin\frac{1}{2}\phi)/\lambda$ the curve of f *versus* x assumes the parabolic shape

$$x^2=a(Z-f). \tag{6}$$

If this is fitted to an experimental f curve at a small value of x, then a may be obtained. In this case (5) reduces to

$$R_{\phi=0°}=(1+aB_1Z^2)/(1+aB_2Z^2). \tag{7}$$

Fitting (6) to Shonka's zero point energy f curve for NaF at $x=0.1$, we obtain $a=0.0175$, whence $R_{\phi=0°}=0.662$.

VI. Comparison of Diffuse, Laue, and Total Scattering of X-Rays

Shonka[16] has measured the ratios of the intensities of the Debye-Sherrer circles produced by the Laue scattering of x-rays from a powdered crystal of NaF. Assuming a wave-length of $\lambda=0.4$A, we have plotted Shonka's ratios against

[14] P. Debye, Verh. deutsch Phys. Ges. **15**, 678 (1913).
[15] I. Waller, Zeits. f. Physik **17**, 398 (1923).
[16] J. J. Shonka, Phys. Rev. **43**, 947 (1933).
[17] R. J. Havighurst, Phys. Rev. **28**, 869 (1926).
[18] E. O. Wollan, Rev. Mod. Phys. **4**, 205 (1932).

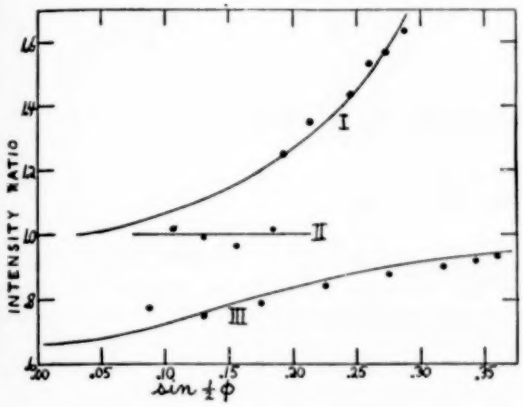

FIG. 2. Ratios of the intensities of the Laue, total and diffuse scattering at 86°K to those at 295°K for NaF. Curve I, Laue scattering (Shonka); curve II, total scattering (Jauncey and Pennell); curve III, diffuse scattering (this research). A wave-length of 0.4A is assumed for curve I in order to plot against sin ½φ.

sin ½φ and the points obtained are shown in the vicinity of curve I in Fig. 2. Jauncey and Pennell[11] have scattered a band of wave-lengths into an ionization chamber with a wide window and have measured the intensity of the "total" scattering from a powdered crystal. This total scattering consists of both the diffuse scattering between the Debye-Sherrer circles and the Laue scattering in these circles. In a more recent experiment Jauncey and Pennell[19] have shown that there is almost no change in the intensity of the total scattering when the temperature of a powdered crystal is changed from 295°K to 103°K. The ratios for the total scattering from NaF are shown as the points in the vicinity of curve II (a straight line). Lastly, in this present research we have obtained the ratios shown in the fourth column of Table I for the diffuse scattering from a single crystal of NaF. These ratios are shown as the points in the vicinity of curve III in Fig. 2. The curves are the theoretical curves for the respective cases. Fig. 2 contrasts very well the behavior of the Laue, diffuse and total scattering of x-rays from NaF with change of temperature from room to liquid air temperature.

[19] G. E. M. Jauncey and Ford Pennell, Phys. Rev. **44**, 138 (1933).

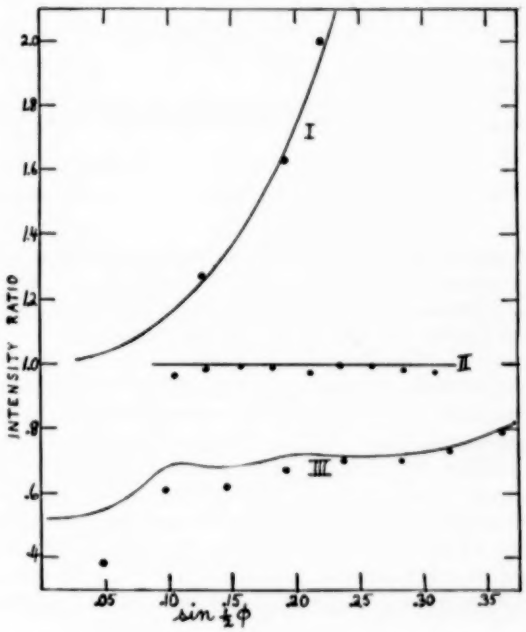

FIG. 3. Ratios of the intensities of the Laue, total and diffuse scattering at 86°K to those at 295°K for KCl. Curve I, Laue scattering (James and Brindley); curve II, total scattering (Jauncey and Pennell); curve III, diffuse scattering (Harvey). A wave-length of 0.4A is assumed for curves I and III in order to plot against sin ½φ.

From the experimental results of James and Brindley,[20] Harvey[10] and Pennell and Jauncey,[19] we have constructed Fig. 3 for KCl in the same way as Fig. 2 has been constructed for NaF. The characteristic temperature for KCl is 230°K. It will be noticed that curve III of Fig. 3 has humps. These humps are characteristic of the theoretical curve for the ratio for diffuse scattering when monochromatic x-rays are used as was the case in Harvey's experiment.[10] Similar humps occur in the theoretical ratio for NaF for monochromatic rays. However, in the present research we used a band of wave-lengths whose intensity distribution is shown in Fig. 1. The effect of such a band is to iron out the humps in the theoretical curve for the ratio plotted against sin ½φ. Hence no humps appear in curve III, Fig. 2, for NaF.

[20] R. W. James and G. W. Brindley, Proc. Roy. Soc. **A121**, 155 (1928).

The Transmission of Waves Through an Ionized Gas

R. W. REVANS,[1] *University of Michigan*

(Received August 26, 1933)

A discharge in mercury vapor at approximately 0.001 mm pressure maintained in a 9 cm spherical bulb between a hot filament and a nearby disk anode was found to become oscillatory at a value of the filament current which depended on the anode potential and was quite definite for a given voltage. By means of a movable probe, the energy of the electrons was determined at various points in the nonoscillating and in the oscillating discharge. When oscillations set in, the electron temperature increased markedly. The frequencies present seemed to consist of a fundamental and a long series of harmonics ranging from about 2×10^4 to 10^6 cycles per sec. The fundamental was constant over a wide range of anode currents and voltages and its frequency was in good agreement with that calculated on the basis of Sir. J. J. Thomson's theory. The overtone that was most intense changed discontinuously with the anode current as though the discharge favored one mode of oscillation at one time as does an organ pipe. It was concluded that the glow was vibrating as a whole in a manner similar to the air in a Helmholtz resonator. A movable probe maintained about ten volts positive with respect to the filament collected currents that showed variations with position and had two or three marked maxima and minima along a diameter of the spherical bulb. In a long cylindrical tube, the currents collected by a probe moved along the tube axis showed no maxima or minima, but those collected by a probe moved along a diameter varied in a manner similar to those in the spherical bulb.

INTRODUCTION

THE existence of electrical oscillations through electrical discharges in gases at low pressures has been known for many years. Such oscillations may be grouped into two broad classes, of essentially different character. The first kind are those whose frequency is a function of the constants of the external circuit used to maintain the discharge, such as capacity-resistance oscillations for the generation of which the discharge tube acts mainly as a valve for controlling the fluctuations of potential in the external circuit. The inductance-capacity oscillations of the Duddell singing arc are of the same character. The second kind are due to the properties of the ionized gas itself, and have been called "ionic oscillations." They have been investigated by a number of observers,[2] including Tonks and Langmuir,[3] and, theoretically, by Sir J. J. Thomson,[4] by whom a complete supporting theory has been developed. It is the object of this paper to describe experiments in which the oscillations have manifested themselves as travelling waves. It is believed that such waves and oscillations may be of great importance in the structure of stellar atmospheres, and theoretical work along these lines is being continued.

APPARATUS

The discharge tube and its connections are shown diagrammatically in Fig. 1. The remainder of the apparatus consisted of a two stage mercury vapor pump, kept running during the observations, and the usual vacuum system. A pressure of less than 10^{-6} mm of residual gas was maintained. Several differently shaped tubes were used, but the majority of observations were with a spherical bulb of 9 cm diameter and a long cylindrical tube of 10 cm diameter and 130 cm length. The tubes were provided with water-cooled ground joints. The cooling water served to keep the mercury vapor at an almost constant pressure of 0.0006 mm for the temperature of the water supply did not vary by more than 0.5°C. A little mercury condensed inside the joints, and as the tube was maintained at a much higher temperature by the heating from

[1] Commonwealth Fellow.

[2] Penning, Phys. Zeits. **27**, 187 (1926); Webb and Pardue, Phys. Rev. **32**, 946 (1929); Fox, Phys. Rev. **35**, 1066 (1931); Chow, Phys. Rev. **37**, 574 (1931); Brown and Cowan, Phys. Rev. **38**, 376 (1931).

[3] Tonks and Langmuir, Phys. Rev. **33**, 195 (1929).

[4] J. J. Thomson and G. P. Thomson, *Conduction of Electricity through Gases*, Part II, page 353.

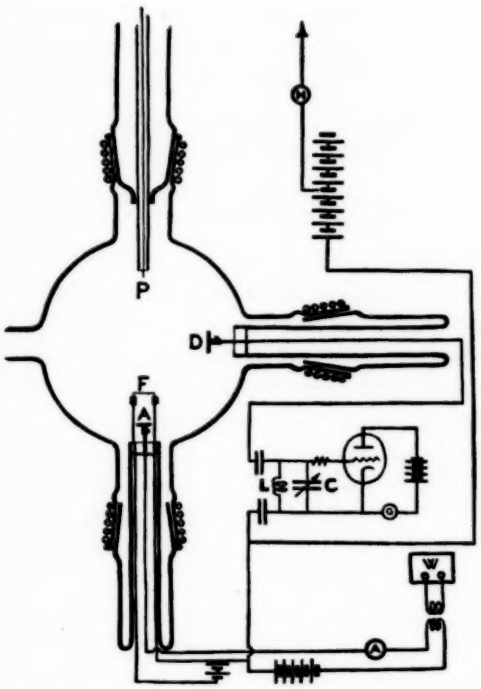

FIG. 1. The discharge tube and control circuits.

the filament, the pressure of the mercury vapor was that of the condensation. The tube was carefully screened with an electrostatic shield. One of the ground joints carried the filament *F* and the anode *A*, which was a circular nickel disk 1 cm in diameter, placed behind the filament in a position that was unimportant. Filaments of various forms were used, either of 5 mil tungsten, straight or spiral, or of oxide coated platinum. Immediately opposite this joint was a second carrying a probe *P*, whose position in the discharge could be altered by means of an electromagnet. The probe was either a small nickel disk or a short fine tungsten wire. The third joint, *D*, carried another plate which could be used as an additional anode, or a collector on which to detect the oscillations. The long tube was provided with a similar set of ground joints and sliding probes, one for moving along the tube axis and another for moving radially across the tube.

The external circuits comprised: (a) The filament heating circuit. (b) The anode circuit, consisting of a battery of 30 accumulators, to provide the arc current, and a milliammeter. The leads were made as short as possible and the resistance of the circuit was reduced to a minimum by shortcircuiting the meter with a key. At times, a coil of 6 turns of copper wire was introduced into this circuit to act as a pickup for the oscillations by coupling it loosely with a wave meter, *W*. The presence of this coil was in no way essential for the production of the oscillations. (c) A detector circuit for oscillations of radiofrequency, consisting of an inductance and capacity, and a three electrode valve, which could be connected either across the filament and anode or the filament and plate *D*. This circuit was also unnecessary to produce the oscillations. (d) The probe-filament circuit, which contained a battery, giving voltages up to 60 volts, and a galvanometer.

METHOD OF OBSERVATION

When the emission from the filament was relatively small, corresponding to an arc current of 20 milliamperes at 40 volts or so, the conditions within the arc were normal. No oscillations could be detected, and there were present in the arc no electrons with energies much higher than would be expected from the potential applied at the anode. The electron temperature was of the order of 10,000 to 20,000°C, by which it is meant that the electrons had a Maxwellian distribution of velocities corresponding to this temperature.

As the filament current was increased, however, a point was reached at which a discontinuity appeared in the anode current, and the glow was thrown into violent oscillation. The value of the filament current at which this set in varied with the anode potential, being, in general, higher with greater voltages. The glow changed its appearance from a uniform discharge filling the tube to a more tenuous glow around the filament, and, in the long tube, failed to reach the end remote from the filament. At the same time, the tube emitted a very faint and highly pitched note. There was then practically no resistance, inductance, or capacity in the whole circuit, nor did the addition of these markedly affect the pitch of the note, except insofar as the applied voltages across the tube were interfered with.

The current-potential characteristics of the

probe at this point at which oscillations commenced underwent a remarkable change as shown in Fig. 2. In these graphs are shown the logarithm

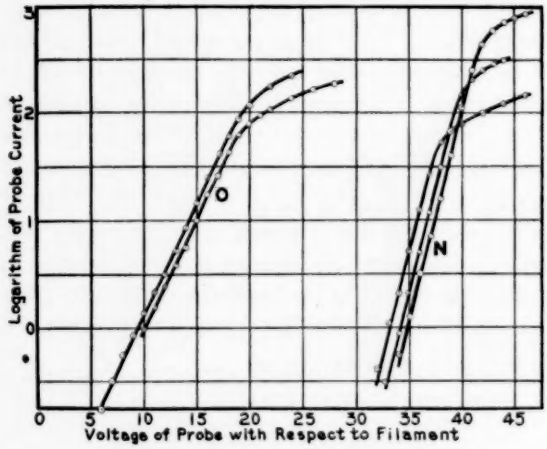

FIG. 2. Semilogarithmic plots of the volt-ampere characteristics of the probe for oscillating (O) and nonoscillating (N) arcs.

of the probe currents plotted with respect to the potential difference between the probe and the filament. The group marked N are for the normal arc, before oscillations commenced, those marked O are for the oscillatory arc immediately afterwards. The general character of the change is independent of the anode voltage, and corresponds to a large increase of the electron temperature, as shown by the decreased slope of the straight portion of the curves. It is remarkable, both for the normal and the oscillatory arcs, for how wide a range of probe current, several hundred-fold, the Maxwellian distribution holds. This change of the electron temperature is, of course, to be expected when the glow is set oscillating, for there will be imposed upon the electrons all the motions of the oscillations, which may have any of a wide range of frequencies.

The oscillatory state is very critical and easily destroyed by a magnetic field. The approach of a magnet to the tube caused the arc current suddenly to jump back to its normal value. For this reason, the shape of the filaments and the heating currents they require probably play a fundamentally important part in the experimental study of these oscillations. With the oxide coated filaments, which required small currents to heat them, the oscillations appeared at lower densities of ionization than with the tungsten wires. Oscillations were more easily produced when straight wire filaments were used than when the filaments were of spiral form.

THE ANODE GLOW

At certain values of the anode voltage and current, a bright blue glow appeared behind the anode. It was not necessarily associated with an oscillatory condition in the rest of the arc, and would appear and disappear without affecting the main discharge. It was generally elusive, and would be present with an anode voltage of say 38 volts and absent when the voltage was 36 or 40. It could be generated or removed with a magnet, and in some runs it did not appear at all. It appears definitely to be associated with the anode, for when the rest of the discharge was oscillatory and its space potential much diminished, the potential in the glow, as measured by another probe, was that of the anode itself.

MEASUREMENTS OF THE FREQUENCIES OF OSCILLATION

The frequency of the strongest oscillation was within the audible range, although near the upper limit. It was measured with a wave meter. Besides this oscillation, its fifth and octave and a range of upper partials could be detected. At all times, even when the low frequency oscillation could not be detected audibly, there was a series of oscillations of frequency 10^6 or so within the radio range. The variations of these frequencies with anode current and potential were extremely complicated. Over wide ranges of the arc current, the frequency would remain constant and then, at a certain value of the current, drop or increase suddenly to remain constant for another range of variation of the current. This seemed to indicate that the discharge favored one mode of oscillation at one time, changing discontinuously to another just as does an organ-pipe. These oscillations of radiofrequency appeared to be higher harmonics of the fundamental. A long series of them was detected with the circuit marked LC. The frequency of the fundamental remained practically constant over the range of current and anode voltage investigated, although

a magnetic field altered the pitch of the note. For this reason, combined with the observations with the sliding probes, one is led to the belief that the glow was vibrating as a whole in a manner similar to the air in a Helmholtz resonator.

Investigations of the Glow with a Sliding Probe

When the sliding probe was made about ten volts positive with respect to the filament, and slid across the oscillatory discharge, the electron current collected showed variations with two or three marked maxima or minima as it passed from an initial position near the filament to the wall on the opposite side of the bulb. In the long tube, no such variations were shown on sliding a probe lengthwise down it. There was merely a decrease in the current collected, which fell off gradually and showed no maxima or minima. But a probe moved across the cylindrical tube showed marked maxima and minima just as with the spherical bulb. These observations are to be taken as proof that the glow is oscillating as a whole under the influence of travelling waves through the charged particles, for maxima and minima develop when reflection is possible. In the case of the long tube there was such a decrease in the intensity of the ionization away from the filament that the waves could not travel down it and form standing oscillations along the tube axis. In the case of the smaller bulb, and the radial section of the long tube in the vicinity of the filament, the density of ionization was high throughout and conditions for a reflected wave from the walls to form nodes and antinodes much more favorable.

In Fig. 3 are shown some of the results. The positions of the nodes and antinodes do not change with the position of the filament, as is indicated by curves *3a*, *3b*, *3c* taken for the same anode voltage and current but with three different positions of the filament as indicated by the dotted lines. Curves 1 and 2 correspond to small current densities with presumably the fundamental and its fifth present, *3a*, *3b*, and *3c* to the octave, which was the favorite mode of oscillation. The appearance of an antinode in curve 2 at the middle of the spherical tube

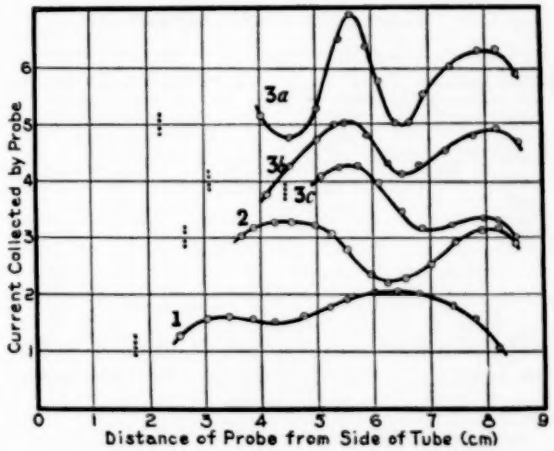

Fig. 3. Variation of the currents collected by the probe with the position of the probe. The dotted lines indicate the positions of the filament.

requires some explanation. It might be that the slab of gas between the filament and the back of the tube was at that time undergoing plane and not spherical oscillation.

Discussion

It has been shown by Sir J. J. Thomson[4] that travelling waves with velocities lying between $(kT_i/M_i)^{\frac{1}{2}}$ and $[(kT_i+kT_e)/M_i]^{\frac{1}{2}}$ can be propagated through an ionized gas, where T_i and T_e are the ion and electron temperatures and M_i the mass of the positive ion. Other waves are also possible, corresponding to the electron oscillations, but these carry little energy. The waves with velocities tending towards the first limit written down above are highly dispersive, and so the oscillations to be expected are those whose frequency is small compared with the free frequency of the electrons. That is, when the frequency is much less than $(ne^2/\pi m)^{\frac{1}{2}}$, where n is the number of electrons or ions per cc and m is the electron mass, the ion waves travel with a velocity approximately given by the second limit above. Since, in this case, the electron temperature is so much greater than that of the ions, this velocity reduces to $(kT_e/M_i)^{\frac{1}{2}}$.

The electron temperatures measured were of the order of 50,000 to 80,000°C, the mass of the mercury ion about 3.32×10^{-22} g, the velocity is about 1.5×10^{5} cm per sec. This gives as the fundamental frequency of oscillation of a bulb

TABLE I. *Anode voltage 38 volts.*

Anode current	Frequency of fundamental
200 m.a.	2.00×10^4
300	1.96
400	1.94
500	1.88
600	1.90
700	1.88
800	1.90

9 cm in diameter approximately 1.7×10^4 per sec. The frequencies measured were, on the average, slightly higher than this, although the agreement is to be regarded as highly satisfactory, considering the disturbances in the glow rendering it non-uniform. Table I gives some of the measured fundamental frequencies, determined by the wave meter. The radiofrequencies were between 10 and 100 times as great.

It seems to be established that an ionized gas is capable of generating and transmitting oscillations of its constituent ions. In the highly ionized gases of the stars and their atmospheres, these oscillations may be of profound importance, especially in disturbed areas such as sunspots, granulations, and faculae.

In conclusion, the author wishes to thank most heartily Sir J. J. Thomson for his continued advice and help, and the Governing Body of Emmanuel College, Cambridge for a studentship which made the work possible. The experiments were completed at the University of Michigan while the author was a Fellow of the Commonwealth Fund.

Field Electron Emission from Liquid Mercury

J. W. BEAMS, *University of Virginia*

(Received August 28, 1933)

Field emission from liquid mercury has been investigated by applying an impulsive potential of approximately 10^{-6} sec. duration between a spherical steel anode and a plane mercury cathode. The field just necessary to produce breakdown gave a measure of the field necessary to produce emission because rotating mirror photographs showed that the field emission from the cathode initiated the discharge. The liquid mercury cathode was cooled to a few degrees above its freezing point and the mercury vapor pressure still further reduced by solid CO_2 traps. The mercury could be distilled repeatedly in vacuo and the surface of the cathode changed by "overflowing." The electric field necessary to produce sufficient field emission to start the discharge depended upon the purity of the mercury surface. It varied from 3.5×10^5 volts per cm for impure mercury to 1.8×10^6 volts per cm for mercury that had been repeatedly distilled in vacuo.

THE fact that electrons can be pulled out of solid metals by electric fields of sufficient intensity has been definitely established by many different investigators.[1, 2, 3] A theory of this phenomenon has also been developed[4, 5] which it is claimed[6] is in reasonable agreement with experiment. However, any quantitative comparison of theory with experiment is usually complicated not only by the trouble of getting a uniformly clean pure metal surface but also by the difficulty of determining the value of the electric field at the surface of the metal. This uncertainty in the determination of the electric field at the surface of the metal, arises from the inherent roughness of the solid metal surface, i.e., the electric field at the point of a small projection may be many times that computed for a smooth plane. Therefore, it seemed worth while to attempt a study[7] of the field electron emission from liquid mercury which could not only be purified by repeated distillation in vacuo but also should probably be comparatively free of inherent surface roughness. A study of the field emission from liquid mercury also is of considerable interest in connection with an understanding of the mercury arc, since it is usually believed to be an important factor in maintaining the requisite electron current from the cathode of the arc.[8, 9] In addition to the above, a knowledge of the field necessary to produce appreciable field emission from mercury might prove of value in connection with the design of discharge tubes to withstand high impulsive potentials.

The usual method of studying field electron currents in which a steady potential is applied to the electrodes in vacuo and the resulting current measured by a galvanometer or electrometer obviously cannot be used when one of the electrodes is mercury. The mechanical forces arising from the electric field (0.11 to 11 atm. for fields of 5×10^5 to 5×10^6 volts per cm) will cause the liquid mercury surface to be completely distorted. Therefore, it is necessary to adopt an experimental method in which the electric field is applied and removed from the mercury surface in such a short time that the resulting forces cannot appreciably distort the mercury surface.

It has been definitely shown that if a high impulsive potential is applied across two plane or spherical electrodes in vacuo the resulting dis-

[1] Wood, Phys. Rev. **5**, 1 (1897).

[2] Millikan and Eyring, Phys. Rev. **27**, 51 (1926); **31**, 900 (1928). Millikan and Lauritsen, Proc. Nat. Acad. Sci. **13**, 45 (1928); Phys. Rev. **33**, 598 (1929).

[3] See Compton and Langmuir, Rev. Mod. Phys. **2**, 121 (1930).

[4] Fowler and Nordheim, Proc. Roy. Soc. **A119**, 173 (1928).

[5] Oppenheimer, Phys. Rev. **31**, 66 (1928).

[6] Stern, Gossling and Fowler, Proc. Roy. Soc. **A124**, 699 (1929).

[7] Beams, Phys. Rev. **43**, 781A (1933).

[8] Langmuir, G. E. Rev. **26**, 735 (1923).

[9] Compton, Phys. Rev. **37**, 1077 (1931); Compton and Lamar, Phys. Rev. **37**, 1069 (1931).

charge is initiated by the field electron emission from the cathode.[10, 11] The value of the field required to produce sufficient emission to start the discharge varies for different cathode materials, their purity and their previous treatment but for tungsten is of the order of magnitude of 5×10^5 volts per cm.

Fig. 1a shows a photograph of the light from the beginning of an impulsive discharge between tungsten electrodes in a vacuum after reflection in a rapidly rotating mirror.[12] Since the image was moving across the photographic plate in a direction perpendicular to a line through the electrodes, it will be observed that the anode becomes luminous before the cathode. This is in accord with the work of Hull and Snoddy who concluded that when the field reaches a certain magnitude the electrons are pulled out of the cold cathode, fall through the high potential difference between the electrodes and bombard the anode. As a result the anode is heated until sufficient vaporization takes place to start the discharge.[11] Fig. 1b shows a similar rotating mirror photograph of an impulsive discharge between a steel ball anode and a liquid mercury cathode. It will be observed that the luminosity starts at the steel anode indicating that the discharge is initiated by the field current from the mercury cathode which heats the steel anode by bombardment and thus initiates the discharge.

FIG. 1a. Photograph of the beginning of a discharge between two fifty mil tungsten wires in a vacuum. The photograph is magnified seven times. The time between the appearance of the luminosity at anode and cathode in this picture was about 1.5×10^{-7} sec.

FIG. 1b. Photograph of the beginning of a discharge between a steel spherical anode and a liquid mercury cathode in a vacuum. The time between the appearance of the luminosity at anode and cathode in this picture was about 2×10^{-7} sec. However, this time as well as that recorded in Fig. 1a depends upon a number of factors such as the electrode spacing, power, etc. The faint streak of light above the cathode is due to stray reflected light.

Fig. 2 shows a schematic diagram of the apparatus. The condenser C is charged until the spark gap G breaks down. This applies a potential across the resistance R_1 and to the steel sphere A until a discharge takes place between A and B. The discharge between A and B in turn lights the sensitive neon tube. The potential source was a static machine for the lower potentials and a high potential transformer, in the primary of which a direct current was mechanically broken, for the higher potentials. The spark gap G consisted of two 10 cm brass spheres. The cathode of G was irradiated with ultraviolet light from a quartz mercury arc to reduce time lag effects. The electrolytic resistance R_1 prevented oscillations and was usually adjusted to give a time constant of 1.2×10^{-6} sec. The 2 cm steel spherical anode was mounted on a steel rod about 0.25 mm

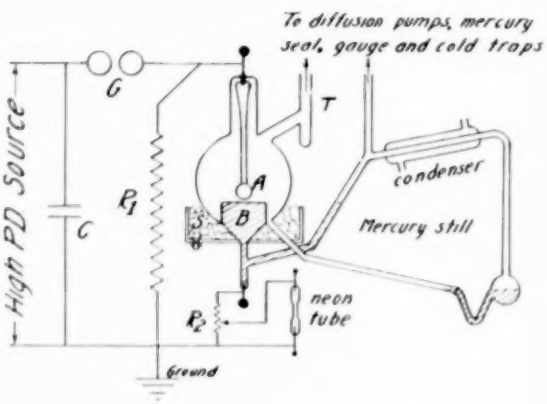

FIG. 2. Diagram of apparatus.

[10] Hull and Burger, Phys. Rev. **21**, 1121A (1928).

[11] Snoddy, Phys. Rev. **37**, 1678A (1931).

[12] See Beams, Phys. Rev. **35**, 24 (1930): R. S. I. **1**, 667 (1930) for general method.

above the maximum height the mercury in B could attain without pouring over the side. It was necessary to avoid violent disturbances of the mercury surface because when the steel sphere and mercury were even reasonably clean the mercury "wetted" the sphere and could be removed only by heating. The electrolytic resistance R_2 prevented violent oscillations in the tube. The neon tube was so arranged that it lighted only when current passed from A to B. It also served as a sensitive means of obtaining the polarity of the discharge. The glass walls of the inner tube containing the mercury B were always electrically shielded from A by the projection of the mercury above the edges of the tube. A freezing mixture of salt and ice S cooled the liquid mercury pool while the trap T, surrounded by solid CO_2, served to reduce the vapor pressure of the mercury in the tube. The surface of B was changed by overflowing and its height regulated by operating the mercury still. A sticking vacuum was always maintained by the mercury diffusion pumps. The mercury was distilled by the Hulett[13] method before being introduced into the clean still. Also the glass tube containing A and B and the traps were baked for 10 hours at 450°C before the mercury was distilled in. The potentials were measured by the width of G. Effects of possible electrical reflections at A were investigated and found to be inappreciable. Distances between A and B were measured by a travelling microscope and the field at B computed by the usual formulas.[14] Care was taken to shield the mercury cathode B from light that might pass through the Pyrex glass, and produce a photoelectric effect on the cathode. Mechanical vibrations of the tube containing B which would cause ripples on the mercury surface were eliminated as far as possible by careful mounting of the tube and by checking the observations late at night, with all pumps, stills, etc., stopped.

When the mercury was first distilled into the tube B, the field necessary to initiate the discharge was about 6.5×10^5 volts per cm. However, as the mercury was repeatedly distilled the field required to initiate the discharge increased at first at the rate of about 10^5 volts per cm per distillation but later much slower until fields of 1.8×10^6 volts per cm were required to start the discharge. Dry nitrogen or hydrogen at about 10 mm pressure when allowed to come in contact with the mercury cathode for a few minutes and then pumped out for an hour seemed to have no appreciable effect on the discharge potential. However, water vapor in sufficient amount or impurities such as grease vapors lowered the discharge potential markedly. Fields of 3.5×10^5 volts per cm were found to initiate the discharge with a cathode containing impurities. In all cases the value of the field necessary to initiate the discharge was critical, i.e., a few percent change in the field caused a change from no discharge to a violent discharge. According to the theory of Fowler and Nordheim[6]

$$I=6.2\times10^{-6}\frac{\mu^{\frac{1}{2}}}{(\mu+w)w^{\frac{1}{2}}}F^{2}e^{-6.8\times10^{7}w^{\frac{3}{2}}/F},$$

where I is the field current in amperes per cm^2, μ is a parameter, which they take as 5, w is the thermionic work function in electron volts, and F is the field strength at the surface of the metal in volts per cm. The thermionic work function for liquid mercury has not been experimentally determined but its practical equivalent, the photoelectric work function has been measured many times and found to be 4.53 electron volts for clean mercury.[15] Substituting then the value 1.8×10^6 volts per cm for F, which is the value of the field at the surface of the mercury cathode if it was a perfectly smooth plane, I is of the order of magnitude of 10^{-160} which is considerably less than one electron per sec. and could not possibly start a discharge. From the rate at which heat is conducted away from the anode one can roughly estimate the power and hence the value of I required to start a discharge in 10^{-6} sec. The minimum value of I in this case comes out around one ampere per cm^2. Therefore, in order to account for the discharge field observed, it is necessary to assume either that there exist sharp points on the mercury surface where the field would be increased by a factor of almost 18, that the effective

[13] Hulett and Minchin, Phys. Rev. **21**, 388 (1905).

[14] Peek, *Dielectric Phenomena in High Voltage Engineering*, 3rd edition, Chapter 2 (1929).

[15] See Hughes and DuBridge, *Photoelectric Phenomena*, p. 75.

work function varied over large ranges (the maximum value would have to be less than a volt) or that both factors were operating together. The observed increase in the value of the field required to produce a discharge with purification of the mercury surface, indicates that the work function of the surface varied over a considerable range. However, it is not likely that the work function alone could account for the large divergence between formula and experiment even though the assumption is made that the cathode might contain small "patches" with widely different work functions. On the other hand, as far as the writer could find, the exact submicroscopic structure of a liquid mercury surface is not definitely known. X-rays scattered from liquid mercury indicate that "quasi-crystals" may exist in the liquid[16] but since these are so loosely bound, ridges in the surface should not necessarily exist. Very small dust particles were possibly present to some extent in the vacuum system although care was taken to keep the mercury as free from them as possible. The constant breakdown potential observed would require the dust particles, if conducting, all to be of approximately the same dimensions and of the same material if they were causing the breakdown. The distortion of the mercury surface by the mechanical forces arising from the electric field (less than 2 atm.) could not produce points on the surface because in the first place the distortion in 10^{-6} sec. is very small and in the second place it is, by comparison, uniformly distributed and hence could not produce points. Of course if points already existed on the surface the field would increase their height. Mercury droplets should not be pulled out of the surface by the field in 10^{-6} sec. because the internal pressure or cohesive force has been experimentally found to be over 5 atm. while the theoretical value is 13,000 atm.[17] Also the effect of the distortion of the mercury surface by the field was experimentally tested by varying the time of application of the field by a factor of 2, without change of breakdown potential. The natural statistical fluctuations in the surface of the mercury cause a certain roughening of the surface but probably not enough to account for the results observed. Ripples, if present, might account for the results, but as mentioned previously these were eliminated as far as possible. Also they could not be observed by an optical arrangement having a magnification of about thirty. It should also be noted that although the temperature of the mercury was always below 0°C there was still a large number of atoms leaving and entering the mercury surface per second, which would give rise to roughnesses of molecular dimension. In view of our lack of knowledge of the submicroscopic structure of a mercury surface one cannot justly compare the theory with the experimental results obtained above. As a matter of fact, if one could be certain of the direct applicability of the theory valuable information of the submicroscopic structure of the mercury surface could be obtained. The remarkable success of the theory in explaining so many of the experimental results obtained by different investigators with solid metal cathodes indicates that the formula is not far wrong, although it seems that there might be some question as to whether or not the "sharp" potential barriers used in the theory are more than rough approximations to their true shape. It is hoped that the measurement of both the photoelectric threshold (and hence the work function of the surface) and the field necessary to initiate breakdown of the same mercury surface, now being undertaken in this laboratory, may help to straighten out some of the uncertainties.

The experimental results reported above support the field emission theory of Langmuir and Compton for the origin of at least part of the large electron current from the cathode of the mercury arc. Lamar and Compton have shown that in the neighborhood of the cathode of a mercury arc the field is at least 5.7×10^4 volts per cm, which as they point out may possibly give fields of millions of volts per cm at points in the cathode spot produced by the violent agitation. It is likely that the mercury in the arc, although distilled with care, contains sufficient impurities to give enough field emission, with fields of less than 10^6 volts per cm to account for the electron current observed near the cathode of the arc. If it were possible to keep the mercury in an arc really clean, which might be very difficult because of

[16] Debye and Menke, Phys. Zeits. 31, 797 (1930).
[17] Int. Crit. Tables, Vol. 4, p. 19.

impurities liberated by ions and excited atoms from the walls, etc., observations such as those of Lamar and Compton of the characteristics of the arc should perhaps show changes, if field emission is an important factor.

It is a pleasure to record my indebtedness to Mr. James A. Chiles, of this laboratory, who not only kindly obtained the picture 1a but loaned the rotating mirror apparatus with which 1b was secured. Also I am very grateful to Dr. L. B. Snoddy and Mr. F. T. Holmes for the privilege of discussing this paper with them.

Magnetic Deflection Method for Angular Distribution of Electrons Scattered by Gas Molecules

A. PHARO GAGGE, *Sloane Physics Laboratory, Yale University*

(Received June 21, 1933)

A method is given for evaluating the scattering coefficient for electrons colliding with gas molecules, if the electrons both before and after collision describe circular paths in a uniform magnetic field. As in previous methods an electron gun and a receiver are needed. The axis about which the gun may be rotated is parallel to the receiver slits and lies some distance from their common plane on a perpendicular thereto through the center of the first slit. The second slit with Faraday collector can be set at such distances from the first slit as to collect only electrons that have lost a definite energy on collision. The chief advantage over previous methods used for angular distribution study is that, since all electronic paths are circular, the angular distribution may be studied up to 180° scattering angle. The fact that the collector may be set for electrons of definite energy allows both elastic and inelastic collisions of slow electrons to be studied. Typical experimental curves are given which show the variation with angle of the scattering coefficient in mercury vapor for 80 and 30 volt electrons. The scattering angles cover the range from 20° to 180°. These results are compared with those of previous observers over that portion of this range which they studied. An application of the method to the inelastic collisions of 23 volt-electrons in mercury vapor is included.

INTRODUCTION

AN inherent difficulty of the Dymond method[1] for the study of electron scattering by gas molecules is that the angular distribution of the scattered electrons cannot be studied up to 180°. The same is true for the zone method of Ramsauer and Kollath.[2] If the paths of the electrons are made circular before and after collision, by placing a uniform magnetic field perpendicular to the incident electron beam it is possible to devise an apparatus free from this limitation. The magnetic field in addition sorts the scattered electrons in accordance with their energies so that groups losing definite energies may be examined separately.

THEORY OF METHOD

As in Dymond's method a gun and a receiver are needed. The electron beam from the gun has a radius of curvature dependent upon the electron energy and magnetic field strength. If the pressure of the gas uniformly distributed throughout the apparatus is small enough to make multiple collisions unlikely, each volume element within the beam acts as a source of scattered electrons. The receiver slits in turn define a beam within which scattered electrons must move in order to be collected. The region common to both beams is that in which effective collisions occur. The general principle of the theory to be given is true for any receiver slit arrangement in which the four slit edges are parallel, but on account of its geometrical simplicity the arrangement to be considered in detail is that in which the parallel slits of the receiver lie in the same plane. This arrangement is similar to that used by Danysz in the β-ray spectrometer.

The essential geometry of the problem is illustrated in Fig. 1 (A, B). To pass through the collector slits S_1 and S_2 the centers of curvature of the electron paths must lie in the small region $ABCD$, formed by arcs of radius, R, whose centers lie at the slit edges. The electrons must enter upon these paths somewhere within the roughly circular area outlined (scattering area). At any point in this area, say P, the tolerance in angle (in the plane of the paper) which permits the scattered electron to reach the Faraday box is MN/R. The *average* tolerance for a given angular position, σ, of P (but varying

[1] E. G. Dymond, Phys. Rev. **29**, 433–441 (1927).

[2] C. Ramsauer and R. Kollath, Ann. d. Physik [5] **12**, 529–561 (1932).

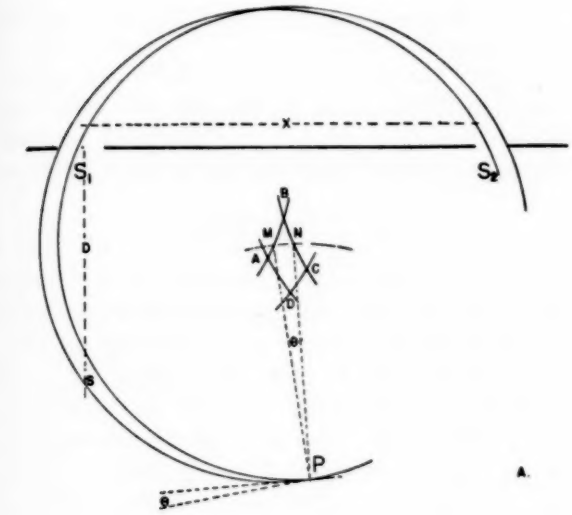

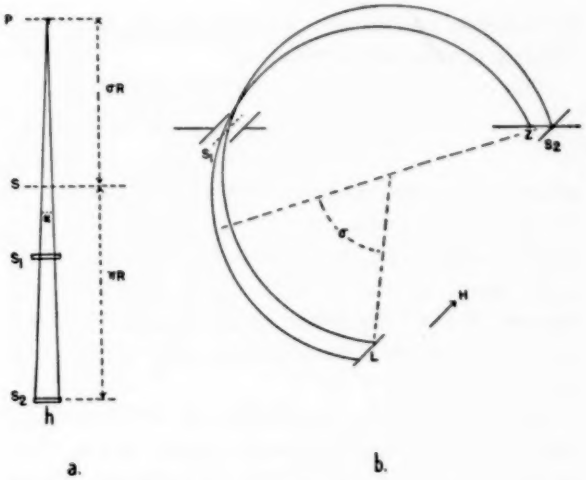

FIG. 2. Paths that do not lie in plane normal to magnetic field.

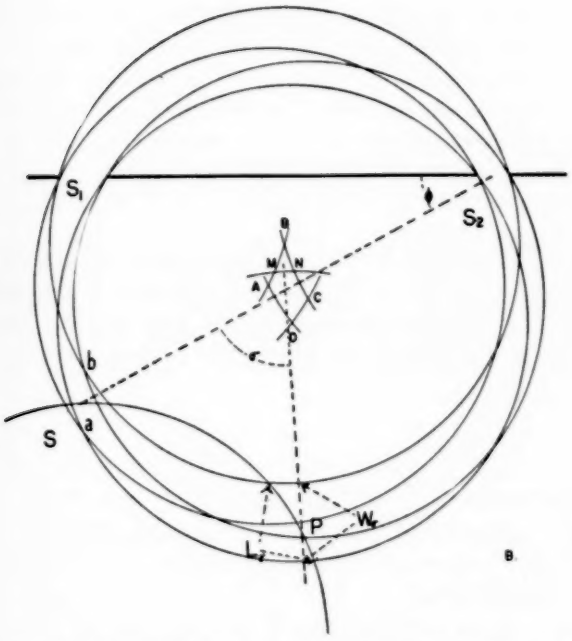

FIG. 1. Diagram of paths in a plane normal to magnetic field.

position of P across the scattering region) is

$$\bar{\theta} = (\text{area } ABCD)/RW_\sigma,$$

where W_σ is the radial distance across the scattering region at the angular position, σ.

The average tolerance in angle α with respect to the plane of the paper is (see Fig. 2a)

$$\bar{\alpha} = h/(\sigma+\pi)R,$$

where h is the length of the slit S_2 and $(\sigma+\pi)R$ is the length of path of the electron. Strictly speaking the electrons scattered away from the plane of the diagram (see Fig. 2b) will have to have a slightly higher average energy to pass through the slit S_2 than do those moving in the plane. For the dimensions of the slits here used this fact need not be taken into account.

Hence the average solid angle $\bar{\omega}$ of the collected beam from P is, from (1) and (2),

$$\bar{\omega} = \bar{\alpha}\bar{\theta} = (\text{area } ABCD)\cdot\frac{h}{(\sigma+\pi)R^2}\cdot\frac{1}{W_\sigma}. \quad (1)$$

For small slit widths the area $ABCD$ is $s_1s_2x/2D$ where x is the distance between the centers of S_1 and S_2 and $D=(4R^2-x^2)^{\frac{1}{2}}$.

The point, S, in Fig. 1B lies at a distance, D, below the center of slit S_1. The incident beam is rotated about an axis through S. If θ is now the angle the incident beam makes with the direction of the scattered beam at S, it may be seen that the incident beam again crosses the collectable area at P. The point, S, is called the primary scattering region, while P is called the secondary scattering region. There will be a θ-value (in the case of the apparatus to be described, 95°) where, as θ is decreased, the initial beam strikes the walls of the receiver, and thus the secondary scattering region vanishes. For S the angle σ is always zero, while for P it

is variable and in no case greater than 80° for this particular arrangement.

The current collected *for a given pressure is*

$$I_\theta = I \cdot (\bar{\omega}_\theta \cdot L_\theta) \cdot S(\theta), \tag{2}$$

where I_θ is the collected current, I the initial beam at S, $\bar{\omega}_\theta$ the average solid angle, L_θ the path length, and $S(\theta)$ the so-called scattering coefficient, which is defined as the scattered current at $\theta°$ to the initial beam, per unit electron current, per unit solid angle, per unit path length.

The path length, L_θ, consists of two parts, L_0, due to the primary scattering region, and L_σ, due to the secondary region. The $\bar{\omega}_0$ (with $\sigma = 0$) and $\bar{\omega}_\sigma$ are given by (1), and therefore

$$\bar{\omega}_\theta \cdot L_\theta = \frac{s_1 s_2 h \chi}{2\pi D R^2} [L_0/W_0 + L_\sigma \pi / W_\sigma (\pi + \sigma)]. \tag{3}$$

From (2) and (3)

$$I_\theta = I \frac{s_1 s_2 h \chi}{2\pi D R^2} [L_0/W_0 + L_\sigma \pi / W_\sigma (\pi + \sigma)] S(\theta). \tag{4}$$

For the apparatus here used $0° < \sigma < 80°$. In general, if R_i is the path radius of the initial beam and, as before, R, the radius of scattered beam, the relation between θ and σ is found to be

$$R_i \sin(\pi - \theta) = R \sin \sigma \cdot (R_i > R). \tag{5}$$

For the "elastic" case when $R_i = R$, $\pi - \theta = \sigma$. The bracketed term in Eq. (9) is called the "dispersion factor." For the Dymond method the equation corresponding to (9) is of the form

$$I_\theta = I \cdot S(\theta) \cdot K \cdot \csc \theta,$$

where K includes the dimensions of the apparatus. In that case the dispersion factor is $\csc \theta$.

The dispersion factor is determined graphically. From 10° to 140° the uncertainty of determination is easily reduced to 5 percent. From 140° to 170° the uncertainty increases to 10 percent on account of the greater range in the values of ω to be averaged. At 180° the uncertainty reduces again to 5 percent. A typical set of factor values is presented in Table II.

The graphical solution is carried out for inelastic collisions in the same way as for elastic collisions except that the more general value of σ in terms of θ given by Eq. (5) is used.

Apparatus

The general plan of the scattering chamber is shown in Fig. 3. The tube is a copper elbow to which the end plates are waxed with picein. The magnetic field from Helmholtz coils is perpen-

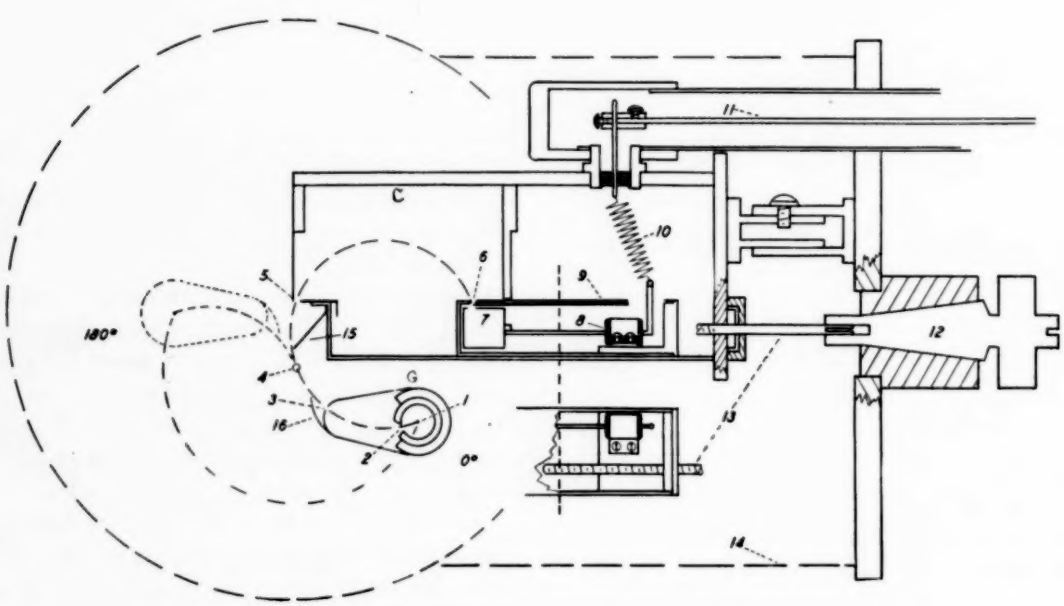

Fig. 3. General arrangement of apparatus.

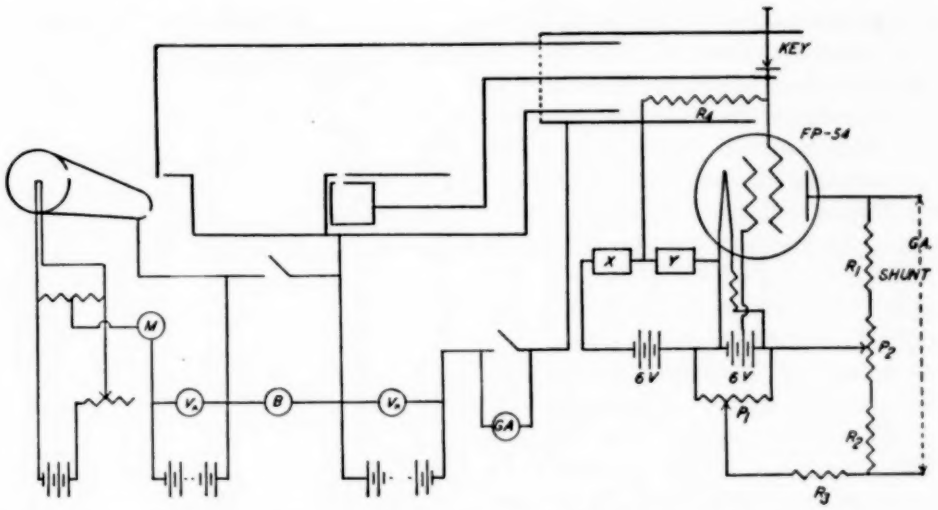

FIG. 4. Wiring diagram: M, microammeter; V_A, voltmeter for accelerating potential; V_R, voltmeter for retarding potential; B and GA, galvanometers; X and Y, resistances of constant sum 10,000Ω; R_1 and R_2, 10,000Ω; R_4, 20,000Ω; R_3, S. S. White Dental Co. high resistance of 10^{10}Ω; P_1 and P_2, 400Ω potentiometers.

dicular to the plane of the figure and deflects electrons from the gun into circular paths. This gun is mounted to rotate about an axis through a point (4) (the primary scattering region). Below the second defining slit (6) is the Faraday collector (7) which is connected to a vacuum tube electrometer. The gun is shown in two positions; at 0° where the primary beam passes directly into the collector and at 180° (dotted lines) where electrons scattered at (4) through 180° pass into the collector. The points (4), (5) and (6) define the path radius of the electrons collected. The slit (6) and Faraday box are mounted in a movable drawer (9) whose position is accurately controlled by a micrometer screw (13). In this way scattered electrons of various energies may be collected. The whole gun system is insulated from the receiver system by very thin washers of mica. A baffle (15) prevents the secondary electrons scattered by the lower step of the receiver from entering slit (5). A baffle (16) similarly protects the receiver from secondary electrons from the inner side of slit (3). (See Table I.)

TABLE I. *Dimensions here used (see Fig. 3).*

Slit (2)	1. mm×8 mm
Slit (3)	0.5 mm×4 mm
Slit (5)	1. mm (s_1)×10 mm
Slit (6)	0.4 mm (s_2)×10 mm (h)
Average radius of "elastic" circle	2 cm (R)
Distance from slit (5) to axis (4)	1.27 cm (D)

ADJUSTMENT AND USE

Fig. 4 is the wiring diagram used. The voltage sensitivity of the vacuum tube electrometer may be determined by making small changes in the resistances of the X and Y plug boxes. The constancy of the high resistance R_4 is checked easily by grounding the Faraday cylinder to its surrounding case and using batteries V_R and galvanometer G_A.

After every disassembly the gun and receiver units are placed in a separate vacuum furnace and baked for four hours at a temperature of 400°C. These parts are sealed into the elbow immediately after removal from the furnace.

The adjustment of the magnetic field is complete when for a given field strength, H, and accelerating potential, V_A, the initial beam passes through the axis of rotation for all angular settings of the gun.* The adjustment of the gun and drawer positions is complete when the Faraday box is able to collect the full initial

* To facilitate this adjustment slit (2) is made wide enough to permit a considerable range of beam curvatures for a given setting of (1), (2) and (3).

beam for 0° position of gun. When both these conditions are realized, the radius of the electron path as determined by the drawer position,* x, should equal the value of the radius conditioned by field, H, and electron energy, V_A. The apparatus is now ready for elastic collision study.

Inelastic collisions may be studied in either of two ways. In the first way the gun is fixed at a definite θ (with proper i for a given V_A) and x is decreased. In this way one will find the elastic peak and also the inelastic peaks. Resetting the drawer at a peak position and rotating the gun the angular distribution for electrons of the selected energy may then be obtained. The second and simpler method is to calculate the position of the drawer for a given energy loss and with drawer so set to vary the angle of scattering. To get fair resolution as one varies x for any fixed θ the retarding potential between (6) and (7) is best adjusted to be two or three volts less than $V_A - V_C$, where V_C is the energy loss in collision. The value of θ for inelastic collisions must be corrected by adding the angle between the line (4)–(6) for the elastic and inelastic settings of (6).

The usual tests for correct operation are applicable here: (1) at very low gas pressures no scattered beams should be found; (2) the collected currents should vary linearly with pressure; (3) the collected currents should have the expected energies when retarding potentials are applied, and (4) the collected currents should vary directly with the current in the initial beam.

Calculations and Curves

The second column in Table II gives for the dimensions in Table I, the graphically determined "dispersion factor," when $R_i = R$ (elastic case). It is found that under these conditions, if one varies s_1, holding s_2 constant, the values in Table II are independent of s_1. The factors for extreme θ's, however, depend greatly on s_2. For the case where $s_2 = 1$ mm instead of 0.4 mm the maximum value at 180° becomes 7.9 while the minimum at about 90° remains unchanged.

In the third column of Table II are the corresponding values of csc θ, dispersion factor of Dymond method. The cosecant term of the Dymond method corrects only for the change in path length of the initial beam which contributes to the scattered current. The value of $\bar{\omega}$ is assumed to be constant for all angles of scattering. However near the limiting case at 180° and near 0° ω may vary widely within the scattering region, and, as yet, no one using this method for large angle scattering (above 165°) has derived a sufficiently accurate value of $\bar{\omega} \cdot L$ to justify his results. The new method gives lower values for $S(\theta)$ in the border region from 150°–172° than those previously reported.

Table II. *Dispersion factors.*

θ	Gagge $[L, W]$	Dymond csc θ	θ	Gagge $[L, W]$	Dymond 2 csc θ
10°	4.68	5.76	100°	1.72	2.04
15°	3.58	3.86	105°	1.80	2.08
20°	2.90	2.92	110°	1.94	2.12
25°	2.40	2.37	115°	2.00	2.20
30°	2.00	2.00	120°	2.18	2.30
35°	1.70	1.74	125°	2.30	2.44
40°	1.50	1.56	130°	2.45	2.62
45°	1.40	1.41	135°	2.60	2.82
50°	1.30	1.31	140°	2.90	3.12
55°	1.20	1.22	145°	3.35	3.48
60°	1.15	1.15	150°	3.90	4.00
65°	1.10	1.10	155°	4.70	4.74
70°	1.05	1.06	160°	6.10	5.84
75°	1.04	1.04	165°	7.7	7.72
80°	1.02	1.02	170°	9.3	11.52
85°	1.00	1.00	175°	10.3	22.94
90°	1.00	1.00	180°	10.6	∞
95°	1.00	1.00			

As an illustration of the results to be expected of the magnetic deflection method, curves are presented in Fig. 5 for elastic scattering in mercury at two electron energies as shown. These two curves are compared with the corresponding curves taken from the recent paper of Jordan and Brode.[3] For the 80 volt curves the two are adjusted to agree at 80°. For the 30 volt curves they are made to fit at 165° to show what disagreement results at smaller angles. It will be noted that the magnetic deflection method reveals a new maximum in the very large angle scattering for these energies.*

* Use is made of the condition $R = (D^2 + x^2)^{\frac{1}{2}}$, or (4), (5) and (6) form a right triangle.

[3] E. B. Jordan and R. B. Brode, Phys. Rev. **43**, 112–115 (1933). In this paper their 80 volt curve is compared with earlier data of Arnot[4] and Tate and Palmer.[5]

* Preliminary curves for scattering in helium and argon do not show any maxima near 180°.

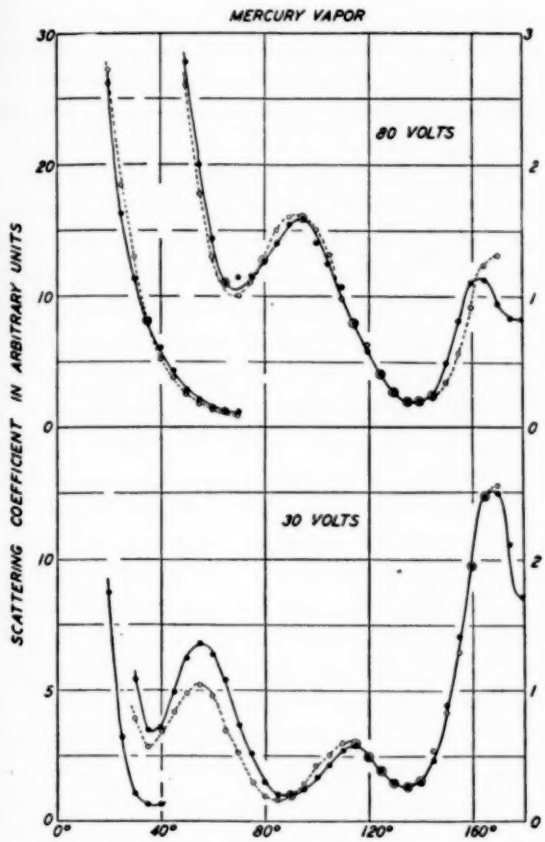

FIG. 5. $S(\theta)$ for 80 volt and 30 volt electrons. The ordinate scales of the two curves are unrelated. Circles, Jordan and Brode; black dots, Gagge.

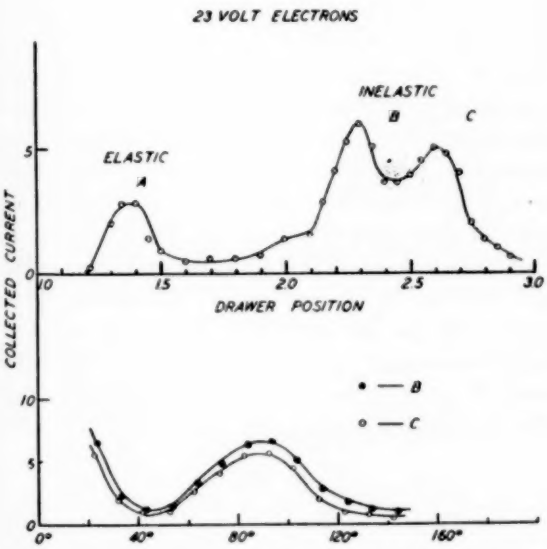

FIG. 6. Analysis of 23 volt electrons scattered in mercury vapor. B—4.9 volt loss $^1S_0-{}^3P_1$; C—6.7 volt loss $^1S_0-{}^1P_1$.

The course of $S(\theta)$ depends upon the values used for the "dispersion factors" (Fig. 5). The absolute values of the scattering coefficient depend also upon the remaining terms in Eq. (4). As an example, the value of $S(80°)$ for 80-volt electrons will be calculated. Using the following data in conjunction with Table I,

$$I_{80°} = -4.9\times10^{-14} \text{ amp.}$$
$$I_0 = -3.1\times10^{-7} \text{ amp.}$$
$$\text{pressure} = 1.2\times10^{-3} \text{ mm Hg}$$
$$\text{dispersion factor } 80° = 1.02,$$

one finds $S(80°)$ for 1 mm Hg to be 0.27. The absolute values found by other investigators for this particular point are

Jordan and Brode[3*]	0.14
Arnot[4]	0.43
Tate and Palmer[5]	1.00

This comparison emphasizes the difficulty of getting absolute values.

Fig. 6 gives some results for inelastic scattering in mercury vapor. In the top curve the gun is set at $\theta° = 80°$, and the collected current is plotted against the drawer position, x. In the lower curve by repeating this value for several values of θ the maximum currents for inelastic scattering are plotted against θ.

DISCUSSION

Certain limitations of the new method as here applied may be mentioned. The maximum electron-energy which can be studied depends on the maximum field the Helmholtz coils can produce. For the inelastic collisions the fractional loss of energy $(V_A - V_C/V_A)$ is the important factor. The smallest fraccional loss that may be studied is 1/7. For small relative losses, x (inelastic) is nearly equal to x (elastic), and the inelastically scattered current may be increased by the presence of electrons of full energy. For fractional losses greater than three-quarters the method runs into geometrical limitations. Perhaps the most doubtful point is the graphical

* Inferred from a statement in their paper that their scattered currents were approximately one-third of Arnot's for similar initial conditions.

[4] F. L. Arnot, Proc. Roy. Soc. **A130**, 665–667 (1930–31).

[5] J. T. Tate and R. R. Palmer, Phys. Rev. **40**, 731–748 (1932).

calculation of the divergence factor in Eq. (9), but in the region from 15° to 150° results are easily as reliable as the corresponding values in the Dymond method. Between 150° and 170° the uncertainty increases but at 180° the graphical method is again as exact as in the 15° to 150° range. Therefore it is believed that values of $S(\theta)$ are significant in the whole range covered by the apparatus and are more reliable in the large angle range than those hitherto obtained by the Dymond method.

The method analyzes inelastically scattered electrons without appreciably altering their characteristics. In addition the system is ideally suitable for analyzing electrons of low energy without introducing an electrostatic accelerating or decelerating field near the supposed field free scattering region.

The author wishes to express his appreciation for the encouragement and generous advice given him throughout this work by Professor John Zeleny, and he is also indebted to Professor L. W. McKeehan for valuable suggestions in the design of the apparatus. Finally, the author is indebted to the Charles A. Coffin Foundation for a fellowship that made this work possible.

Zeeman Effect and Uncoupling Phenomena in the CaH Bands

W. P. CUNNINGHAM AND WILLIAM W. WATSON, *Sloane Physics Laboratory, Yale University*

(Received August 18, 1933)

The effect of the strong l-uncoupling in the $^2\Pi$ state on the Zeeman patterns of the lines of the $^2\Pi \rightarrow {}^2\Sigma$ CaH band at 7000A is discussed.

AMONG the large number of diatomic molecules whose known electronic states exhibit through their spin and Λ-doublings various degrees of spin and l-uncoupling the CaH molecule is a prime example. It has been shown[1] that the upper $^2\Pi$ state of the 7000A band and the upper $^2\Sigma$ state of the 6389A band of CaH stand in a relation of "pure precession" with each other. That is, these two states share the same l, and differ only in that $\lambda = 1$ for the $^2\Pi$ state and $\lambda = 0$ for the $^2\Sigma$. Strong uncoupling of both the l and the spin from the internuclear axis occurs in this $^2\Pi$ state, so that at $K = 33$ the component of l in the direction of the rotational axis of the molecule is about 0.25. The effect of this large uncoupling on the Zeeman patterns of the lines in both of these band spectra has already been discussed.[2, 3] In particular, the details of the Zeeman patterns for the higher rotational lines of the $^2\Sigma \rightarrow {}^2\Sigma$ band were examined with consideration of the energy of interaction of this perpendicular component of l with the applied magnetic field. Since the uncoupling relations between these CaH states form an exaggerated example of relations that exist generally between the electronic states of all molecules, the completion of this discussion with a brief quantitative analysis of the Zeeman effect data for the $^2\Pi \rightarrow {}^2\Sigma$ band is desirable.

Of the two kinds of levels, $^2\Pi_e$ and $^2\Pi_d$, which constitute the $^2\Pi$ state, only the $^2\Pi_d$ levels display large spin doubling due to l-uncoupling. In fact, this doubling in the $^2\Pi_d$ sublevels is practically identical with the spin doubling in the interacting $^2\Sigma$ level, whereas in the $^2\Pi_e$ levels it is almost negligible. Therefore it is to be expected that for the Q branch lines, which originate in the c sublevels of the $^2\Pi$ state, the Zeeman patterns even for quite large values of K should be those given by Hill's[4] treatments of the Zeeman effect in $^2\Pi$ and $^2\Sigma$ states. For the P and R branch lines, however, which involve the $^2\Pi_d$ levels, the effect on the Zeeman patterns of the magnetic energy due to the interaction of the perpendicular component of l and the applied field should be appreciable.

We first calculate the magnetic energy levels of extreme M value as a function of K with the aid of Hill's equations which give the perturbing effect of the field on $^2\Pi$ levels intermediate between case a and case b for spin uncoupling. Then the positions of these levels are corrected by the addition of the energy $\rho \times \Delta\nu_n$, where ρ is the component of l in the direction of K and $\Delta\nu_n$ is the normal Zeeman displacement. The details of these calculations need not be given here as they are quite similar to those outlined in reference 3. From the resulting energy level diagram the outlines of the broad blocks of unresolved components forming the Zeeman patterns of the band lines are, with due regard for the selection rules governing the various transitions, computed.

The comparison of the Zeeman patterns thus calculated with some of the measurements on the spectrograms of the 7000A CaH band with $H = 18{,}200$ gauss is made in the accompanying diagrams. On the scale of abscissae 0 gives the position of the no-field line, + indicates shifts to higher frequencies, − to lower frequencies. The

[1] R. S. Mulliken and A. Christy, Phys. Rev. **38**, 87 (1931).

[2] W. W. Watson and W. Bender, Phys. Rev. **35**, 1513 (1930).

[3] W. W. Watson, Phys. Rev. **39**, 278 (1932).

[4] E. L. Hill, Phys. Rev. **34**, 1507 (1929).

solid curving lines indicate the extreme transitions, as calculated from Hill's formulas, which define the two groups of unresolved components making up the Zeeman pattern of every line in such band spectra. The dotted line in the middle of each group gives the $M'=M''=0$ transition, while the dashed lines in the R_1 and R_2 groups indicate the predicted pattern outlines when the additional $\rho\times\Delta\nu_n$ energy is included. It is assumed that the orientation of ρ parallel to K corresponds to the F_1 levels, the anti-parallel orientation to the F_2 levels. This added magnetic energy has the effect of broadening the patterns of the R_1 lines and narrowing those of the R_2 lines.

The extent of the observed groups of Zeeman components is given by the horizontal solid lines at the appropriate K'' levels. More complete measurements are prohibited by the many instances of overlapping patterns. Also one can see the broader and consequently weaker group of components for many of the lines, but the exact determination of the limits of such "blurs" on the spectrograms is impossible. The observations that are given in Figs. 1 to 4, however, are definite and unambiguous. They indicate clearly the presence of the additional magnetic energy due to the coupling of ρ and the field for the R branch lines, whereas the limits of the groups of components for the Q lines are given within experimental error by the uncorrected predictions from Hill's equations. In the R_2 patterns there is a curious crossing-over of the extreme components of the narrower group at about $K=25$. This $+$ group for these higher R_2 lines consequently becomes a narrow intense line, the observed position of which is indicated by the small circles.

Equally good quantitative explanation is in the same way given for the striking differences

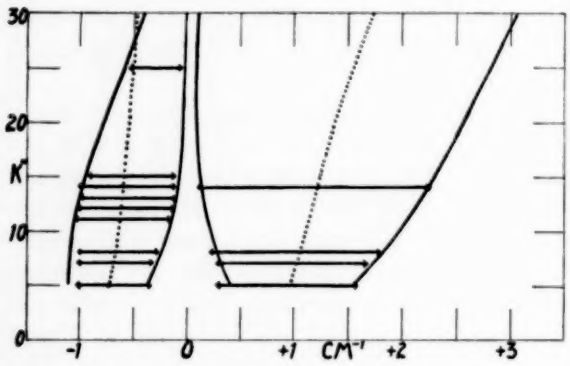

FIG. 1. Zeeman effect patterns of Q_1 lines. $^2\Pi\rightarrow{}^2\Sigma$ CaH band.

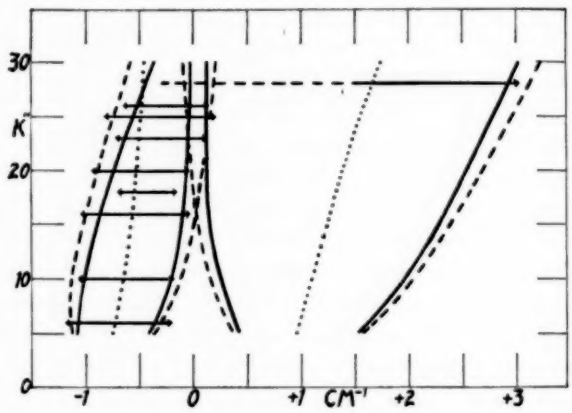

FIG. 3. Zeeman patterns of R_1 lines.

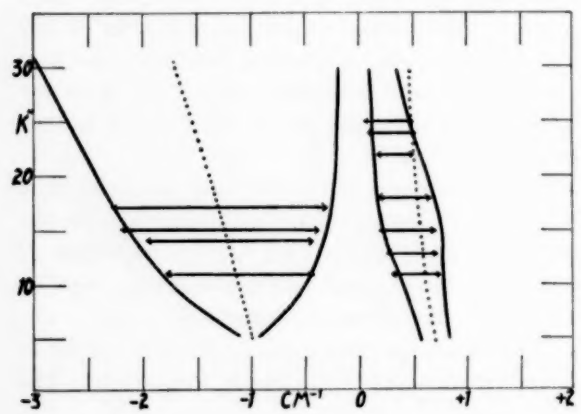

FIG. 2. Zeeman patterns of Q_2 lines.

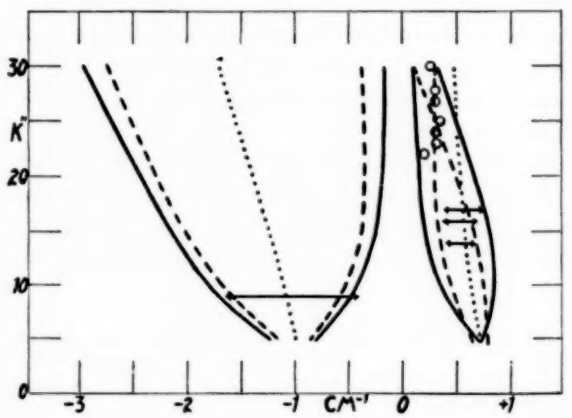

FIG. 4. Zeeman patterns of R_2 lines.

in the patterns of the P_1 and P_2 branch lines for the higher rotational levels.[5] The broad groups of components in the patterns for the P_1 lines are as predicted by the overlapping of the two groups of components in our Fig. 3 for the corresponding R_1 lines. This fusion of the two groups would not occur were it not for the magnetic energy associated with the l-uncoupling. Similarly the shifts of the narrow groups of + components of the higher P_2 lines are accurately given by calculations such as those here shown for the R_2 lines arising from the same levels.

[5] Cf. reference 2, Fig. 3A and Table IV. Note, for example, the $K' = 24$ doublet in this figure.

Limitations of the Theory of Complex Spectra

H. H. MARVIN, *University of Nebraska*

(Received September 6, 1933)

The theory of two-electron systems is extended to include d^9p and d^9d, and comparison is made with experimental data for the $3d^94p$ and $3d^94d$ configurations of Ni I. Greater discrepancies appear here than in d^9s or p^5p, but the multiplets are placed in the correct order. Though the neglected interactions are important, yet the values obtained for the parameters of the largest interactions seem not to be seriously disturbed.

THE theory of two-electron systems, developed by Houston,[1] Slater,[2] Johnson[3] and others, takes into account the electrostatic interaction of the electrons and the magnetic interaction of the spin of each one with its own orbit, but neglects their mutual magnetic interactions. It accounts for the arrangement of the spectral terms of electron configurations such as ps and ds, though with errors which are in some instances several percent of the intervals between neighboring terms. It is less successful in dealing with configurations which do not have one electron in the s state, failing in some cases to place the terms in the correct order. It is most successful in configurations p^5s and d^9s, the errors in the term values seldom amounting to more than one percent. The almost closed shells p^5 and d^9 act in a sense like single electrons, merely inverting and rearranging the multiplets.

Inglis and Ginsburg[4] have found that the theory places the terms in the correct order in the $2p^53p$ configuration of neon. The errors in term values, relative to the separation of adjacent terms, are considerably larger than in p^5s configurations. Thus, the situation is more favorable than in pp, but less so than in p^5s. These authors suggest that the neglected interelectronic magnetic interactions become more important with increasing complexity of the configuration. The spin-orbit interaction of an electron in a p^5 shell is large because the effective nuclear charge is great, while this interaction is zero for an s electron. This accounts for the fact that the theory is more successful with p^5s than with ps. The spin-orbit interaction of the outer electron in p^5p is likely to be of the same order of magnitude as the neglected magnetic interactions. This accounts for the larger relative errors encountered in fitting this configuration.

The arc spectrum of nickel affords an opportunity to study the limitations of the theory of two-electron systems in a closely related group of configurations, $3d^94s$, $3d^94p$ and $3d^94d$, each of which has one electron outside of a d^9 shell. Term values given by Russell,[5] and g-factors for the Zeeman effect determined by Marvin and Baragar[6] are available for comparison.

The latter authors have shown that Houston's formulae[1] for the ds system fit the $3d^94s$ configuration of nickel very well. The parameters in the formulae have the values $X=-7.868$[7] and $\gamma=-301.6$. Introducing Slater's notation for the electrostatic interaction of the electrons, the triplet-singlet interval is ${}^1D-{}^3D=(2/5)G^2(32;40)=X\gamma=2373$. The value of the interaction integral is $G^2=5933$. The parameter of the magnetic spin-orbit energy of a $3d$ electron is, in Johnson's notation,[3] $a=2\gamma=-603.2$.

Johnson[8] has given expressions for the electrostatic energies of the multiplets of d^9p. These, referred to ${}^3P$ as zero, are

$$
\begin{aligned}
&{}^1F\colon\ 5F_2+90G_3=\alpha, && {}^3F\colon\ 5F_2=\beta,\\
&{}^1D\colon\ 14F_2=(14/5)\beta, && {}^3D\colon\ 14F_2=(14/5)\beta,\\
&{}^1P\colon\ 20G_1=\gamma, && {}^3P\colon\ 0.
\end{aligned}
$$

[1] Houston, Phys. Rev. **33**, 297 (1929).
[2] Slater, Phys. Rev. **34**, 1293 (1929).
[3] Johnson, Phys. Rev. **38**, 1628 (1931).
[4] Inglis and Ginsburg, Phys. Rev. **43**, 194 (1933).
[5] Russell, Phys. Rev. **34**, 821 (1929).
[6] Marvin and Baragar, Phys. Rev. **43**, 973 (1933).
[7] The value of X in reference 6 is in error. The values of a^3D_2 and a^1D_2 are 873 and 3417, instead of 872 and 3402.
[8] Johnson, Phys. Rev. **43**, 632 (1933).

The magnetic energy matrix for dp, given by Johnson,[3] which is valid for d^9p also, can be referred to $^3P_0$ as zero by adding $\frac{1}{2}(3a_1-a_2)$ to each diagonal term. Then by adding the electrostatic energies to the diagonal terms and setting the determinant of the matrix equal to zero the secular equations for d^9p are obtained.

The adjustment of the five parameters α, β, γ, a_1 and a_2 to fit the secular equations to the $3d^94p$ configuration of nickel was extraordinarily difficult. The procedure finally adopted was to balance the deviations of the individual terms from their empirical values, departing as little as possible from the sums of terms with the same J. The values $\alpha=615.7$, $\beta=391.3$, $\gamma=3090.7$, $a_1=-516.5$ and $a_2=50$ were adopted, after many trials. Thus, $F_2=78.28$, $G_1=154.54$ and $G_3=2.493$. Slater's interaction integrals are $F^2=35F_2=3728$, $G^1=15G_1=2317$ and $G^3=245G_3=610.8$. The solutions of the secular equations with these parameters are given in Table I, together with the g-factors calculated by the method described at the end of this paper.

The electrostatic energies of the multiplets of d^9d, given by Johnson,[5] are, when referred to ^3G,

$$^1G: 140G_4=\alpha,$$
$$^1F: 12F_2+10F_4=\beta,$$
$$^1D: 7F_2-35F_4+28G_2=\delta,$$
$$^1P-3F_2+85F_4=\epsilon,$$
$$^1S: -10F_2-125F_4+10G_0=\kappa,$$
$$^3G: 0,$$
$$^3F: 12F_2+10F_4=\beta,$$
$$^3D: 7F_2-35F_4=\gamma,$$
$$^3P: -3F_2+85F_4=\epsilon,$$
$$^3S: -10F_2-125F_4=\iota.$$

The magnetic energy matrix for dd, given by Johnson,[3] which is valid for d^9d, can be referred to $^3G_5$ by subtracting a_1+a_2 from each diagonal term. The secular equations are formed in the manner already described.

The adjustment of the parameters to fit the secular equations to the $3d^94d$ configuration of nickel was not especially difficult. No combination could be found which would bring $^3P_0$ and $^1S_0$ near enough to each other. The adjustment was made so that the sum of terms with each value of J is equal to the sum of the empirical terms. The values $\alpha=44.70$, $\beta=244.3$, $\gamma=74.34$, $\delta=139.2$, $\epsilon=83.04$, $\iota=-398.5$, $\kappa=1881.9$, $a_1=-590$ and $a_2=10$ were adopted. Thus, $F_2=18.97$, $F_4=1.67$, $G_0=228.04$, $G_2=2.32$ and $G_4=0.32$. Slater's interaction integrals are $F^2=49F_2=929.5$, $F^4=441F_4=736.5$, $G^0=G_0=228.0$ $G^2=49G_2=113.7$ and $G^4=441G_4=141.1$. The solutions of the secular equations with these parameters are given in Table II, together with the calculated g-factors.

The multiplets are placed in the correct order in $3d^94p$, and in $3d^94d$ with one exception. The errors in the term values are large, however, indicating that the energy of the neglected interactions is greater than the magnetic spin-orbit energy of the outer electron. The parameter of the spin-orbit interaction of the $3d$ electron is

TABLE I. *Energy levels and g-factors for Ni, $3d^94p$.*

Term	W(cm^{-1}) obs.[5]	W(cm^{-1}) calc.	g obs.[6]	g calc.
$z^3F_4^0$	29481	29292	1.28	1.250
$z^3F_3^0$	29321	29344	1.08	1.051
$z^3F_2^0$	30619	30613	0.72	0.841
$z^3D_3^0$	29669	29924	1.31	1.274
$z^3D_2^0$	29888	29872	1.04	1.041
$z^3D_1^0$	30913	31142	0.54	0.557
$z^3P_2^0$	28569	28920	1.46	1.426
$z^3P_1^0$	29501	29642	1.45	1.443
$z^3P_0^0$	30192	30192	0/0	0/0
$z^1F_3^0$	31031	30754	1.02	1.093
$z^1D_2^0$	31442	31213	1.02	1.024
$z^1P_1^0$	32982	32621	1.00	1.002

TABLE II. *Energy levels and g-factors for Ni, $3d^94d$.*

Term	W(cm^{-1}) obs.[5]	W(cm^{-1}) calc.	g obs.[6]	g calc.
e^3G_5	49158	49158	1.20	1.200
e^3G_4	49175	49159	1.05	1.023
e^3G_3	50678	50646	0.77	0.769
e^3F_4	49333	49374	—	1.218
e^3F_3	49314	49352	—	0.993
e^3F_2	50834	50981	—	0.934
f^3D_3	49271	49258	1.32	1.289
f^3D_2	49328	49338	—	1.128
f^3D_1	50717	50732	—	0.719
e^3P_2	49159	49209	1.43	1.279
e^3P_1	49171	49236	—	1.159
e^3P_0	50276	49830	—	0/0
e^3S_1	48953	48898	1.92	1.809
e^1G_4	50706	50680	1.02*	1.056
e^1F_3	50832	50840	—	1.105
f^1D_2	50754	50546	—	0.997
e^1P_1	50537	50507	—	1.338
e^1S_0	51457	51900	—	0/0

* Value not less than that given.

determined with fair accuracy. Its value is $a=-603.2$ for $3d^9 4s$ which is not perturbed by any other configuration, and $a_1=-590$ for $3d^9 4d$ which is not subjected to strong perturbation. This agrees with the value obtained from the $3d^9$ configuration of Ni II. The doublet interval here is $5/2a_1=-1506.9$, from which $a_1=-602.8$. In view of the excellent agreement of these values of the parameter it is probable that the low value $a_1=-516.5$ in $3d^9 4p$ is connected with the strong perturbation of this configuration by the quintets of $d^8 s(^4F)\cdot 4p$.

The discrepancies between observed and calculated g-factors are about as large as those which Inglis and Ginsburg found in Ne, $2p^5 3p$. The deviations are somewhat larger in $3d^9 4d$ than in $3d^9 4p$.

It is evident that exact results cannot be expected from the theory in its present state in any but the simplest configurations. Nevertheless, the parameters of the larger electrostatic and magnetic interactions of the electrons in shells which contain a considerable number may be determined accurately enough to be of use in the study of atomic structure.

Calculation of the Zeeman Effect

The formulae for the g-factors in complex configurations are so cumbersome that it is best to leave them in determinant form. The development is according to the same plan, whatever the degree of the secular equation. A single example serves to explain the method.

The secular equation for three energy levels with the same J, such as $^3F_3$, $^1F_3$ and $^3D_3$ in a dp or a $d^9 p$ configuration, may be written

$$\begin{vmatrix} A_1-W & B_{12} & B_{13} \\ B_{12} & A_2-W & B_{23} \\ B_{13} & B_{23} & A_3-W \end{vmatrix}=0. \qquad (1)$$

The first row and column belong to $^3F_3$, the second to $^1F_3$ and the third to $^3D_3$. The A's are functions of the electrostatic and the magnetic parameters; the B's are functions of the magnetic parameters only. The first order Zeeman effect is taken into account by adding $Mg_1\omega$, $Mg_2\omega$ and $Mg_3\omega$, respectively, to the diagonal terms, and replacing W by $W+Mg\omega$. M is the magnetic quantum number, ω is the Larmor precession; g_1, g_2 and g_3 are the Landé g-factors for $^3F_3$, $^1F_3$ and $^3D_3$, respectively, in (LS) coupling, and g is the unknown for intermediate coupling.

The solution of the modified secular equation for g, ignoring products, squares and higher powers of the small terms which represent the Zeeman effect, is

$$g=(g_1U_1+g_2U_2+g_3U_3)/(U_1+U_2+U_3). \qquad (2)$$

U_1, U_2 and U_3 are the first minors of A_1-W, A_2-W, A_3-W, respectively, in the determinant in Eq. (1). The three roots of Eq. (1) are substituted in turn into Eq. (2) to obtain the values of g in intermediate coupling for the three terms.

The method is as readily applied to quadratic or quartic secular equations. The number of rows and columns in the determinant of the energy matrix is equal to the number of spectral terms for which values of g are sought.

New Terms in the Spectra of N III, N IV, N V, O III, O IV, and O V

WILLOUGHBY M. CADY,[1] *California Institute of Technology*

(Received August 10, 1933)

Certain spectrum plates from a new type of discharge have been analyzed. The source was a condensed discharge through air at a pressure of a few microns to a few hundred microns taking place in a quartz tube of about 2 mm bore and 9 cm long. From fifty to five hundred discharges of a large high-tension condenser sufficed for good exposures between λ105 and 796A, and showed known lines of carbon, nitrogen, oxygen and silicon. New lines have been identified, which establish new levels in N V, O IV and O V, and which join for the first time isolated groups of known levels in N III, N IV and O III.

THIS report is concerned with a new violent gaseous discharge, and the spectra that it emits in the extreme ultraviolet.

PART I. THE DISCHARGE

The tube used in this investigation was merely a length of quartz capillary (2 mm bore by 9 cm long) sealed, in the end-on position, about 3 cm from the slit of a vacuum grating spectrograph. One electrode was an aluminum cap waxed over the end of the capillary; the other electrode was the slit assembly of the spectrograph. An adjustable leak admitted air continuously to the capillary. The spectrum was excited by the repeated discharge of a condenser (0.33 or 0.42 μf, charged to a direct potential of some 25 kv) through the tube and a spark-gap in series with it.

The individual flashes were very brilliant, sometimes rupturing the capillary. The quartz was not, in general, much eroded, however, even after several hundred flashes, and the slit remained fairly clean. This discharge has the added advantage of being reproducible in the sense that, under proper conditions, with the flashes evenly spaced a second or two apart, each flash is of the same violence as every other; it is suggested that this property, lacking in the hot spark, may make this source useful for spectrophotometry in the extreme ultraviolet.

PART II. THE PLATES

Plates were obtained with this "flash discharge" at Harvard in the summer of 1932 with the grazing incidence spectrograph previously described[2] and at the University of California at Berkeley in the summer of 1933 with a somewhat similar instrument. Of these, the Harvard plates were the more intense, probably because of a difference in slit-width; fifty flashes (0.33 μf, 25 kv) produced plates of great brilliance, and one exposure of ten flashes gave over one hundred lines. The Harvard spectra extended from λ105 to 335A. Longer wave-lengths were absorbed completely by the residual air in the spectrograph and in the practically discharge-free space between the capillary and the slit; the short-wave limit is interesting in that it is apparently over 100A "harder" than had been reached previously with a gaseous discharge. At Berkeley, one exposure was secured; five hundred flashes (0.42 μf, 25 kv) were used in exposing a plate to the region between λ192 and 796A.

The excitation was evidently very violent in the Harvard discharge, which showed O VI strongly; the inductance of the condenser-spark-capillary circuit was probably less than in the Berkeley circuit. The Berkeley plate showed no O VI, some O V, and strong O IV. The pressure in the capillary was a few tenths of a millimeter at Harvard, and a few microns at Berkeley; accordingly nitrogen, which is provided in part by the flowing air, was more prominent in the former plates.

The spectra observed in the flash discharge were, beside those mentioned in the title, C III, C IV, N II, O II, O VI and Si IV. None of these

[1] National Research Fellow.

[2] Cady, Phys. Rev. **43**, 322 (1933).

six additional spectra was bright. In fact, deliberate attempts to introduce impurities into the Harvard spectra all failed. Unless such attempts can be made to succeed, the use of this type of source will be limited to the spectra of oxygen and nitrogen.

The resolving power was, on all the plates, such as to divide lines about 0.06A apart. The wave-lengths, probably accurate to about 0.02A, were calculated from standards, by using quadratic interpolation and a correction curve. The standards were from an unpublished list of oxygen lines[3] measured by Edlén at Upsala in 1931; (some of these standards are given their series designations for the first time, in Part III, below).

Part III. The Analyses

New data have been secured with the source and plates above described, which pertain to several spectra, as follows: in some cases, N V, O IV, O V, new high terms have been found, which fix ionization potentials; and in the others, N III, N IV, O III, known low terms have been connected by new lines with known high terms. The nitrogen spectra first, and then those of oxygen will be treated in the order of decreasing ionization. In the lists of lines, there is put first the intensity as estimated visually, together with any special remarks (*n*, nebulous; *N*, very nebulous; *B*, blend with another line; *E*, listed among Edlén's standards, from which the wave-length and frequency are copied), next the wave-length and frequency, and finally the series designation. In the term tables, there are written first the configuration and multiplet symbol, then the *J*-value, the absolute term value relative to the first ionization limit, and lastly the fine-structure separations. The values of odd terms are, as usual, italicized.

Nitrogen V

This spectrum was splendidly developed in the Harvard discharge, and its analysis presented no difficulty. The lines as observed are given in Table I. The long *S*, *P*, and *D* series afford independent but concordant determinations of the ionization limit. Table II gives the absolute term values. The terms from $2s\ ^2S$ to $3d\ ^2D$ inclusive are from the work of Edlén and Ericson.[4]

Table I. *Lines of N V.*

Int.	λ(A)	ν(cm⁻¹)	Designation
1	133.941	746,597	$2s\ ^2S_{1/2} - 8p\ ^2P^\circ$
3	136.402	733,127	$2s\ ^2S_{1/2} - 7p\ ^2P^\circ$
3	140.334	712,586	$2s\ ^2S_{1/2} - 6p\ ^2P^\circ$
0*n*	146.769	681,343	$2p\ ^2P^\circ - 10d\ ^2D$
4	147.427	678,302	$2s\ ^2S_{1/2} - 5p\ ^2P^\circ$
2*N*	148.188	674,818	$2p\ ^2P^\circ - 9d\ ^2D$
3*BE*	150.127	666,103	$2p\ ^2P^\circ - 8d\ ^2D$
1	153.124	653,065	$2p\ ^2P_{1/2}{}^\circ - 7d\ ^2D$
1	153.180	652,827	$2p\ ^2P_{3/2}{}^\circ - 7d\ ^2D$
3*N*	158.021	632,827	$2p\ ^2P^\circ - 6d\ ^2D$
6	162.559	615,165	$2s\ ^2S_{1/2} - 4p\ ^2P^\circ$
2	166.868	599,276	$2p\ ^2P_{1/2}{}^\circ - 5d\ ^2D$
2	166.942	599,010	$2p\ ^2P_{3/2}{}^\circ - 5d\ ^2D$
1	168.559	593,264	$2p\ ^2P_{1/2}{}^\circ - 5s\ ^2S_{1/2}$
1	168.618	593,056	$2p\ ^2P_{3/2}{}^\circ - 5s\ ^2S_{1/2}$
7	186.089	537,377	$2p\ ^2P_{1/2}{}^\circ - 4d\ ^2D$
7	186.176	537,126	$2p\ ^2P_{3/2}{}^\circ - 4d\ ^2D$
3	190.172	525,840	$2p\ ^2P_{1/2}{}^\circ - 4s\ ^2S_{1/2}$
5	190.257	525,605	$2p\ ^2P_{3/2}{}^\circ - 4s\ ^2S_{1/2}$
10	209.293	477,799	$2s\ ^2S_{1/2} - 3p\ ^2P^\circ$
9	247.568	403,929	$2p\ ^2P_{1/2}{}^\circ - 3d\ ^2D$
9	247.724	403,675	$2p\ ^2P_{3/2}{}^\circ - 3d\ ^2D$
8	266.197	375,662	$2p\ ^2P_{1/2}{}^\circ - 3s\ ^2S_{1/2}$
8	266.385	375,397	$2p\ ^2P_{3/2}{}^\circ - 3s\ ^2S_{1/2}$

Table II. *Terms of N V.*

Term	J	Term value	
$2s\ ^2S$	1/2	789,700	
$2p\ ^2P^\circ$	1/2	*709,245*	259
	3/2	*708,986*	
$3s\ ^2S$	1/2	333,726	
$3p\ ^2P^\circ$	1/2	*311,921*	75[5]
	3/2	*311,846*	
$3d\ ^2D$	3/2, 5/2	305,319	
$4s\ ^2S$	1/2	183,393	
$4p\ ^2P^\circ$	1/2, 3/2	*174,535*	
$4d\ ^2D$	3/2, 5/2	171,864	
$5s\ ^2S$	1/2	115,956	
$5p\ ^2P^\circ$	1/2, 3/2	*111,398*	
$5d\ ^2D$	3/2, 5/2	109,972	
$6p\ ^2P^\circ$	1/2, 3/2	*77,114*	
$6d\ ^2D$	3/2, 5/2	76,245	
$7p\ ^2P^\circ$	1/2, 3/2	*56,573*	
$7d\ ^2D$	3/2, 5/2	56,170	
$8p\ ^2P^\circ$	1/2, 3/2	*43,103*	
$8d\ ^2D$	3/2, 5/2	——[6]	
$9d\ ^2D$	3/2, 5/2	34,254	
$10d\ ^2D$	3/2, 5/2	27,729	

[3] Cady, reference 2, footnote 11.

[4] Edlén and Ericson, Zeits. f. Physik **64**, 64 (1930).

[5] Calculated from the stellar lines 4604, 4620; Paine, Astrophys. J. **77**, 299 (1933).

[6] The lines $2p$–$8d$ are masked by the O IV standard, ν666,103.

Nitrogen IV

Here the low triplet terms[7] had never been connected to the high triplet terms.[8] This has now been accomplished with the recognition of five lines, displayed in Table III. Table IV gives all known triplet terms.

TABLE III. *Lines of N IV.*

Int.	λ(A)	ν(cm⁻¹)	Designation
3	283.403	352,844	$2s2p\ ^3P_0^\circ - 2s3d\ ^3D_1$
3	283.490	352,746	$2s2p\ ^3P_1^\circ - 2s3d\ ^3D_2$
3	283.580	352,634	$2s2p\ ^3P_2^\circ - 2s3d\ ^3D_3$
1	322.571	310,009	$2s2p\ ^3P_1^\circ - 2s3s\ ^3S_1$
1	322.712	309,874	$2s2p\ ^3P_2^\circ - 2s3s\ ^3S_1$

TABLE IV. *Triplet terms of N IV.*

Term	J	Term value	
$2s2p\ ^3P^\circ$	0	*557,000*	
			68
	1	*556,932*	
			136
	2	*556,796*	
$2p^2\ ^3P$	0	448,670	
			63
	1	448,607	
			132
	2	448,475	
$2s3s\ ^3S$	1	246,930.0	
$2s3p\ ^3P^\circ$	0	*218,242.9*	
			15.8
	1	*218,227.1*	
			35.4
	2	*218,191.7*	
$2s3d\ ^3D$	1	204,168.8	
			3.5
	2	204,165.3	
			8.6
	3	204,156.7	

Nitrogen III

Three faint lines have been found, which probably represent unresolved multiplets connecting the low quartet terms[9] of N III with the higher terms[10] based on N IV $2s2p\ ^3P^\circ$. Table V shows these lines. This identification is supported, in the absence of sufficient resolution to resolve these three multiplets, by the great regularity in the separation of the doublet transition $2s\ ^2 2p - 2s\ ^2 3s$ from the quartet transition $2s2p^2 - 2s2p3s$ along the sequence: C II, N III, O IV. The quartet lines in question were only 444 cm⁻¹ from their predicted position. The term $2s2p3s\ ^4P_{1/2}^\circ$ is 230,365 above $2s2p^2\ ^4P_{1/2}$, as calculated from λ434; this figure, with Freeman's estimate of the absolute value of $2s2p3s\ ^4P_{1/2}^\circ$ as 163,078.3 below N IV $2s2p\ ^3P_0^\circ$, places the ground state $2s2p^2\ ^4P_{1/2}$ of the quartet system at 393,443 below the limit, $2s2p\ ^3P_0^\circ$.

TABLE V. *Lines of N III.*

Int.	λ(A)	ν(cm⁻¹)	Designation
0N	304.828	328,054	$2s2p^2\ ^4P - 2s2p4d\ ^4D^\circ$
2N	362.916	275,546	$2s2p^2\ ^4P - 2s2p3d\ ^4D^\circ$
0	434.057	230,384	$2s2p^2\ ^4P - 2s2p3s\ ^4P^\circ$

Oxygen V

The series limit for the singlet system has now been determined more accurately than before, so that absolute values can now be assigned to the singlet terms as well as to the triplets. The virtue in this relative adjustment of $2s^2\ ^1S_0$ and $2s2p\ ^3P_0^\circ$ lies in the possibility for a more precise estimation of the O IV quartets with respect to O V $2s^2\ ^1S_0$. Table VI is a list of all the O V lines that have been identified in this source. Of the thirty-six new levels in O IV, reported as found, before a recent meeting of the Physical Society,[11] I have abandoned about ten as untrustworthy. Tables VII and VIII give the singlet and triplet terms of O V, all referred to O VI $2s\ ^2S_{1/2}$. Of the terms in Table VII, all are new except those in $2s^2$, $2s2p$, $2p^2$ and $2s3p$; all in Table VIII are new except those in $2s2p$, $2p^2$, $2s3s$, and the series $2snd$. The old terms noted here are due to Bowen and Millikan,[7] to Edlén,[12] and to Bowen as quoted by Bacher and Goudsmit.[13] The very recent and presumably more accurate measurements of Kruger[14] on the separations in a few known multiplets of O V have not been incorporated in the lists for this spectrum.

---

[7] Bowen and Millikan, Phys. Rev. **26**, 150 (1925).
[8] Freeman, Proc. Roy. Soc. **A127**, 330 (1930).
[9] Bowen, Phys. Rev. **29**, 231 (1927).
[10] Freeman, Proc. Roy. Soc. **A121**, 318 (1928).
[11] Cady, Phys. Rev. **44**, 128A (1933).
[12] Edlén, Nature **127**, 744 (1931); Zeits. f. Physik **73**, 476 (1931). Also Paine, Zeits. f. Astrophys. **7**, 1 (1933).
[13] Bacher and Goudsmit, *Atomic Energy States.*
[14] Kruger and Schoupp, Phys. Rev. **44**, 105 (1933).

TABLE VI. *Lines of O V.*

Int.	λ(A)	ν(cm⁻¹)	Designation	Int.	λ(A)	ν(cm⁻¹)	Designation
1	134.424	743,915	$2s^2\ ^1S_0 - 2s4p\ ^1P_1^\circ$	10	202.180	499,609	$2p^2\ ^3P_1 - 2p3d\ ^3P_1^\circ$
5*n*	138.028	724,491	$2s2p\ ^3P^\circ - 2s5d\ ^3D$?	10	202.396	494,081	$2p^2\ ^3P_2 - 2p3d\ ^3P_2^\circ$
3	139.030	719,269	$2s^2\ ^1S_0 - 2p3d\ ^1P_1^\circ$	10	203.810	490,653	$2p^2\ ^3P_1 - 2p3d\ ^3D_2^\circ$
0	139.492	716,887	$2s2p\ ^1P_1^\circ - 2s8d\ ^1D_2$	10	203.904	490,427	$2p^2\ ^3P_2 - 2p3d\ ^3D_3^\circ$
0*n*	142.119	703,636	$2s2p\ ^1P_1^\circ - 2s7d\ ^1D_2$	3	205.108	487,548	$2p^2\ ^1D_2 - 2p3d\ ^1P_1^\circ$
5*n*	144.809	690,565	$2p^2\ ^3P - 2p5d\ ^3D^\circ$	8*E*	207.794	481,246	$2p^2\ ^1D_2 - 2p3d\ ^1D_2^\circ$
3	146.350	683,293	$2s2p\ ^1P_1^\circ - 2s6d\ ^1D_2$	5*E*	215.034	465,043	$2s2p\ ^3P_0^\circ - 2s3s\ ^3S_1$
2*E*	151.452	660,275	$2s2p\ ^3P_0^\circ - 2s4d\ ^3D$	6*E*	215.104	464,891	$2s2p\ ^3P_1^\circ - 2s3s\ ^3S_1$
3*E*	151.488	660,118	$2s2p\ ^3P_1^\circ - 2s4d\ ^3D$	8*E*	215.245	464,587	$2s2p\ ^3P_2^\circ - 2s3s\ ^3S_1$
4*E*	151.551	659,844	$2s2p\ ^3P_2^\circ - 2s4d\ ^3D$	8*E*	216.018	462,924	$2p^2\ ^1D_2 - 2p3d\ ^1F_3^\circ$?
4	153.962	649,511	$2s2p\ ^1P_1^\circ - 2s5d\ ^1D_2$	10*E*	220.352	453,819	$2s2p\ ^1P_1^\circ - 2s3d\ ^1D_2$
2	156.152	640,402	$2s2p\ ^3P_1^\circ - 2s4s\ ^3S_1$	4*E*	227.376	439,800	$2p^2\ ^3P_1 - 2p3s\ ^3P_2^\circ$
2	156.225	640,102	$2s2p\ ^3P_2^\circ - 2s4s\ ^3S_1$	8*E*	227.510	439,541	$2p^2\ ^3P_1 - 2p3s\ ^3P_1^\circ$ $2p^2\ ^3P_2 - 2p3s\ ^3P_2^\circ$
2	158.800	629,723	$2p^2\ ^3P_1 - 2p4d\ ^3P_1^\circ$	4	227.662	439,248	$2p^2\ ^3P_2 - 2p3s\ ^3P_1^\circ$
4	158.911	629,283	$2p^2\ ^3P_2 - 2p4d\ ^3P_2^\circ$	5*E*	231.823	431,364	$2p^2\ ^1S_0 - 2p3d\ ^1P_1^\circ$
6	159.348	627,557	$2p^2\ ^3P - 2p4d\ ^3D^\circ$	4*E*	248.460	402,479	$2s2p\ ^1P_1^\circ - 2s3s\ ^1S_0$
2*E*	164.583	607,596	$2s2p\ ^3P_1^\circ - 2p3p\ ^3P_2$	2	286.440	349,113	$2p^2\ ^1D_2 - 2s3p\ ^1P_1^\circ$
3*E*	164.658	607,319	$2s2p\ ^3P_1^\circ - 2p3p\ ^3P_1$ $2s2p\ ^3P_2^\circ - 2p3p\ ^3P_2$	3	712.668	140,318	$2s3p\ ^1P_1^\circ - 2p3p\ ^1S_0$?
2	164.710	607,123	$2s2p\ ^3P_2^\circ - 2p3p\ ^3P_1$	6*E*	758.676	131,809	$2s2p\ ^3P_1^\circ - 2p^2\ ^3P_2$
5	170.192	587,572	$2s2p\ ^1P_1^\circ - 2s4d\ ^1D_2$	5*E*	759.438	131,676	$2s2p\ ^3P_0^\circ - 2p^2\ ^3P_1$
6*E*	172.168	580,828	$2s^2\ ^1S_0 - 2s3p\ ^1P_1^\circ$	4*E*	760.228	131,540	$2s2p\ ^3P_1^\circ - 2p^2\ ^3P_1$
0	177.191	564,363	$2s2p\ ^1P_1^\circ - 2s4s\ ^1S_0$	7*E*	760.446	131,502	$2s2p\ ^3P_2^\circ - 2p^2\ ^3P_2$
5	177.799	562,433	$2s2p\ ^1P_1^\circ - 2p3p\ ^1S_0$?	5*E*	761.130	131,384	$2s2p\ ^3P_1^\circ - 2p^2\ ^3P_0$
8*E*	185.747	538,367	$2s2p\ ^1P_1^\circ - 2p3p\ ^1P_1$	6*E*	762.002	131,233	$2s2p\ ^3P_2^\circ - 2p^2\ ^3P_1$
4*E*	192.750	518,807	$2s2p\ ^3P_0^\circ - 2s3d\ ^3D$	4	774.537	129,109	$2s2p\ ^1P_1^\circ - 2p^2\ ^1S_0$
5*E*	192.804	518,661	$2s2p\ ^3P_1^\circ - 2s3d\ ^3D$				
6*E*	192.904	518,393	$2s2p\ ^3P_2^\circ - 2s3d\ ^3D$				
10*E*	194.593	513,893	$2s2p\ ^1P_1^\circ - 2p3p\ ^1D_2$				

TABLE VII. *Singlet terms of O V.*

Term	J	Term value	Term	J	Term value	Term	J	Term value
$2s^2\ ^1S$	0	918,800	$2p3p\ ^1D$	2	246,109	$2s4p\ ^1P^\circ$	1	*174,885*
$2s2p\ ^1P^\circ$	1	*760,002*	$2p3d\ ^1F^\circ$	3	*224,154* ?	$2s4d\ ^1D$	2	172,430
$2p^2\ ^1D$	2	687,078	$2p3p\ ^1P$	1	221,635	$2s5d\ ^1D$	2	110,491
^1S	0	630,893	$2p3d\ ^1D^\circ$	2	*205,832*	$2s6d\ ^1D$	2	76,709
$2s3s\ ^1S$	0	357,523	$2p3d\ ^1P^\circ$	1	*199,527*	$2s7d\ ^1D$	2	56,366
$2s3p\ ^1P^\circ$	1	*337,972*	$2p3p\ ^1S$	0	197,633 ?	$2s8d\ ^1D$	2	43,115
$2s3d\ ^1D$	2	306,183	$2s4s\ ^1S$	0	195,639			

TABLE VIII. *Triplet terms of O V.*

Term	J	Term value		Term	J	Term value		Term	J	Term value	
$2s2p\ ^3P^\circ$	0	*836,400*		$2p3p\ ^3P$	0	——		$2p4d\ ^3D^\circ$	2, 3	*76,988*	
			136								
	1	*836,264*			1	228,844		^3P	0	——	
			307				190				
	2	*835,957*			2	228,654			1	*75,001*	
											−171
$2p^2\ ^3P$	0	704,880		$2p3d\ ^3D^\circ$	1, 2, 3	*214,050*			2	*75,172*	
			156								
	1	704,724		$^3P^\circ$	0	——		$2p5d\ ^3D^\circ$	2, 3	*13,980*	
			269								
	2	704,455			1	*210,248*					
							−140				
$2s3s\ ^3S$	1	371,367			2	*210,388*					
$2s3d\ ^3D$	1, 2, 3	317,587		$2s4s\ ^3S$	1	195,855					
$2p3s\ ^3P^\circ$	0	——		$2s4d\ ^3D$	1, 2, 3	176,128					
	1	*265,185*		$2s5d\ ^3D$	1, 2, 3	112,070					
			261								
	2	*264,924*		$2s6d\ ^3D$	1, 2, 3	77,280					

Oxygen IV

I had independently identified the new O IV quartets (connecting known low terms with known high terms), from Edlén's list of standards; Kruger[14] has given a more complete list of these quartets, with which my identifications, as far as they go, agree completely. The diffuse series of O IV doublets has been extended beyond Freeman's[8] $2s^2 3d\ ^2D$, as given in Table IX. The absolute value of the ground state $2s^2 2p\ ^2P_{1/2}{}^\circ$ is thereby set at about 624,200 below O V $2s^2\ ^1S_0$, in good agreement with Freeman's earlier estimate, 623,500.

TABLE IX. *Lines of O IV.*

Int.	λ(A)	ν(cm^{-1})	Designation
0	174.097	574,392	$2s^2\ 2p\ ^2P_{1/2}{}^\circ - 2s^2\ 6d\ ^2D$
1	174.227	573,964	$2s^2\ 2p\ ^2P_{3/2}{}^\circ - 2s^2\ 6d\ ^2D$
2*n*	181.174	551,956	$2s^2\ 2p\ ^2P_{1/2}{}^\circ - 2s^2\ 5d\ ^2D$
2*n*	181.302	551,566	$2s^2\ 2p\ ^2P_{3/2}{}^\circ - 2s^2\ 5d\ ^2D$
3*E*	195.863	510,561	$2s^2\ 2p\ ^2P_{1/2}{}^\circ - 2s^2\ 4d\ ^2D$
4*E*	196.009	510,181	$2s^2\ 2p\ ^2P_{3/2}{}^\circ - 2s^2\ 4d\ ^2D$

In the quartet system of O IV, the absolute value of $2s2p^2\ ^4P_{1/2}$ below O V $2s2p\ ^3P_0{}^\circ$ is about 631,000 (which is about 548,600 below O V $2s^2\ ^1S_0$). This value gives the correct quantum defects, and presents a fairly good check on Slater's theory[15] in $2s2p^2$, although the check is rather poor in $2p^3$.

Several standard lines, listed by Edlén as O IV, remain unidentified. These may belong to transitions between configurations each containing $2s2p$ or $2p^2$, while the third electron jumps from $3s$ to $2p$, $3p$ to $2s$, or $3d$ to $2p$.

Oxygen III

Some of the higher quintet levels in O III have been observed by Mihul,[16] but the quintet ground state was apparently unknown. It is expected that this will be $2s2p^3\ ^5S_2{}^\circ$. Now, the interval between the quintet resonance line $2s2p^3\ ^5S_2{}^\circ - 2s2p^2 3s\ ^5P_3$ and the triplet line $2s^2 2p^2\ ^3P_2 - 2s^2 2p 3s\ ^3P_2{}^\circ$ should be roughly as great as the corresponding interval in N II. On this assumption, we compute from the known lines of N II and O III that the O III resonance radiation should appear near ν277,300. This line and its satellites are obviously represented by the lines of Table X. The separations, 156 and 139, between these lines agree with the known separations, 161.2 and 124.4, of the upper state.

TABLE X. *Lines of O III.*

Int.	λ(A)	ν(cm^{-1})	Designation
4	359.034	278,525	$2s2p^3\ ^5S_2{}^\circ - 2s2p^2\ 3s\ ^5P_3$
3	359.235	278,369	$2s2p^3\ ^5S_2{}^\circ - 2s2p^2\ 3s\ ^5P_2$
2	359.415	278,230	$2s2p^3\ ^5S_2{}^\circ - 2s2p^2\ 3s\ ^5P_1$

It is a pleasure to acknowledge my debt to Professor T. Lyman of Harvard University, under whose sanction the earlier part of this work was carried out; to Professor H. E. White of the University of California in Berkeley, for his permission to use the two-meter spectrograph of his design; to Mr. R. J. Hopkins of that university, for his cooperation in taking the Berkeley plate; and to Professor I. S. Bowen of this Institute, for many illuminating discussions during the course of the analysis.

Note added in proof. After the present report had been submitted for publication, there appeared two very beautiful and complete papers on the same subject, by Edlén.[17] In one of these are extensive wave-length lists, embracing all the standards cited above;[3] the average discrepancy between the published and the unpublished lists is only 0.0017A, which is well within my experimental error. The term analyses proposed here differ nowhere from those of Edlén.

[15] Condon and Shortley, Phys. Rev. **37**, 1025 (1931).

[16] Mihul, Comptes Rendus **184**, 1055 (1927).

[17] Edlén, Zeits. f. Physik **84**, 746 (1933); **85**, 85 (1933).

Standard Copper Wave-Lengths in the Region 100A to 450A

P. GERALD KRUGER AND F. S. COOPER, *Department of Physics, University of Illinois*

(Received August 23, 1933)

The copper spectrum has been photographed in the region 100A to 450A with a twenty-one foot grazing incidence vacuum spectrograph. The wave-length of sharp copper lines (approximately two every Angstrom) have been determined by interpolating between known aluminum and oxygen lines with the formula $\lambda=\lambda_0+Ax+Bx^2+Cx^3\cdots$. A discussion of the errors in the wave-lengths is given.

I. INTRODUCTION

PREVIOUSLY available standard wave-lengths in the region 100–450A consisted of aluminum lines which had been measured by Söderqvist and Edlén.[1] In addition, the authors had an unpublished list of oxygen standards due to B. Edlén. However, there were not a sufficient number of these standards for convenient interpolation when using an instrument of high dispersion. Thus, in order to bridge the gaps in the above lists, the secondary standards listed in Table II were established.

The copper spectrum was chosen because it has a large number of strong, sharp lines well distributed throughout the region. Moreover, the copper spectrum is more easily excited than either oxygen or aluminum.

II. EXPERIMENTAL

The instrument[2] used was a 21-foot grazing incidence vacuum spectrograph which was constructed by the Mann Instrument Company of Cambridge, Massachusetts, and which has dispersions given in Table I. The grating was ruled on glass 30,000 lines per inch by R. W. Wood and H. M. O'Bryan at The Johns Hopkins University.

TABLE I. *Dispersion: Angle of incidence 87°.*

100A	0.215 A/mm
200A	.295
300A	.356
450A	.432

[1] Söderqvist and Edlén, Zeits. f. Physik **69**, 356 (1931).
[2] P. G. Kruger, Rev. Sci. Inst. **4**, 128 (1933).

The electrodes were made of copper, size 1 inch by 1/4 inch diameter, thin copper shells cored with aluminum, and a copper shell packed with an oxide of boron. The latter was used as the lower (positive) electrode with an upper (negative) electrode of solid copper in obtaining the oxygen spectrum. The copper shells on the aluminum electrodes tended to prevent uneven wearing away of the aluminum, and also served to indicate any relative shift of the lines of adjacent aluminum (oxygen) and copper spectra. The vacuum spark was less than a millimeter in length when operated in a vacuum of 10^{-5} mm of Hg or better at a d.c. potential of 100 kv.

III. CALCULATION

Interpolations between the above-mentioned standard oxygen and aluminum lines were made by use of the relation,

$$\lambda=\lambda_0+Ax+Bx^2+Cx^3+\cdots, \qquad (1)$$

where λ_0 is a known standard, x is the distance along the plate from λ_0 to λ (i.e., the difference of the two comparator readings, and hence either positive or negative), and A, B, C are constants.

This relation is derived from the grating equation (where ϕ is the angle of diffraction) by expressing $\sin\phi$ in terms of the radius, R, of the Rowland circle, and the length of arc, X, from the center of the grating to λ_0, plus (or minus) an increment of arc, x, from λ_0 to λ, thus

$$\lambda=e\sin\theta-e\sin\phi$$
$$=e\sin\theta-e\cos[(X+x)/2R]. \qquad (2)$$

The last term may be expanded in terms of two angles, one constant and the other variable. By further expanding cos $(x/2R)$ and sin $(x/2R)$ as power series, and collecting terms in powers of x, the following equation is obtained.

$$\lambda = e\left(\sin\theta - \cos\frac{X}{2R}\right) + \left(\frac{e}{2R}\sin\frac{X}{2R}\right)x + \left(\frac{e}{8R^2}\cos\frac{X}{2R}\right)x^2 + \left(-\frac{e}{48R^3}\sin\frac{X}{2R}\right)x^3 + \cdots, \quad (3)$$

whence, comparing Eq. (1),

$$C = -A/24R^2. \quad (4)$$

The constants A and B for any region are calculated from λ_0 and two other known standards λ_1 and λ_2 lying 6–10 cm distant from, and on opposite sides of, λ_0. This is done by solving the simultaneous equations,

$$\begin{aligned} \lambda_1 - \lambda_0 &= Ax_1 + Bx_1^2, \\ \lambda_2 - \lambda_0 &= Ax_2 + Bx_2^2, \end{aligned} \quad (5)$$

for A and B. For values of x less than 10 cm the value of the term Cx^3 is less than 0.001A.

For larger values of x the cubic term is used. In this case Eqs. (5) become cubic equations, but they may be reduced to equations with one less constant by the use of Eq. (4), and solved as before. That is, Eqs. (5) become

$$\begin{aligned} \lambda_1 - \lambda_0 &= A(x_1 - x_1^3/24R^2) + Bx_1^2, \\ \lambda_2 - \lambda_0 &= A(x_2 - x_2^3/24R^2) + Bx_2^2. \end{aligned} \quad (6)$$

C is then found from Eq. (4) by using the measured value of R which is sufficiently accurate. In dividing the spectrum into these regions, care was taken that a known standard occurred near the middle of the region (λ_0), and that the remainder of the standards were as advantageously distributed as possible for drawing a correction curve.

IV. Discussion

The wave-lengths of the lines were determined by making measurements on three different plates. Four readings were taken per line on each of the three plates so that a total of twelve settings were made on each line.

From these data, the wave-lengths were calculated in the manner outlined in Part III, each separate calculation covering a range of 30–60A. Correction curves were then drawn using all the available primary standards in the region, and the corrections so determined were applied to the calculated wave-lengths. These corrections served to compensate for minor deviations from the formula, and also to smooth out small irregularities within the primary standards. The maximum corrections rarely exceeded 0.07A and were usually much smaller. In selecting the regions for calculation, care was taken to see that the regions from different plates overlapped. Consequently maximum corrections on one set of data coincided with small corrections on another.

The number of standards available for drawing these correction curves was adequate except at long wave-lengths (350–470A). Here there were a few regions where the oxygen standards were so widely spaced that the correction curves may be open to some question. In the region 400–435A, second order copper lines were used to supplement the oxygen lines.

While making the measurements it was noticed that there was a slight shift between the oxygen and copper spectra. This was observable due to the appearance, in the oxygen spectrum, of copper lines from the copper shell of the electrodes, and was probably caused by a temperature change between exposures, though the temperature was kept constant to about ± 0.04°C during a set of exposures.

This shift was measured and found to be positive (add $\Delta\lambda$ shift to correct λ) on one plate, negative by the same amount on the second and negative by a slightly larger amount on the third plate. Since the shift in $\Delta\lambda$ was practically constant for a plate this error was easily corrected by adding or subtracting the proper amount when the averages were taken. Further, the three sets of data were given different weights in various wave-length regions, the weights being determined from the size of the correction curve and its smoothness.

In Table III there are listed various wave-

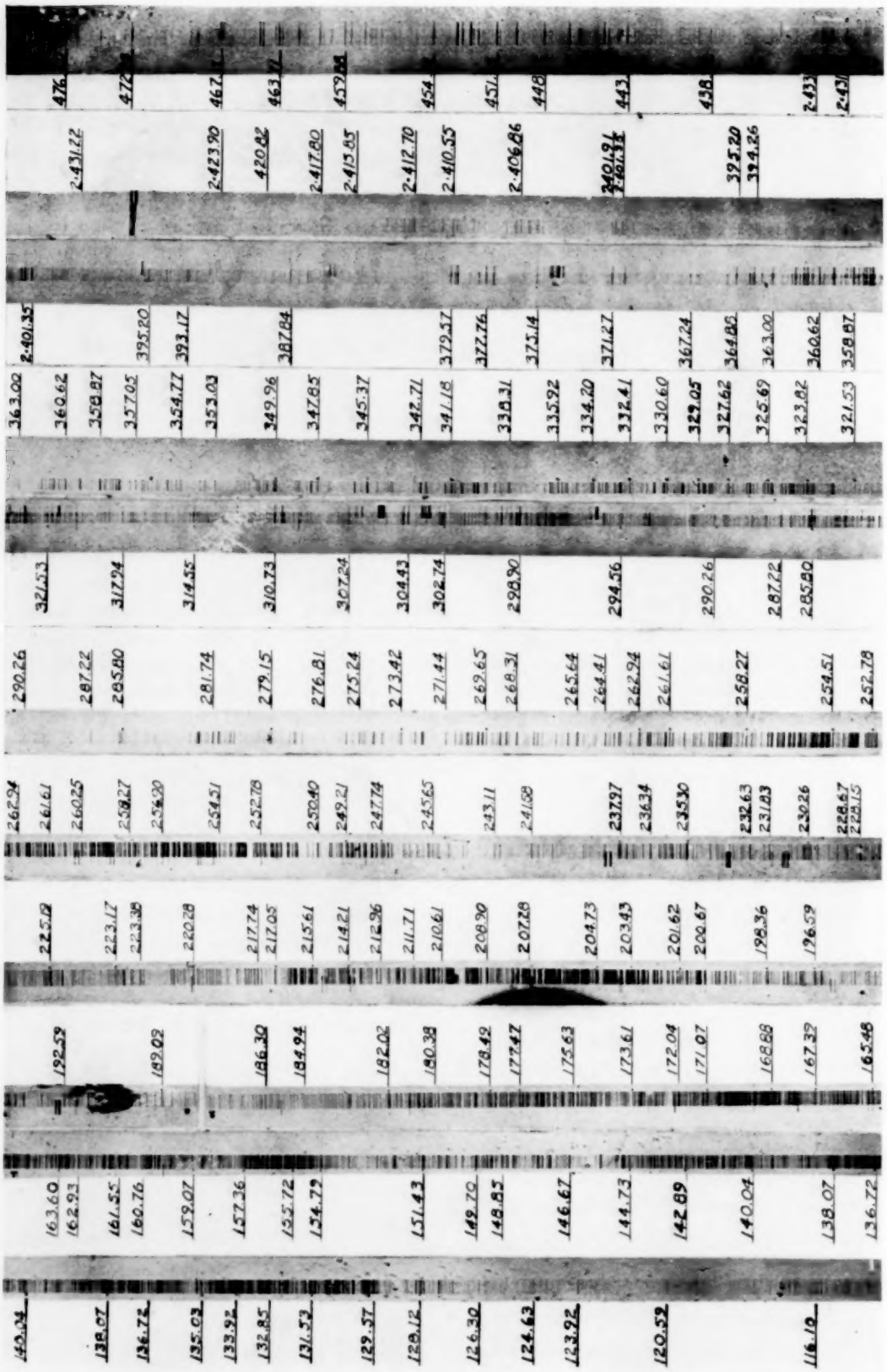

Fig. 1. The copper spectrum with standard lines indicated. Overlapping spectra are due to oxygen, aluminum, and boron.

TABLE II. *Standard wave-lengths of copper lines.*

Int.	λ (vac.)	Int.	λ (vac.)	Int.	λ (vac.)	Int.	λ (vac.)	Int.	λ (vac.)	Int.	λ (vac.)	Int.	λ (vac.)
	A		A		A		A		A		A		A
10	109.123	40	155.136	9	194.357	2	237.406	10	274.269	10	332.405*	4	2–407.148
12	109.215	15	155.718	10	196.363	10	237.969	15	274.601	100	332.893	5	2–407.623*
7	109.818	20	156.153	30	196.585	15	241.583	10	275.244	30	333.562	5	2–407.677*
7	110.637	20	156.557	30	197.128	4	242.882	10	275.829	30	334.204	7	2–409.443*
10	110.741	20	156.847	30	197.598	4	243.108	10	276.805	20	335.016	10	2–410.548
10	111.756	40	157.359	5	198.364	1	244.411	10	277.761	15	335.470	10	2–411.093
12	112.532	15	158.080	7	198.850	2	245.418	20	278.128	25	335.919	8	2–411.210
6	113.120	20	158.702	10	199.723	2	245.653	10	279.150	25	336.279	15	2–412.702
8	113.928	10	159.072	7	200.417	1	246.286	8	280.802	8	336.577*	10	2–413.234
7	114.033	10	159.462	100	200.674	2	246.852	50	281.492	25	338.314	5	2–413.681*
7	115.143	4	159.919	75	200.860	10	247.336	40	281.744	10	339.038*	3	2–413.813*
8	115.766	15	160.530	50	200.958	25	247.742	20	282.440	15	339.420	3	2–414.558*
10	116.099	50	160.763	15	201.329	10	248.153	6	285.798	30	339.887	3	2–415.853*
7	116.229	30	161.551	20	201.615	50	248.426	10	285.873	20	341.183	10	2–417.799
7	117.079	25	161.748	20	202.065	7	248.858	8	287.215	25	341.483	10	2–418.949
15	120.594	20	162.078	60	203.010	20	249.213	0	289.358*	20	342.432*	5	2–419.292*
9	123.286	10	162.651	60	203.432	15	249.415	0	290.259*	80	342.713	5	419.355*
20	124.630	20	162.926	15	204.056	10	249.908	2	291.800*	5	343.059*	5	420.820*
20	126.298	30	163.271	40	204.725	30	250.400	10	293.257*	8	344.075*	3	2–421.876*
20	127.105	25	163.598	60	205.278	4	250.816	3	293.409*	5	344.179*	8	2–422.213*
25	127.444	20	164.259	30	205.610	20	251.278	0	294.094*	8	344.866*	5	2–422.310*
25	128.012	15	164.675	10	205.984	20	251.670	5	294.561*	90	345.368	2	2–423.400*
25	128.123	30	165.127	60	206.355	20	251.947	5	295.350*	60	346.004	3	426.668*
30	128.255	25	165.481	35	206.842	15	252.223	1	295.516*	30	347.854	0	2–428.414*
15	128.523	8	166.023	20	207.282	75	252.780	10	297.057*	15	348.413	10	2–431.215
10	129.398	12	166.308	15	207.733	15	253.083	10	297.647*	30	349.964	1	2–431.349*
40	129.567	10	166.645	35	207.925	15	253.465	5	298.017*	10	350.056	1	2–431.995*
20	129.697	5	166.958	15	208.502	15	253.786	20	298.901*	8	350.421	9	2–432.120*
10	129.890	10	167.392	60	208.902	50	254.510	15	299.217	5	350.824	0	2–432.502*
15	130.438	15	168.111	30	209.241	70	254.772	5	300.074	5	351.538	7	2–432.626*
18	130.671	15	168.423	30	209.648	45	255.214	1	300.823*	15	353.031	4	2–432.899*
20	130.739	30	168.881	15	210.217	35	255.417	1	301.437*	10	353.568	2	2–433.034*
15	131.015	15	169.488	15	210.612	30	256.365	5	302.000*	8	354.771	1	438.929*
15	131.533	15	169.765	50	211.109	40	256.898	8	302.735*	20	355.425	5	443.233
35	131.590	15	170.007	20	211.707	20	257.315	10	304.434	5	355.977*	10	443.666
7	132.149	15	170.645	10	212.339	20	257.626	8	304.656	3	356.643*	3	444.214*
12	132.528	15	171.074	10	212.964	15	258.004	4	307.238	10	357.052	15	444.999*
50	132.848	20	171.215	8	213.617	45	258.265	20	310.380	100	357.897	2	445.391*
40	133.389	40	172.036	20	214.206	4	258.609	15	310.727	90	358.865	10	446.359
40	133.916	5	172.810	10	214.460	80	258.927	20	312.505	50	359.873	25	446.995
60	134.550	10	173.193	10	214.861	20	259.199	9	312.833	30	360.618	25	448.420
20	135.025	5	173.605	50	215.611	20	259.558	2	313.890*	25	361.220	25	450.015
30	135.846	10	173.990	50	216.063	25	259.871	6	314.545	15	361.838	25	451.152
45	136.724	9	174.507	25	216.454	25	260.245	6	315.873*	8	363.003	5	452.223*
40	136.936	8	174.885	8	217.052	25	260.967	4	316.873*	10	363.967	4	452.500*
75	138.074	30	175.484	20	217.743	30	261.606	7	317.937	5	364.876	30	452.654
50	138.115	25	175.633	4	219.227	20	261.806	2	318.763*	9	364.870	20	453.130*
50	140.042	15	176.232	6	219.927	20	262.442	2	319.845*	3	367.238*	40	453.425
30	141.694	10	176.824	6	220.277	30	262.938	5	320.134	10	370.622	10	454.791
20	142.158	20	177.466	4	221.065	8	263.329	5	321.534	10	371.267	5	457.760
60	142.892	10	177.809	15	222.378	30	263.760	15	322.617	5	375.138*	10	458.709
50	143.033	5	178.286	4	222.718	15	264.029	60	323.816	10	377.355	10	459.511
15	143.634	15	178.489	4	223.368	20	264.414	70	324.485	15	377.756	15	459.881
25	144.728	15	179.223	25	225.497	50	265.641	50	324.607	25	379.326	2	460.653
35	145.651	15	179.630	10	225.991	20	266.061	20	325.038	8	379.573	10	461.319
10	145.671	15	180.384	2	226.785	10	266.584	20	325.687	5	386.943*	10	462.545
100	146.669	20	180.986	10	228.146	10	267.203	20	326.575	8	387.841	20	463.712
20	147.544	30	182.019	6	228.667	25	267.562	15	327.383	3	393.172*	20	464.640
80	148.846	8	182.669	8	230.260	60	268.309	20	327.620	3	394.256*	20	464.824
80	149.703	10	183.396	7	230.451	50	268.773	50	328.412	5	395.202*	15	467.106
26	150.662	7	183.705	2	230.928	40	269.044	25	328.536	30	2–401.346	3	468.505
70	151.429	7	184.938	7	231.833	20	269.653	40	328.737	20	2–401.718	2	468.890
8	152.312	15	186.296	8	232.632	30	270.298	20	328.831	10	2–401.913	20	472.342
8	152.348	5	189.085	4	234.256	20	270.740	100	329.047	8	2–405.921	2	472.775
10	152.383	20	191.719	30	235.299	20	271.443	30	329.805	7	2–406.010	2	474.137
15	152.929	7	192.585	4	235.785	15	272.424	30	329.851	8	2–406.369*	2	474.176
8	152.853	7	193.409	5	236.343	10	272.807	5	330.602*	8	406.439	2	475.500
40	154.785	8	194.050	8	236.714	20	273.417	8	331.573*	5	2–406.860	20	476.201

TABLE III. *Reliability of copper wave-lengths.*

Wave-length region	Comments
109–120A	Poor
120–132A	Fair
132–150A	Consistent (probably fair)
150–240A	Good
240–260A	Consistent (from two plates only)
260–290A	Good
290–302A	From one plate only
302–323A	Good (from two plates only)
323–328A	Good
328–345A	Good (from two plates only)
345–371A	Consistent (probably good)
371–432A	Consistent (two plates only)
432–476A	Poor (two plates only)

length regions followed by characterizing words or phases which indicate the error to be expected in that region. Poor means unreliable data to about ± 0.010A. Fair means that an error of ± 0.005A may be expected and good means that the error is about ± 0.003A. Consistent means that the three sets of data agree well but that the absolute value may be open to question. An asterisk has been placed after lines in Table II which were measured on one plate only.

Unfortunately, the grating used throws very little energy into the second order. Thus only the strongest lines appear in the second order (those preceded by a 2 in Table II at about 400A) and it was impossible to check first and second orders completely. Where a check was possible, first and second order lines agree to about ± 0.003A.

Fig. 1 shows several reproductions of spectrograms with appropriate wave-lengths of Table II designated.

The Thermionic Constants for Platinum

H. L. VAN VELZER, *Department of Physics, Pennsylvania State College*

(Received July 24, 1933)

The thermionic constants for platinum in the form of cylindrical filaments were investigated. The slope of the supersaturation curves was taken as a criterion of filament condition. It was found that a very stable state, probably not indicative of a pure surface was obtained which withstood aging at 1650°K for 175 hours. For this condition the ϕ and A values are very high. Aging at 1785°K produced a new surface for which the supersaturation slopes were correct, and for which the constants were assumed to be approaching correct values. If A is taken to be 60 amp./cm²·deg.², ϕ is estimated to be 5.29 volts.

INTRODUCTION

THERMIONIC emission of platinum has been the subject of numerous investigations.[1] The most recent and significant has been that of DuBridge[2] who was able to check the thermionic with the photoelectric work function. His best values are: $\phi = 6.27$ volts and $A = 1.7 \times 10^4$ amp./cm²·deg.². The present paper deals with an attempt to evaluate these constants by an independent method.

Some earlier work[3] with tungsten has shown the adaptability of Schottky curves for indicating filament conditions. For constant temperatures ln I plotted against $(dv/dx)^{\frac{1}{2}}$ should, in the supersaturation region, give straight lines having a slope of $e^{\frac{1}{2}}/kT$. Unless the filament was in excellent condition these curves were very erratic; but a value of e correct to 0.2 percent was obtained under conditions where the curves were smooth straight lines. Similar experiments applied to platinum are described below. This method does not lend itself to photoelectric measurements, but possesses the advantage that cylindrical filaments may be used instead of strips. These withstand aging at much higher temperatures because of their smaller area and the reduced effect of local heating.

TUBES

The filaments used were wires of 5, 7 or 10 mil diameter and were of the purest platinum obtainable from Baker and Company, Newark, N. J. The manufacturers state that there are generally present spectroscopic traces of iron, magnesium and calcium. Anodes and guard rings were of 5 mil nickel. The tubes were of two types as shown in Fig. 1. Both are satisfactory but the type at the left is subject to the disadvantage that the tungsten spring may become permanently extended during bakeout, thus allowing the filament to become eccentric. However, the resultant change in gradient may be calculated, and is quite small.

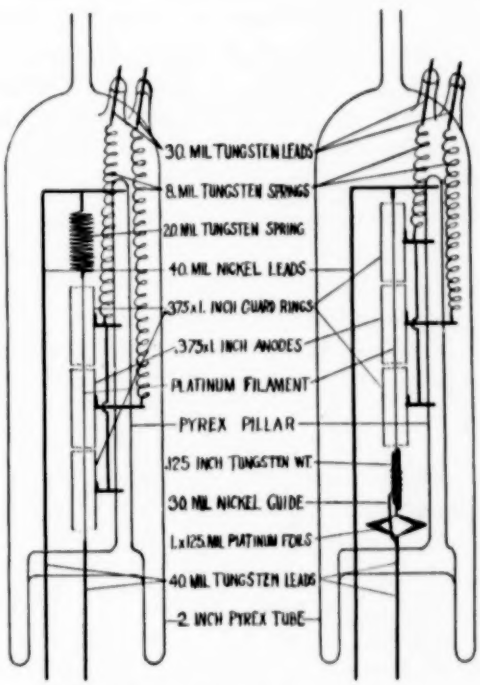
30 MIL TUNGSTEN LEADS
8 MIL TUNGSTEN SPRINGS
20 MIL TUNGSTEN SPRING
40 MIL NICKEL LEADS
.375 x .1 INCH GUARD RINGS
.375 x .1 INCH ANODES
PLATINUM FILAMENT
PYREX PILLAR
.125 INCH TUNGSTEN WT.
30 MIL NICKEL GUIDE
1 x .125 MIL PLATINUM FOILS
40 MIL TUNGSTEN LEADS
2 INCH PYREX TUBE

FIG. 1. Diagram of tube.

[1] Dushman, Rev. Mod. Phys. **2**, 396 (1930).
[2] DuBridge, Phys. Rev. **31**, 736 (1928); **32**, 961 (1928).
[3] Van Velzer and Ham, Phys. Rev. **33**, 1081 (1929).

Charcoal was used with liquid air on all tubes during operation and in some, magnesium was flashed into an auxiliary bulb immediately before beginning runs. The presence of charcoal bulbs necessitated a long bakeout. This was continued at temperatures of from 450 to 490°C for from 200 to 600 hours, after which the pressure with ovens on was between 10^{-4} and 10^{-5} mm of Hg. Liquid air was introduced around a trap on the system before the end of the bakeout. After baking, the metal parts were heated by a high frequency current and the filament was flashed at about 1750°C, in some cases for several hours. The pressure was now about 10^{-7} mm of Hg. Immediately after seal-off all of the joints were coated with Canada Balsam as a precautionary measure.

No attempt was made to measure the pressure in the tubes after removal from the pumps; but tungsten filament tubes of similar design and exhaust have been so tested by connecting their elements in an ionization gauge circuit with anode as plate and guard rings as collectors, the usual voltages being employed. This arrangement has been found to be about six times as sensitive as the usual design, but after liquid air had been placed around the charcoal for several hours (required for temperature equilibrium) the positive ion currents were less than 10^{-9} ampere.

The circuit diagram is shown in Fig. 2. The anode circuit includes, in series, a calibrated resistor of from 10^6 to 10^9 ohms. The potential across this was determined with a Compton electrometer set at a stable value of about 340 mm/volt.

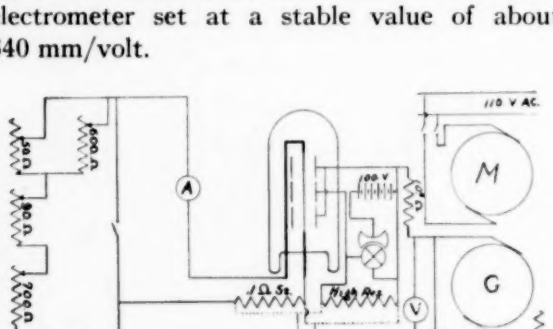

FIG. 2. Circuit diagram.

TEMPERATURE SCALE

The determinations made were based on the temperature current relations given for tungsten by Langmuir and Jones.[4] Emissivities were corrected from the data of Forsythe.[5] In all cases crossed or nearby platinum and tungsten filaments were equated in brightness by viewing them through a telescope. Comparisons were made over a range of from roughly 1000°K to 2000°K. The final relation between heating current and absolute temperature is a weighted least square solution obtained from 170 points. In terms of a filament one centimeter in diameter it is expressed as $T=0.44460I+43.220I^{\frac{1}{2}}+315.40$. The probable error in the region investigated is 1.2°C.

PROCEDURE

The charcoal was immersed in liquid air for several hours to attain temperature equilibrium. The filament was then heated to some aging value, usually of from 1650 to 1790°K; and runs were taken each 24 hours. At the beginning of each run the electrometer sensitivity was determined and tests made for electrical leakage. With the filament current held constant by means of the potentiometer, thermionic currents were then measured at anode potentials from 150 to 1250 volts.

RESULTS

As aging progressed, four distinct types of characteristics were noted. At first the currents were large and erratic, usually increasing with time unless the filament temperature was raised above a critical value. The Schottky curve obtained with such filaments is shown in Fig. 3.

Second, there was a rather protracted stage, lasting in one case for 175 hours at an aging temperature between 1650 and 1690°K. This condition is characterized by Schottky slopes of from two to five times the theoretical value, which slopes sometimes increased at first, then decreased. The curves, too were not straight but concave downwards, though in the later runs they tended to straighten. As aging proceeded the consistency of the data increased and the

[4] Jones and Langmuir, G. E. Rev. 310 (1927).

[5] Forsythe, Int. Crit. Tables, Vol. V, 245.

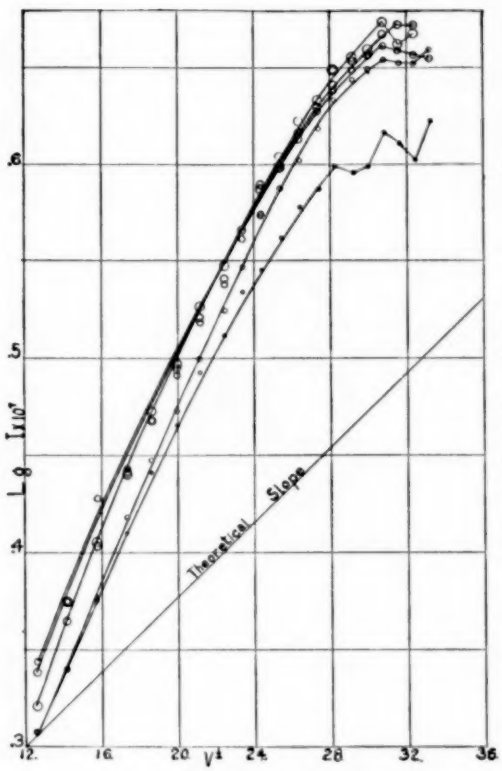

FIG. 3. Schottky curves during first stage for 7 mil filament. Aging has been preliminary, curves are erratic, slopes are high.

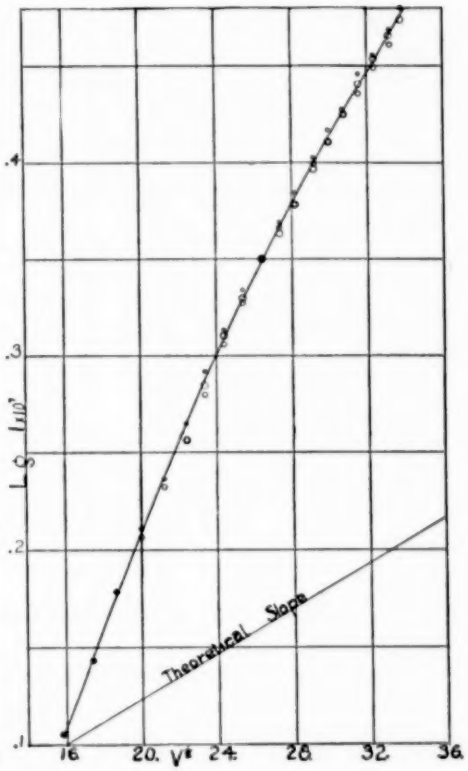

FIG. 4. Schottky curves during second stage for 7 mil filament. Aging has been protracted: 175 hours at 1650 to 1690°K. Data are consistent but curves are not linear and slopes are high.

currents decreased slightly. A curve, typical of this stage is shown in Fig. 4.

A third stage is that in which slopes of the correct value were found as shown in Fig. 5. The attainment of this condition required flashing at a temperature around 1785°K; but the filaments remained in the same condition at lower temperatures as shown in curves 2 and 3 of Fig. 5. In fact, with a filament in this stage the liquid air was removed from the charcoal for several weeks, and after recooling the filament condition was found unchanged. Apparently a requirement necessary for transition to this stage is some evaporation of platinum. It was found that at 1785°K, the filament current remaining constant, the filament diameter decreased sufficiently to cause the temperature to rise an amount sufficient to cause a continuously increasing emission.

A fourth stage appeared when evaporation had continued to such an extent that the slope fell noticeably below the theoretical value as shown in Fig. 6. This decrease appears because (dv/dx_0) entering with an exponent $\frac{1}{2}$ increases the slope more slowly than T decreases it. The seven mil filament used in this case was found after burnout to have a minimum diameter of 5.5 mils. The dotted line in curve 7 shows the slope calculated for this diameter. It will be observed that changes in slope due to decrease in filament diameter are quite small, and are easily distinguishable from the preceding effects.

DISCUSSION OF RESULTS

It is difficult and unnecessary to assume a mechanism which will account for the above results. The early, erratic stages seem, however, to indicate the evolution of some volatile material from the filament surface, and the presence of a surface layer of low work function; the emission being increased due to a decreasing thickness of the layer of impurity. The stable

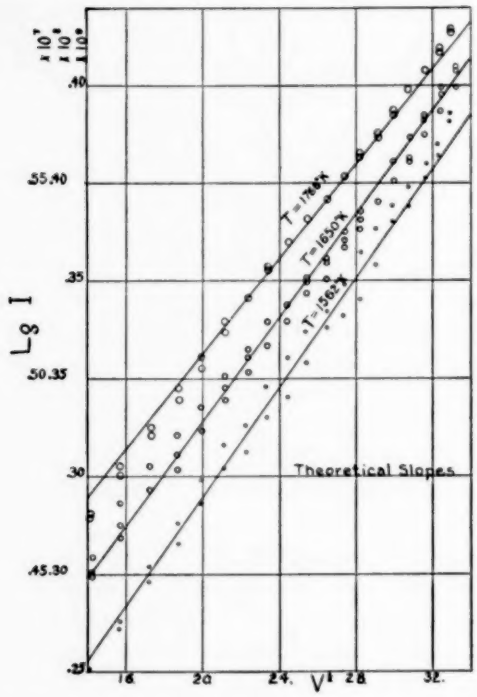

FIG. 5. Schottky curves during third stage for 7 mil filament. Filament has been aged up to 1785°K. Straight lines shown are the theoretical slopes corresponding to the three temperatures.

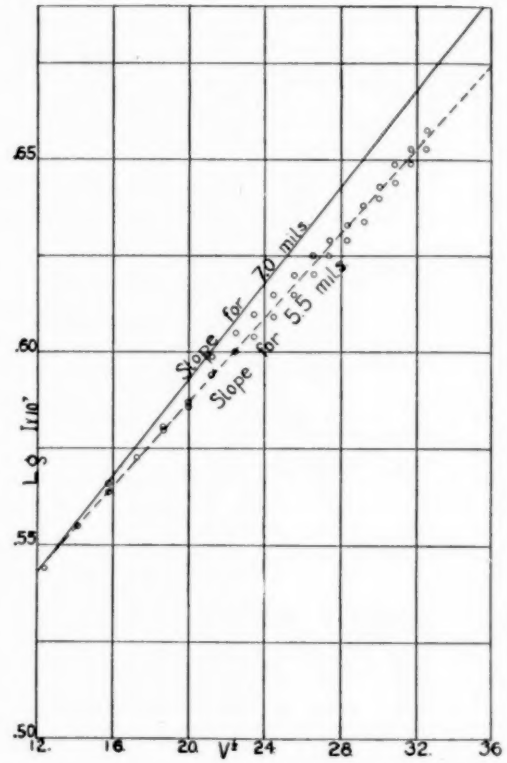

FIG. 6. Schottky curves during fourth stage. Evaporation has occurred so that data fall below the slope calculated for a 7 mil filament but fit slope calculated for 5.5 mil filament; the measured diameter after burnout.

condition yielding high slopes might be attributed to a diffusion of some less volatile material outward to the filament surface. More certainly, evaporation is involved in the transition to the condition in which correct slopes are found. The stability of this condition, then, might point to the previous completion of the process of purification of the interior of the filament by diffusion.

FORCED AGING

Some of the filaments used burned out at low temperatures for reasons which were not apparent. Most of the filaments did not survive long enough to give curves of the correct slope. For this reason, and in order to obtain a more comprehensive view of the phenomena, tests were made in the following fashion: A filament which had been aged at 1755°K for 12 hours was subjected to gradually increasing temperatures for 15 minute intervals. At the end of each 15 minute interval the temperature was reduced to some convenient lower value and thermionic currents measured at anode potentials of 200 and 1250 volts. From these readings the slope of the Schottky curve was computed. The results are shown in Fig. 7. Although the thermionic currents reached an apparently stable value at an aging temperature of about 1917°K the Schottky slopes remained high until a temperature of 1990° was reached. From this point on they decreased rapidly to the theoretical value. The region from 1917 to 1990°K probably corresponds to stage two in previous tests; and is of such a stable character that it seems likely that thermionic and photoelectric work functions would agree. In this way the entire aging process was compressed into 7 hours. The results seem to indicate that the aging temperature is of more importance than the time of aging. The diameters of the filaments were not decreased by evaporation enough to detect with a micrometer after burnout. A filament heated to 2000°K for 30 minutes should[6] decrease in diameter only 0.16

[6] Jones, Langmuir and Mackay, Phys. Rev. **30**, 201 (1927).

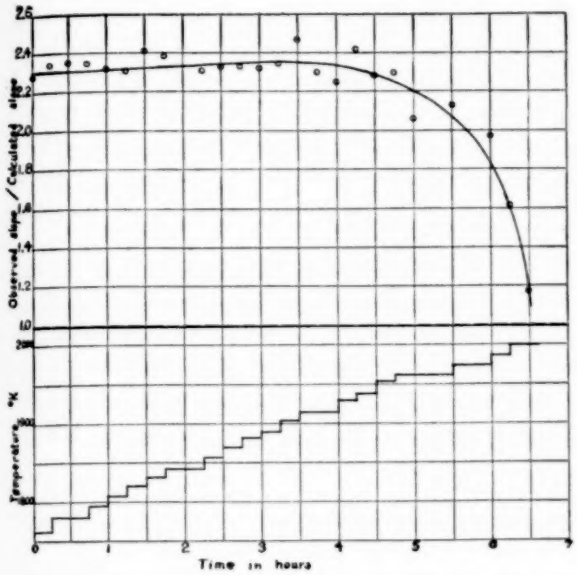

FIG. 7. Diagram showing results of forced aging. Ratio of observed to calculated slopes approaches unity only after aging had progressed to within 45° of the melting point. Slopes were consistent after aging temperatures of 1917°K had been reached.

mil; whereas heated to 1785°K for 175 hours it should decrease 1.6 mils—approximately as found in the longer runs.

CALCULATION OF THERMIONIC CONSTANTS

During the second stage, when the filament condition seemed to be quite stable, although the Schottky slopes were high, values of ϕ and A came out quite high. Because of the lack of straightness of the supersaturation curves it was impossible to determine the slopes of the Richardson curves with accuracy, but the best obtainable values were: $\phi = 7.4$ volts, and $A = 1.3 \times 10^5$ amp./cm^2·deg.^{2}. These are even higher than those found by DuBridge: $\phi = 6.27$ volts and $A = 1.7 \times 10^4$ amp./cm^2·deg.^{2}.

The Richardson plots for a filament which had reached the final stage are shown in Fig. 8. The upper curve yields the values $\phi = 5.66 \pm 0.07$ volts and $A = (1.5 \pm 0.7) \times 10^3$ amp./cm^2·deg.^{2}. The lower curve, taken after further aging, gives $\phi = 5.40 \pm 0.03$ volts and $A = 170 \pm 20$ amp./cm^2·deg.^{2}. These are probably not the final values since slightly lower values might have been obtained had the filament withstood further treatment. Nevertheless they do indicate that the final values of the constants for pure platinum

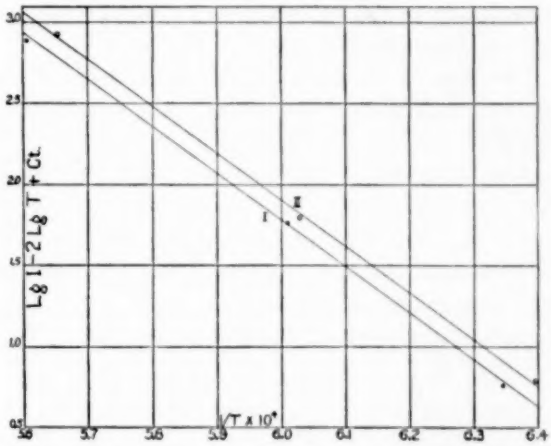

FIG. 8. Richardson curves for two sets of runs each taken at three temperatures. The upper curve gives values of ϕ of 5.66 ± 0.07 volts and $A = (1.5 \pm 0.7) \times 10^3$ amp./cm^2·deg.^{2}. The lower curve gives $\phi = 5.40 \pm 0.03$ volts and $A = 170 \pm 20$ amp./cm^2·deg.^{2}.

are considerably lower than those reported by DuBridge, and in particular that the value of A is approaching the theoretical value of 60 amp./cm^2·deg.^{2}. The above values are subject to some uncertainty because of electrometer fluctuations and the fact that complete data were taken for only three different temperatures. Nevertheless the results are sufficiently consistent that the Richardson slopes can be determined to within about 0.6 percent and the value of A within about 12 percent. Errors due to

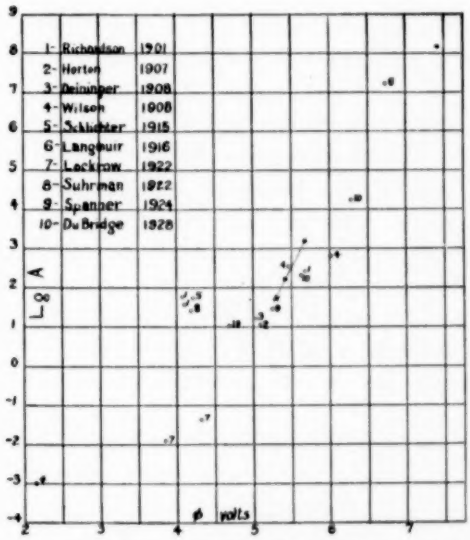

FIG. 9. Compilation of results of several experimenters. Data should give a straight line. X shows probable value of ϕ, 5.29 volts, on the assumption that A should be 60 amp./cm^2·deg.^{2}.

uncertainty in the calibration of the electrometer and the resistors are certainly less than this.

The high value of A for platinum previously reported has been the cause of some speculation and explanations have been proposed by Fowler[7] and by DuBridge. The present results indicate that this high value is characteristic of a fairly stable but not pure surface condition, and that for a surface cleaned at very high temperatures the value is not far from 60.

Richardson and DuBridge[8] have shown that for a given surface log, A is a linear function of ϕ. The values of these constants for platinum tabulated by Dushman are plotted in Fig. 9. Assuming the straight line as drawn to be correct it is seen that a platinum surface for which $A=60$ should show a work function of about 5.29 volts. Possibly this is close to the true value for clean platinum.

The author wishes to express his appreciation to Dr. W. R. Ham who directed the problem and to Mr. Karl D. Larsen who assisted throughout the work. Assistance was also furnished many times by other members of the Physics Department of The Pennsylvania State College.

[7] Fowler, Proc. Roy. Soc. **A122**, 36 (1929).

[8] Richardson, *Emission of Electricity from Hot Bodies*, p. 135; DuBridge, Proc. Nat. Acad. Sci. **14**, 788 (1928).

Variation with Temperature of the Electrification Produced in Air by the Disruption of Water Drops and Its Bearing on the Prevalence of Lightning

JOHN ZELENY, *Sloane Physics Laboratory, Yale University*

(Received August 24, 1933)

The total charge carried by the negative ions which are produced in the air when a water drop is disrupted by falling through a horizontal stream of air was measured for different stream velocities at temperatures between 1°C and 63°C. The dependence of this charge upon the size of the drop was found from observations made with drops differing in volume between 0.076 cc and 0.092 cc. For blasts exceeding that necessary just to disrupt the drops, the charge obtained per drop disrupted increases rapidly both with the velocity of the blast and with increase of temperature. The rate at which the charge changes with increase of temperature of the drop depends upon the magnitude of the air stream employed for producing the disruption. For drops of 5.8 mm diameter falling from a height of 2 cm through a horizontal cylindrical stream of 1 cm diameter and having an average velocity of 20 m/sec., the relation between the numbers of negative ions produced per drop disrupted at the temperatures 1.3°C, 24.2°C, 42.1°C and 62.5°C, respectively, was found to be 1 : 3 : 6.4 : 11. In the range of temperatures found in the atmosphere at different times the amount of electrification produced in the air when raindrops are disrupted by air currents of a given magnitude may be at least three times as large when the rain-water is warm as when it is cold. Rain temperature is therefore an important factor in determining the frequency and the intensity of lightning discharges.

PREVAILING theory considers the disruption of raindrops as the primary action that causes the electrification of thunder clouds.[1] The two electricities are supposed to become separated while the filaments and films formed from the drops by the wind, after rupture, are rapidly contracting into droplets. Temperature influences the action, mechanically, because the surface tension and the viscosity of water change with temperature; and possibly, electrically, owing to the dependence of electrical conductivity upon temperature. Warm water drops are more easily disrupted by a given air turbulence than are cold ones of the same size. The force due to surface tension that urges a broken water filament to contract decreases about 0.2 percent per 1°C rise in temperature but the effect of this change upon the speed of contraction is more than offset by the much greater decrease in the viscosity of water which amounts to about 3 percent for a rise of 1°C, in the range under consideration. Accordingly, the rapidity with which water filaments and films contract should increase markedly with rise of temperature and hence the electrification of air, accompanying the disruption of water drops, may also increase. If this be the case, then, other things being equal, the electric charge acquired by clouds can more readily reach values sufficient for the production of lightning with warm drops than with colder ones, and this may be one of the main reasons that lightning is more violent and of more frequent occurrence in warm weather than in cold. Lightning displays of greatest severity occur in certain tropical regions and lightning is said to be unknown in the polar regions.

No direct work on the influence of temperature on the electrification produced in air when water drops are disrupted by an air current has been reported. However, J. J. Thomson[2] found that when drops splash against a solid object the electrification of the water was nearly twice as large at 95°C as it was at 15°C. Usener[3] under like conditions also found an increase of electrification as the temperature of the water was raised from 11°C to 41°C.

In the experiments to be described drops of pure water at different temperatures, falling from a vertical tube, were disrupted, more or less, by passing through a horizontal jet of air, and the

[1] G. C. Simpson, Phil. Trans. Roy. Soc. **A209**, 379 (1909); P. Lenard, Ann. d. Physik **65**, 629 (1921).

[2] J. J. Thomson, Phil. Mag. **37**, 341 (1894).

[3] H. Usener, *Dissertation*, Bonn, 1895.

electrification of the air thus produced, per drop disrupted, was measured. The results show that the number of negative ions found in the air under these conditions increases quite rapidly with rise of temperature.

As shown by Lenard[4] for the case where water drops strike an obstruction, the amount of charge found in the air is greatly affected by the purity of the water used. Most of the experiments to be reported were carried out with water of the highest obtainable purity. The water after a first distillation was redistilled in the presence of potassium permanganate in a special still in the Sterling Chemistry Laboratory and kindly furnished by Dr. L. S. Darken. The initial specific conductivity was about 4×10^{-7} ohm^{-1} cm^{-1} and after standing a week in a fused quartz vessel its specific conductivity increased to 1.06×10^{-6}. Some measurements, which will be mentioned, were made with singly distilled water which on standing some days in a tin-lined vessel had a specific conductivity of 1.8×10^{-6}. The results shown on any one curve were always obtained on the same day with a single filling of the reservoir of the apparatus, since at times the absolute values obtained for the amount of electrification differed somewhat for different samples of water.

It may be worthy of mention that a series of observations made first with water immediately after it had been distilled directly into the reservoir of the apparatus and then repeated later on the same day and again on the next day showed an increase with the age of the water in the number of negative ions obtained by disruption of drops at the same temperature. Since it is believed that the final equilibrium state of polymerization of water is attained quite slowly, these results may point to a dependence of the electrifications here studied upon the state of polymerization of the water used.

In addition to the purity of the water, the number of ions formed in air per drop disrupted is naturally also dependent upon the size of the drops and upon the nature and velocity of the air stream used for effecting the disruption.

The apparatus used for the final measurements is shown in elevation in Fig. 1, drawn to scale and separated into three parts. It consists of the glass

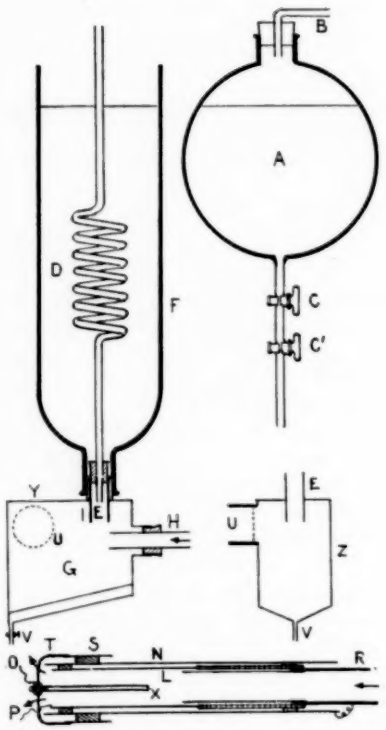

FIG. 1. Diagram of apparatus.

water reservoir A (15.5 cm in diameter) from which the water flowed through the greaseless, regulating stopcocks C and C' into the helical coil D which was immersed in the temperature water bath F, provided with a heating element and a stirrer, not shown. The water fell in drops from the end of the tube E which had an external diameter of 5.9 mm and whose walls were but 0.2 mm thick, to promote regularity of outflow. After separation from E, the drops passed through the brass shield tube I and fell centrally through an air stream issuing from the brass tube H, which had an internal diameter of 10.3 mm. In passing through the fastest air streams that were used, the drops were drawn out into curved sheets over a centimeter in width and about three times as long, which after bursting formed droplets that reached the bottom of the vessel G at an angular position of about 45° from the origin. The rates of outflow of drops used varied between one and two drops per second. The volume of the drops was determined by a direct count of the drops and a measurement of their total volume by a burette placed below the

[4] P. Lenard, Wied. Ann. **46**, 584 (1892).

outlet *V*. The chamber *G* in which the drops were disrupted is made of brass. It is provided with a removable top *Y* and two glass windows, not shown, which are covered on the inside with wire gauze. The temperature of the water drops was measured by a thermal junction, not shown, which was placed inside of the tube *E*.

The air used for disrupting the drops came from the air pressure system of the laboratory and passed in succession through a regulating device, a flow gauge, a large glass wool filter, and a charged cylindrical condenser for removing ions, before entering the chamber *G* through *H*. To prevent contamination of the water in *A* from above, the air before entering at *B* was passed through wash bottles of sulphuric acid, caustic potash and distilled water. The glass reservoir *A* and the other glass parts through which the water passed were purposely made of soft glass and before use were treated chemically and then had steam pass through them for several hours.

The ions produced in the air by the disruption of the drops were removed from it by the cylindrical ion collector *RS*, whose end *R* fits into the tube *U*. The air entered the ion collector through the grounded tube *R* and passed between the rod *X*, charged through *O* to 240 volts, and the cylindrical tube *L* which is connected by *P* to a quadrant electrometer and a condenser. The rod *X* is supported by a metal strip *T* fastened to the insulated cylinder *S*. *L* is electrically shielded by the grounded tube *N*. The whole ion collector is further enclosed in an earthed metal box attached to the electrometer case.

After leaving *E* the drops fell about 2 cm before entering the air stream, and then fell a further 5 or 6 cm before striking the bottom of *G*. For this small height of fall, there was almost no spattering when the drops struck the bottom of *G*. Nevertheless the air acquired some ions by this process and also at the contraction into droplets of the filament present behind each drop as it broke away from *E*. Some results on the combined effect of these secondary processes will be given presently. Only for air stream velocities above about 16 meters per second were the drops definitely disrupted, and at this stage the number of negative ions in the air was found to increase rapidly with increase of stream velocity. This fact permits a separation of the effect due to drop disruption from that due to the other processes just named.

Some typical results of the variation with temperature of the electrification produced in air by all causes per drop disrupted are shown in Fig. 2. The ordinates give the amount of electricity per drop in electrostatic units corresponding to the temperatures indicated by abscissas. The singly distilled water mentioned above was

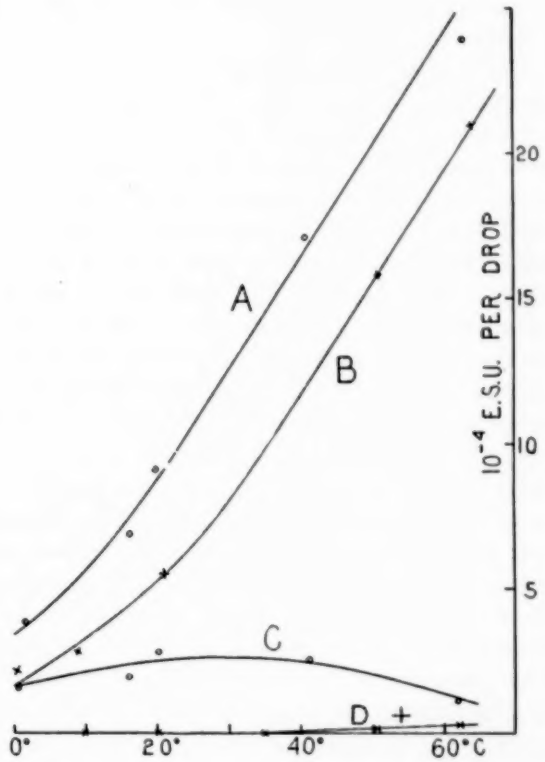

FIG. 2. Variation with temperature of charge on ions per drop disrupted. Curve *A*. Highly purified water. Negative ions. Air blast = 19.1 m/sec. Curve *B*. Distilled water. Negative ions. Air blast = 19.1 m/sec. Curve *C*. Highly purified water. Negative ions. Air blast = 9.88 m/sec. Curve *D*. Distilled water. Positive ions. Air blast = 19.1 m/sec.

used for curves *B* and *D* and the average air blast velocity was 19.1 m/sec. Curve *B* gives the charge on the negative ions present and curve *D* the charge on the positive ions. The amount of positive charge is seen here to be negligibly small, although under some other conditions positive charges as high as ten percent of the negative charge were found. Owing to the scarcity of positive ions the loss of negative ions by recombina-

tion must have been relatively small in the time of about one-tenth of a second taken by the air to get from chamber G to the ion collector. In this short time the loss of ions by diffusion to the wall of the fairly large tube must also have been small. This conclusion is confirmed by some experiments in which the air blast did not strike the falling drops and the ions present were produced solely by the other means mentioned. In this case the charge reaching the ion collector was found to be independent of the rate of flow of air, above a certain rather small limit.

Curve A of Fig. 2 gives the amount of negative charge per drop for water of the highest purity with the same air blast of 19.1 m/sec. The charge here is seen to be larger at all temperatures than that shown by curve B where less pure water was used. Curve C was obtained with the same pure water when the air blast was reduced to 9.88 m/sec. This blast was not sufficient to disrupt the drops and the curve is entirely different from curves A and B both in shape and in the magnitude of the charges obtained. The charge shown by curve C must have arisen from one or both of the other causes to which reference has been made. Curves A and B show that the number of negative ions produced in the air by the disruption of water drops increases rapidly with increase of temperature of the drops. The values at the different temperatures are not strictly comparable because the size of the drops obtained from the same orifice also varied with temperature, decreasing from 0.100 cc at 1°C to 0.084 cc at 62°C for the rates of outflow actually used. The drops increase in size with increase of rate of outflow. It will be shown below how the number of ions obtained increases with increase in the size of the drops disrupted.

Because of the presence of ions other than those produced by the blast, it was important to make measurements at each temperature with air blasts of various magnitudes. The results of such measurements for the four different temperatures given in the caption are shown by the curves of Fig. 3, each of which gives the relation between the negative charge obtained per drop disrupted and the average velocity of the air blast used, expressed in meters per second. Water of the highest purity was used. The results for curves A, B and C were all obtained during a continuous run employing water that had been distilled 24 hours before the experiments were started, a single filling of reservoir A (Fig. 1) sufficing for the purpose. The data for curve D were obtained on the following day by using a different filling of reservoir A with water that had been distilled at the same time as that used on the previous day.

Each curve has a more or less flat portion in the region of the lower blast velocities and a second part where the charge per drop increases rapidly with increase of the air stream. The ions represented by the flat portions of the curves are interpreted as originating not at drop disruption but rather in the process involved when the drops break off from the tube that discharges them and also at the place where the drops impinge on the bottom of the chamber G. Observations made by the light of a spark showed that the drops were not disrupted until the blast reached approximately the value (about 16 m/sec.) for which the curves show the beginning of the rapid rise in the number of ions observed.

Further evidence on this point was obtained from measurements made with a curved air nozzle so placed in the apparatus that the drops did not enter the direct blast but fell at the side of the blast tube. The water temperature was 25.5°C and the rate at which air was passed through the apparatus was varied to cover the range employed previously for the results in Fig. 3. For the upper half of this range the negative charge per drop remained constant at 2×10^{-4} e.s.u. For still lower rates of flow the charge per drop at first increased to 2.4×10^{-4} e.s.u. and then diminished again for the lowest rates of flow used. The value 2×10^{-4} e.s.u. is nearly the same as the charge at the minimum point on curve B of Fig. 3, for which the temperature was nearly the same as here. Therefore it seems safe to assume that all charges obtained with blasts of less velocity than that corresponding to the minimum points of the curves in Fig. 3 are not due to disruption of drops by the blast but rather to one or both of the other processes already described.

The shape of the curves in Fig. 3 for the lower air blast velocities may be explained by assuming, first, that at the lowest velocities where it takes the air of the order of a half second to pass from chamber G to the ion collector a consider-

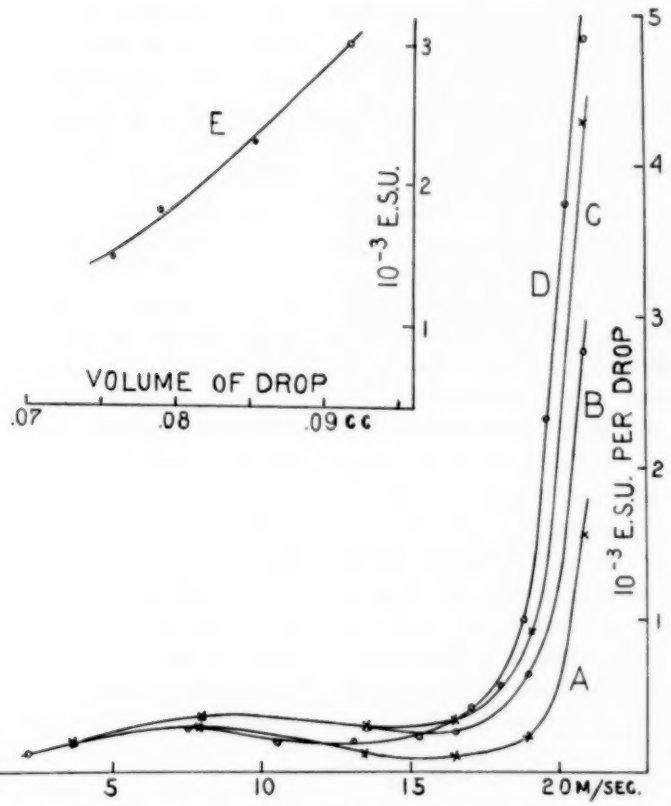

FIG. 3. Variation, with speed of air, of charge on negative ions per drop disrupted for different temperatures. Curve *A*. 13°C. Volume of drop = 0.1031 cc. Curve *B*. 24.2°C. Volume of drop = 0.0986 cc. Curve *C*. 42.1°C. Volume of drop = 0.0945 cc. Curve *D*. 62.5°C. Volume of drop = 0.0853 cc. Curve *E*. Variation of negative charge with volume of drop. 22.7°C. Air blast = 20.4 m/sec.

able number of the ions become lost by diffusion to the walls of the tubes, and second, that as the drops become more and more deformed by the increasing blasts the number of ions liberated when the drops strike the bottom of the chamber *G* becomes less and less.

The right-hand portions of the curves *A*–*D* in Fig. 3 represent, then, the combined charges produced by drop disruption and all other causes. Because of the comparatively small effect of the latter for the higher blast velocities, no large error can arise by assuming the magnitude of the charges produced by them within this range to remain equal to the minimum value at the dip of each curve, although with more complete disruption of the drops the ionization due to one of the components involved very likely decreases. The charge arising from drop disruption alone is then obtained by simple subtraction. This will be done below in making a comparison of the effects of this disruption at different temperatures.

Before such a comparison can be made it is necessary to find how the number of ions liberated depends upon the size of the drop disrupted, because the drops varied in magnitude with the temperature used. Measurements were made at 22.7°C with a blast velocity of 20.4 m/sec. with water nozzles of four different diameters. The total negative charge obtained per drop is plotted against the volume of the drops in curve *E*, shown as an insert in Fig. 3. For drops of the range of sizes here used it is seen that the charges obtained per drop disrupted increase very considerably with increase in the size of the drops. In applying the variation found, to reduce the charge obtained with a drop of one size to that of

another size, it will be assumed arbitrarily that the rate of change with size is approximately the same at the different temperatures used.

The results represented by the curves in Fig. 3 verify the explanation already given for the marked difference in the character of curves *A* and *C* of Fig. 2 that the blast used for getting the data of the latter curve was not sufficiently strong to disrupt the drops and that the charges obtained arose from secondary causes alone. Moreover, it is evident from a study of the curves in Fig. 3 that the way in which the amount of electrification obtained by the disruption of water drops varies with the temperature of the drops depends in large measure upon the magnitude of the air blast used for producing this disruption. Warm drops may even be disrupted by blasts which are unable to disrupt colder drops at all. To illustrate the effects of temperature here being studied, it will suffice to make the computations for one representative blast speed. Hence the relative amounts of the charges obtained when the blast velocity used was 20 m/sec. and the drops were at the four different temperatures shown, will alone be given, after correction has been made as indicated above for the differences in the size of the drops and for the charges arising from other causes than the disruption of the drops by the air blast. Under these conditions the number of negative ions obtained at 1.3°C, 24.2°C, 42.1°C and 62.5°C, respectively, varied as 1 : 3 : 6.4 : 11.

This comparison shows that for differences of temperature such as are found in the atmosphere on different days the amount of electrification developed in the air when rain-drops are disrupted by given air currents may be at least three times as large when the rain is warm as when it is cold. The temperature of rain-drops is therefore an important factor in determining the frequency and the intensity of lightning discharges. As is well known, warm weather also favors the formation of the strong upward air currents which are an important feature of thunder storms.

It should be remarked that the value of 16 m/sec. found here for the blast velocity required to disrupt the drops used when at room temperature is higher than the value, 10.8 m/sec., given by Lenard[4] for drops of the same size. It must be remembered, however, that in these experiments the drops were under the action of the disrupting forces of the blast only while falling a distance of 1 cm. Had the blast stream had a larger cross section, the air speeds necessary for drop disruption would have been smaller. The charge here obtained for each drop disrupted is of the same order as the values given by Simpson and by Lenard, but these charges are much smaller than those often found on rain-drops. Thus Benerji and Lele[5] recently reported having observed thunderstorm rain-drops with charges of 3.7 e.s.u. and non-thunderstorm drops with charges as high as 2.4 e.s.u. Such large charges may result from repeated rupture of drops and coalescence of the droplets thus formed under conditions in which the atomization by the turbulent air is more complete than it was in the experiments here reported.

I am glad to acknowledge here the valuable aid received from my assistant, Mr. H. J. Hoge, during the performance of the experiments.

[5] S. K. Benerji and S. R. Lele, Nature **130**, 999 (1932).

Magnetic Analysis of Nickel Films Deposited by Evaporation*

H. N. Otis,† *Sloane Physics Laboratory, Yale University*

(Received August 28, 1933)

The magnetic properties of nickel films deposited from vapor on surfaces at several temperatures and, in some cases, annealed to various degrees have been studied at room temperature. Films deposited at room temperature are magnetically hard, having low initial susceptibility (χ_0). For films deposited on a metal with a higher coefficient of linear expansion than nickel, raising the temperature of deposition or annealing at higher temperatures increases χ_0. For films on a metal with a lower coefficient of linear expansion than nickel χ_0 first increases with deposition or annealing temperature but decreases upon high temperature annealing. The results are explained on Becker's theory by assuming that the films are deposited under strain, these deposition strains becoming less at higher temperatures.

SORENSON,[1] Edwards[2] and Miller[3] measured the magnetic properties of thin films of nickel, deposited by evaporation on aluminum, finding the temperature of deposit important in fixing the course of magnetization. Howey[4] later evaporated films onto various backings, under better vacuum conditions, at deposition temperatures from 125°C to 320°C. Differences in films on Al, Cu, Pt and Mo, all measured at room temperature, were explained as due to differential contraction of film and backing in cooling after deposit. All these investigators found their films magnetically hard; the initial susceptibilities (χ_0) were small. Nickel films deposited by electrolysis,[5] or by sputtering,[6] are also hard to magnetize, but here interpretation is more difficult because of the greater probability of gaseous inclusions during deposit.

The effect of strain upon magnetization has been discussed by Becker,[7] who proposes that, in the absence of an external magnetic field, the stability of the direction of I (intensity of magnetization) in each domain is determined by the stress to which that domain is subject. (This neglects the effect of crystal structure which is found to be small in comparison with that of supportable stresses.) Experiments by Becker and Kersten,[8] and by Kersten[9] on nickel variously strained agree well with the theory. Their curves for nickel wires under tension are very similar to the usual magnetization curves for nickel films.

The purpose of the present investigation was to extend temperatures of deposit down to room temperature and to study the effects of annealing. The results have been examined in the light of Becker's theory to ascertain the internal state of the films at various stages. A similar study of electrolytic films has recently been reported by Elenbaas.[5]

The Still

The still, in which the nickel films were formed, had to meet three requirements. First, rapid evaporation must be possible so that relatively thick films could be built up in reasonable times. Second, means must be furnished for heating or cooling the surface on which deposition occurred, and for measuring the temperature of this surface. Third, vacuum conditions must be good enough to minimize any effects of residual gases. The still, as constructed to meet these requirements, is

* Part of a dissertation presented for the degree of Doctor of Philosophy at Yale University.

† Now located at Hunter College.

[1] A. J. Sorenson, Phys. Rev. **24**, 658 (1924).

[2] R. L. Edwards, Phys. Rev. **29**, 321 (1927).

[3] K. J. Miller, Phys. Rev. **32**, 689 (1929).

[4] J. H. Howey, Phys. Rev. **34**, 1440 (1929).

[5] W. Elenbaas, Zeits. f. Physik **76**, 829 (1932).

[6] L. R. Ingersoll and S. S. deVinney, Phys. Rev. **26**, 86 (1925) reported films sputtered in hydrogen to be non-magnetic.

[7] R. Becker, Zeits. f. Physik **62**, 253 (1930).

[8] R. Becker and M. Kersten, Zeits. f. Physik **64**, 660 (1930).

[9] M. Kersten, Zeits. f. Physik **71**, 553 (1931).

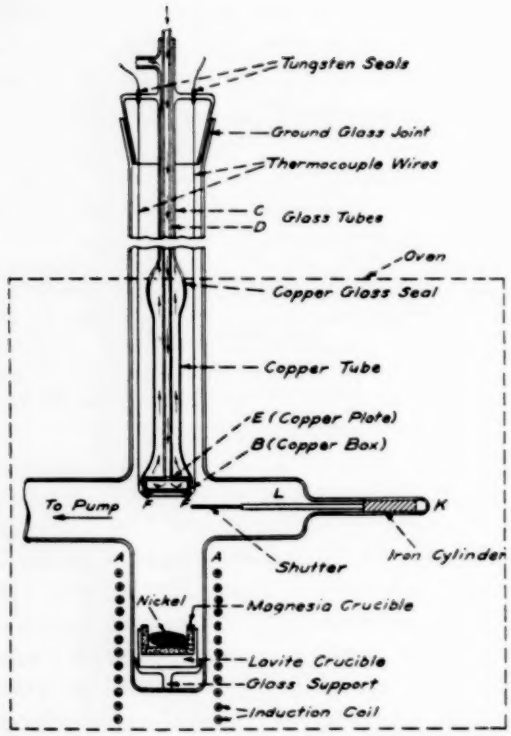

FIG. 1. Design of tube for deposition of nickel films.

shown in cross section in Fig. 1. The vertical tube, of Pyrex, was 5 cm in diameter. The metal disk upon which a film was to be deposited was clamped by small screws between the nickel ring *F* and the water-cooled copper box *B*. Copper parts were silver-soldered together to permit baking out before the water was circulated. The shutter could be moved by a solenoid slid over the side tube *K* so as to protect the prepared surface from nickel vaporized in preliminary operations. A Gaede two stage steel mercury vapor pump backed by a Cenco Hyvac oil pump and protected by a large bore liquid air trap was used and pressures were measured by an ionization manometer. The tube could be baked out or operated at higher than ordinary room temperature by surrounding it with an oven placed as indicated. With a 3 kva high frequency generator the nickel could be melted in from four to five minutes under the usual good vacuum conditions, pressures ranging, except as noted below, between 10^{-4} and 10^{-5} mm Hg. A chromel-alumel thermocouple gave the temperature of *B*.

The crucibles were made of pure MgO, which has been shown[10] to introduce only very slight impurities into a nickel melt. The nickel was prepared electrolytically by the method of Fink and Rohrman[11] and melted under hydrogen into a pellet of the desired shape in a molybdenum-wound furnace.

The film supports were thin disks of Cu, Mo, glass, and mica, 2.54 cm in diameter. Each was initially cleaned with benzene, alcohol and ether, dried in a desiccator and weighed. It was then mounted in the still and the ground glass joint sealed with low vapor pressure Boltwax. To ensure low pressure, surface cleanliness and minimum gas evolution during deposit the following procedure was followed. With shutter closed the nickel was melted and kept molten until the pressure fell below 10^{-4} mm. The tube was then baked at 500°C for from 4 to 10 hours, during which time the nickel was repeatedly frozen and remelted until melting caused no rise in pressure. The still was then allowed to cool to the desired temperature, water circulated if this was room temperature, the shutter drawn aside and a final melting for a controlled time gave the desired deposit. When the melt had cooled the film support was removed and weighed to find its thickness. It was assumed that the film density was that of pure bulk nickel.

MAGNETIC MEASUREMENTS

The torsion magnetometer used for magnetization curves and hysteresis loops has been described elsewhere.[12] Some of the films, initially magnetized, had to be demagnetized before the magnetization curves could be found. Complete loops were taken and agreement between values of *I* at loop tips was taken as proof of initial demagnetization. Only magnetization curves and the upper parts of the descending branches of hysteresis loops are shown in the figures.

RESULTS

Limiting magnetization curves and (partial) loops for films deposited on metals at room

[10] W. H. Swanger and F. R. Caldwell, Bur. Standards J. Research **6**, 1131 (1931).

[11] C. J. Fink and F. A. Rohrman, Trans. Am. Electrochem. Soc. **57**, 325 (1930); **58**, 403 (1930).

[12] H. N. Otis, Rev. Sci. Inst. **4**, December (1933).

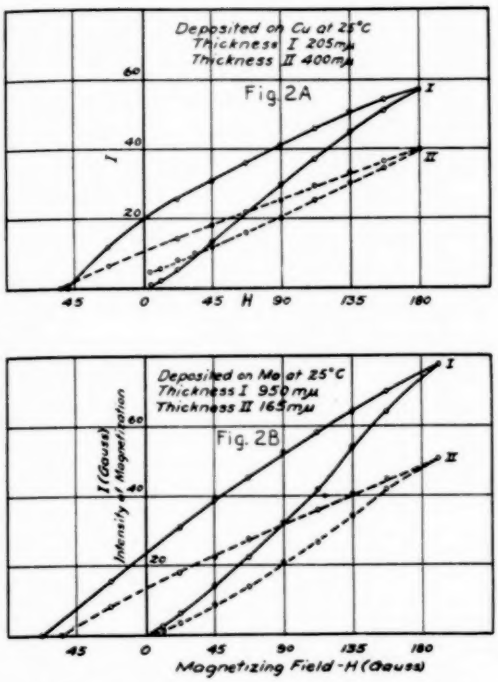

FIG. 2. Magnetization curves for nickel films deposited at room temperature.

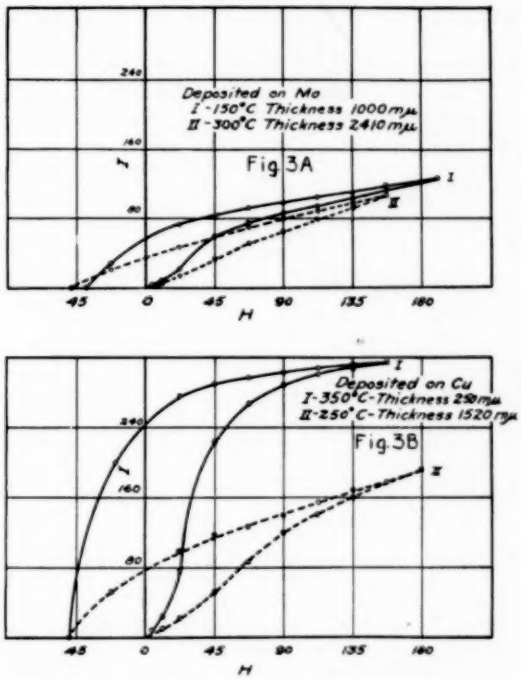

FIG. 3. Magnetization curves for nickel films deposited on molybdenum and copper at from 150° to 350°.

temperature are shown in Figs. 2A and 2B. All results fell between curves I and II.

These films were all relatively thin because peeling always occurred as soon as the thickness exceeded 800 to 1000 mμ. Direct observation showed that peeling over the entire surface occurred suddenly. This peeling might be due to (1) evolution of gases from the support, (2) entrapping of residual gases by the vapor stream, (3) temperature changes of the support. To test (1) and (2) a Mo disk was outgassed in vacuum at 1500°C for 15 hours, then quickly mounted in the still and extreme precautions taken to keep the pressure during deposit below 10^{-5} mm. Peeling occurred as usual. To test (3) a typical run was carried out with the thermojunction soldered to the face of a film support and thus exposed to the stream of nickel vapor. Its temperature rose less than 10°C. In a further test of (3) a film was deposited directly on box B, but still peeled at about the critical thickness. Furthermore, a film deposited on a nickel disk peeled as usual. To test (2) by itself the rate of deposit was reduced to one-tenth its usual value —this required only a slight change in the temperature of the molten nickel—without changing the thickness at which peeling occurred. It must be concluded that peeling results from some intrinsic property of nickel condensed at room temperature.

Figs. 3A, B are typical of films deposited on Mo and Cu at from 150° to 350°C (magnetic measurements at 25°C). Peeling never occurred when the temperature of deposit exceeded 100°C.

Figs. 4A, B, C, D show the effects of annealing, in vacuum for 6 hours at the temperatures indicated, films deposited on Mo and Cu at low and at high temperatures.

Figs. 5A, B show typical magnetic behavior for films on glass and mica. Such films never peeled, and it seems likely that this immunity is due to the higher temperature attained by films on these poor thermal conductors.

Fig. 6 presents magnetization curves for magnetically soft and magnetically hard films up to $H = 1300$. The latter is still far from saturation to judge by its terminal slope.

DISCUSSION

Suppose the stresses in any magnetic domain are resolved into a hydrostatic stress of either

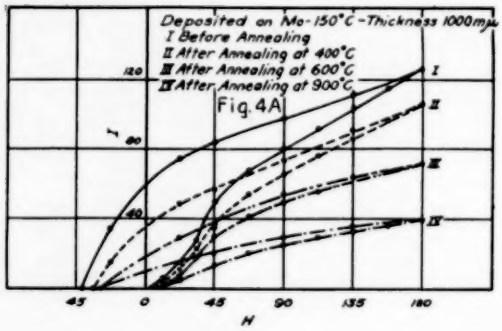

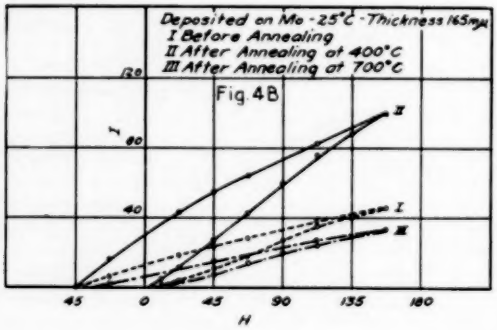

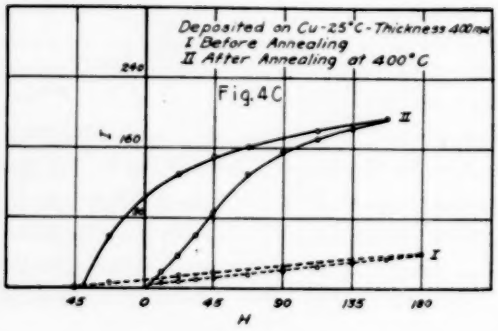

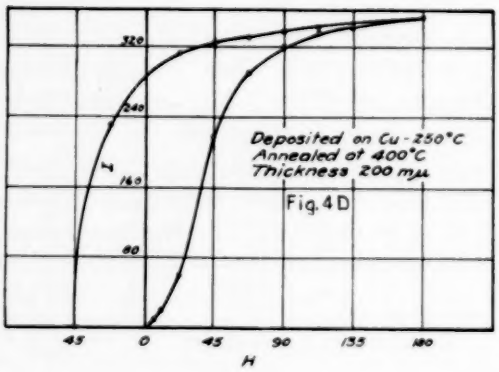

FIG. 4. Magnetization curves which show the effects of annealing.

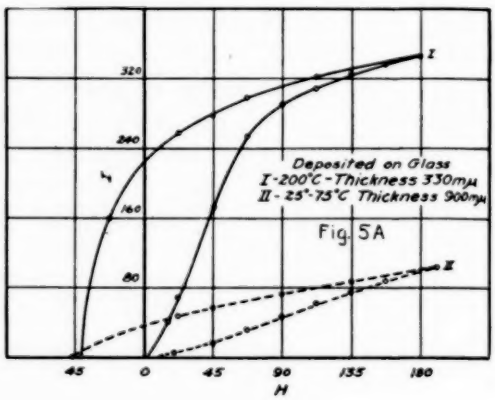

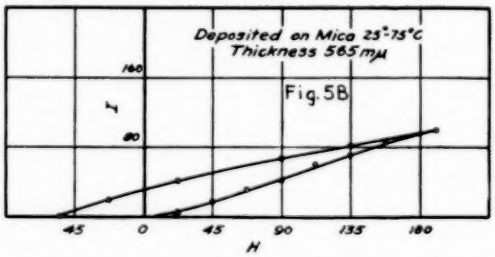

FIG. 5. Magnetization curves for nickel films deposited on glass and mica.

sign and a tension or compression. Becker's theory now states that in nickel, wherein the longitudinal magnetostriction is negative for all crystallographic directions, the magnetization I is parallel to the directed stress if the stress is compressional, at right angles thereto if the stress is tensile. The initial susceptibility for a specimen is then[9]

$$\chi_0 = (I_\infty^2/3\sigma)\overline{\lambda^{-1}}\cdot\overline{\sin^2\epsilon} \qquad (1)$$

where $I_\infty \equiv$ saturation intensity of magnetization, $\sigma \equiv$ directed stress, $\lambda \equiv$ magnetostrictive strain, $\epsilon \equiv$ angle between the strain-determined direction of I in a domain and the direction of the applied H. Bars indicate mean values of the quantities under them. Substituting known values for I_∞ and $\overline{\lambda^{-1}}$ and expressing σ in kg·mm^{-2} we get

$$\sigma = (23.9/\chi_0)\,\overline{\sin^2\epsilon}. \qquad (2)$$

In a film with free upper surface any tension or compression must have its axis in the plane of the film. It will be shown that these stresses are probably tensile, so we take $\overline{\sin^2\epsilon}=1$ and (2) becomes

$$\sigma = 23.9/\chi_0. \qquad (3)$$

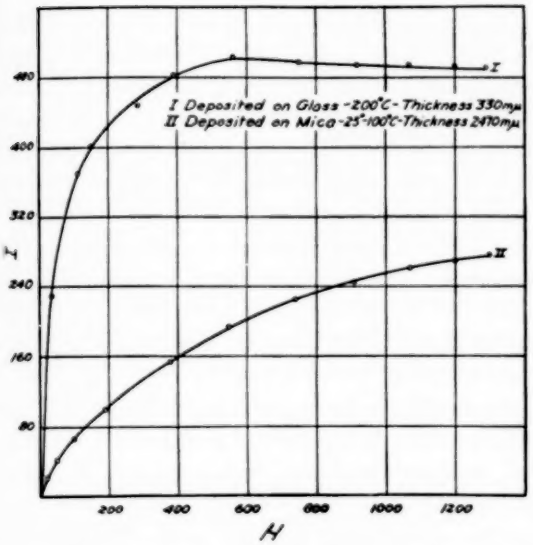

FIG. 6. Magnetization curves for magnetically soft and magnetically hard films.

Values of σ thus computed for the films of Figs. 2, 3, 4 are given in column 6 of Tables I, II.

We first note the similarity (Fig. 2) of films deposited on cold Mo and on cold Cu. The striking differences observed by Howey[4] have disappeared with the suppression of differential contraction of film and support.

TABLE I. *Column 3 gives the kind of metallic support used, column 4 the temperature of deposit, column 5 the initial susceptibility, and column 6 the stress, in kg·mm^{-2} computed from (3).*

Film No.	Fig.	Support	T_D	χ_0	σ
1	2A I	Cu	25°C	0.18	133
2	2A II	Cu	25	0.16	149
3	2B I	Mo	25	0.21	114
4	2B II	Mo	25	0.14	171
5	3B II	Cu	250	0.75	32
6	3B I	Cu	350	1.60	15
7	3A I	Mo	150	0.50	48
8	3A II	Mo	300	0.40	60

The magnetic analysis supports the opinion, already suggested by peeling, that in cold deposited films stresses exceed the breaking strength (about 30 kg·mm^{-2}) of bulk nickel. That this stress is tensile was shown by the curvature of very thin mica on which a film was deposited. When peeling occurs the flakes are convex toward the support, which may mean either that the nickel first deposited is under least tension or that the flake suffers further cold work as it lets go. If the former is the correct explanation it might arise from slow annealing at room temperature of the highly overstrained metal.

TABLE II. *Column 3 gives the kind of metallic support used, column 4 the temperature of deposit, column 5 the annealing temperature, column 6 the initial susceptibility, column 7 the stress in kg·mm^{-2} computed from (3).*

Film No.	Fig.	Support	T_D	T_A	χ_0	σ
7	4A I	Mo	150°C		0.50	48
	4A II			400°C	0.36	66
	4A III			600	0.20	119
	4A IV			900	0.13	184
9	4B I	Mo	25		0.15	159
	4B II			400	0.36	66
	4B III			700	0.14	170
2	4C I	Cu	25		0.16	149
	4C II			400	1.60	15
10	4D	Cu	250	400	1.50	16

The Becker stresses in films deposited at higher temperatures should show the effect of any differential thermal contraction of film and support. Nickel films on copper would be subjected to edgewise compression, films on molybdenum would be stretched.[13] If the tensile stresses due to deposition are unaltered by rise in temperature of deposit films on copper should become magnetically softer, films on molybdenum magnetically harder as the temperature of deposit increases. These changes do occur after the temperature of deposit exceeds about 150°C, but up to that point, at least, χ_0 increases for films on Mo (cf. film 7 at 150°C with films 3, 4 at 25°C) though not as rapidly as for films on Cu. Furthermore the increase for films on Cu (cf. film 5 at 250°C with film 1 at 25°C) is too rapid to be due only to the compression of the hot deposited films by differential contraction. It is apparent that deposition stresses themselves vary with the temperature of deposit and that, if tensile, they decrease as this temperature rises.

Comparison of films 5 and 6 shows that deposition stresses are not completely absent at 250°C,

[13] A rough calculation, neglecting shears, assuming no flow taking place during cooling, and taking the elastic constants of the films to be those for bulk nickel, gives a compressional stress of 12 kg·mm^{-2} per 100°C change in temperature for nickel on copper, and a tensile stress of 27 kg·mm^{-2} per 100°C change in temperature for nickel on molybdenum.

for if they were the value of σ would be higher for film 6 than for film 5. (Since both would be compressive we should have $\overline{\sin^2 \epsilon} = 1/2$ and $\sigma = 12/\chi_0$, but this would not alter *relative* values.) We must therefore conclude that in film 5, at least, the stress is still tensile, and *a fortiori* it must be tensile in film 7. The difference between σ for these two films is then seen to be smaller than that calculated on our simple assumption of homogeneous stresses, though the values fall in the expected order.

Howey,[4] whose curves for nickel deposited at elevated temperatures agree well enough with Figs. 3A, B, found that for deposit at 125°C a film on Mo was magnetically harder than a film on Cu. Values of σ calculated from his χ_0 values are greater than can be accounted for by differential contraction so that both films must have been in tension when at room temperature and deposit strains must also have been tensile.

The results of annealing (Table II) are, for anneals at 400°C, similar to the results of deposit at 300° or 350°C (cf. films 9 and 8, 2 and 6). This is taken to mean that deposit strains are relieved at these temperatures even during the process of condensation. The apparent anomaly presented by films on Mo which have higher χ_0 if deposited at 150°C than if deposited at room temperature or at 300°C, or if annealed at 400°C and upward, is due to the fact that deposit stresses decrease more rapidly than the thermal stretching increases in the lower range of temperatures, and do not decrease at all in the upper range. As before, however, the simple assumptions regarding thermal contraction are seen to be quantitatively inadequate on comparing σ for films 2 and 9 which should, on this basis, differ more than they do.

The peeling of films deposited on cold metal is now naturally attributed to stresses, mainly tensile, arising during deposition. To explain peeling at a critical thickness it must also be supposed that the breaking strength is greater for thin films than for bulk nickel and greater the thinner the film, so that the stretched thin film becomes unstable when its thickness exceeds about 800 mμ. Cracks, traces of gas, or temperature gradients can then initiate break-up.

Tension in electrodeposits has frequently been observed,[14] and it has often been assumed that such stresses were due to inclusion of gas within the metal lattice. The present work suggests that the mere formation of a metallic lattice, atom by atom, at a sufficiently low temperature, creates intense stresses.

For films on glass and mica χ_0 increased as the deposition temperature was raised. This is consistent with the low coefficient of expansion for these supports. The absence of peeling is attributed partly to the higher surface temperatures resulting from poor thermal conductivity, but since this temperature probably did not exceed 100°C there must be some other difference between these films and those on metals. The superior smoothness of glass and mica probably increases the tensile strength of the films since films on metals often started to peel at fine scratches in the supports.

The flattening of magnetization curves well below the saturation value for bulk nickel ($I = 480$) calls for explanation. Four possible sources of error in I have been considered. (1) The film weight may be incorrect, especially when of the order of 10^{-4} g. (2) Magnesia may evaporate and condense with the nickel. This seems unlikely at melt temperatures below 1800°C, since the vapor pressure of MgO is said to be negligible up to this point. (3) The nickel may be partly oxidized. The low gas pressure makes this improbable. (4) The nickel may alloy with the support. This should cause larger defects in I for thinner films, which was not observed. A chemical analysis of a thick film (4500 mμ), deposited on copper at 400°C, which gave a magnetization curve similar to Fig. 4D, gave a nickel content agreeing within 0.5 percent with the weight of the film. This virtually disposes of (1), (2) and (3) above. To get additional information regarding (4) a thin film (200 mμ) was deposited on copper at 350°C and annealed in the still for 6 hours at 400°C. The I-values were not lower than usual—the film was chosen for Fig. 4D as completely typical—where-

[14] e.g., G. Gore, Phil. Trans. **148**, 185 (1858); **152**, 323 (1858). E. J. Mills, Proc. Roy. Soc. **A26**, 504 (1877). G. G. Stoney, Proc. Roy. Soc. **A82**, 172 (1907). R. M. Bozorth, Phys. Rev. **26**, 390 (1925).

as alloying should have been especially effective here if ever. It is suggested that the defects in I point to the existence of portions of the film subject to such great stresses or so imperfectly crystallized as to be nonmagnetizable even in relatively intense magnetic fields.

Magnetically soft films show magnetic saturation at about the expected value of I, as is seen in Fig. 6 which contrasts the two sorts of film up to $H=1300$.

No regular variation of magnetic properties with thickness of film was disclosed in these experiments. Results at the lower deposit temperatures, which were the most consistent, show that any effect of thickness must be small.

More extended application of Becker's theory to the data here collected does not seem justified in view of the uncertainty of I and the numerous evidences of local variations in the harder films.

It is a pleasure to acknowledge indebtedness to Professor L. W. McKeehan, who suggested the investigation, and whose advice and encouragement have been invaluable. The author wishes also to thank Dr. J. H. Howey for many helpful discussions, and Mr. L. H. Ott for collaborating in preparing the nickel.

The Ferromagnetism of Nickel Colloids

S. RAMACHANDRA RAO, *Annamalai University, Annamalainagar, South India*

(Received August 21, 1933)

Colloidal nickel was prepared by an electrical dispersion method and tested magnetically. The intensity of magnetization of the colloid at particle diameters less than about 1.5μ was found to be below that of the mass metal. This experimental result is discussed in the light of Heisenberg's and Bitter's theories of ferromagnetism.

I. INTRODUCTION

A CONSISTENT theory which can account for the known magnetic properties of ferromagnetic bodies has been engaging the attention of several investigators during the last few years.[1] The classical theories of Ewing and Langevin amplified later by Weiss[2] postulated the existence of large local fields within these bodies. The rather arbitrary assumptions of these theories have been partly removed by the new quantum mechanical treatment of Heisenberg.[3] His theory, however, presupposes the existence of microcrystals within the crystal, the resultant spins of these microcrystals having random orientations, which compensate each other in the absence of an external magnetic field. These conclusions together with the ideas of Zwicky[4] on the existence of a block structure in crystals and the calculations of Bitter[5] on the magnetic properties of an assembly of microcrystals suggest a possible relation between the specific intensity of magnetization and the particle size as the volume of the particle is reduced to colloidal dimensions. The highly diamagnetic elements like bismuth and graphite have shown a dependence of the specific susceptibility on the size of the particle.[6]

The experiments of Montgomery[7] suggest a similar dependence in the case of nickel and the large amount of work accomplished with nickel films gives additional evidence.[8] The interest aroused by these experiments made it desirable to attempt a similar study by a different method.

II. EXPERIMENT

The aim of the experiment was to prepare specimens of pure colloidal nickel and determine experimentally their specific intensity of magnetization. The nickel was a single crystal of the pure metal which was kindly supplied by Dr. U. Nakaya (to whom my thanks are due) of the Hokkaido Imperial University, Sapporo, Japan. The apparatus for colloidalization was of the enclosed arc type[9] and is shown in Fig. 1. L_1 and L_2 are stout copper leads with strips of cleaned nickel fixed at the ends facing each other. A gap of $\frac{1}{2}$ to 1 mm was left as the sparking distance between the nickel poles. After thorough cleaning, pumping, warming and drying, the sparking tube was filled to the level 1 with freshly distilled normal propyl alcohol. The tube was reconnected to the pump and the pressure was maintained at about 2.5 cm. To minimize the heat produced and any chemical action, very low sparking currents of 2 to 8 milliamperes from an induction coil were used. The time of sparking extended usually from 2 to 4 hours. Although no appreciable heat was produced during sparking, the main tube was wrapped with cotton and kept cool with water.

After sparking, the cruder particles were allowed to settle for about half an hour. The tube

[1] A useful discussion is given in Proc. Phys. Soc. **42**, 355 (1930). See also Van Vleck, *The Theory of Electric and Magnetic Susceptibilities*, p. 316.

[2] E. C. Stoner, *Magnetism and Atomic Structure*, p. 75; also J. de Physique [7] **1**, 166 (1930).

[3] W. Heisenberg, Zeits. f. Physik **49**, 619 (1928).

[4] F. Zwicky, Phys. Rev. **43**, 270 (1933).

[5] F. Bitter, Phys. Rev. **37**, 90 (1931).

[6] S. R. Rao, Ind. J. Phys. **7**, 35 (1932).

[7] C. G. Montgomery, Phys. Rev. **39**, 163 (1932).

[8] A brief discussion on metal films is given in Section 4 in this paper.

[9] Theodor Svedberg, *The Formation of Colloids*, p. 28.

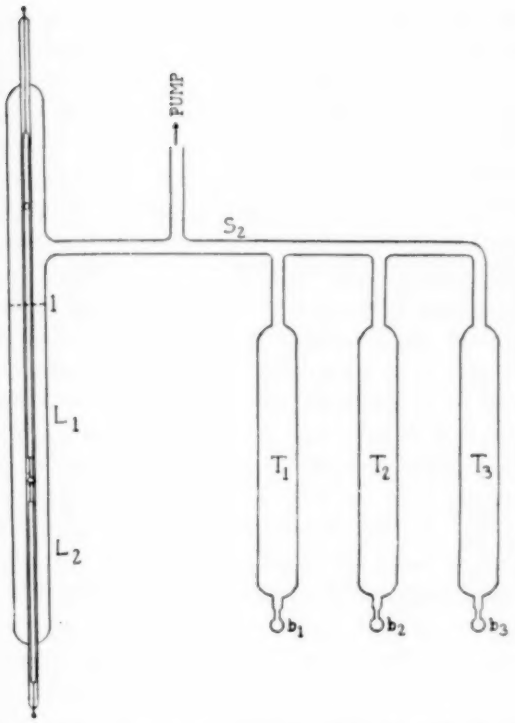

FIG. 1. Arrangement of apparatus for colloidalization of nickel.

connected to the pump was now sealed and the solution was transferred to T_1 and the connecting tube was sealed off at S_2. The fine particles were next allowed to settle for about an hour. These collected in the small bulb blown at the end of T_1. The clear solution was next decanted gradually to T_2 until the bulb b_1 was just full of propyl alcohol. This bulb was now sealed off. The process was repeated in T_2 where the settling was allowed for about two hours, and again in T_3 where the time of settling was increased still further. These times were, however, varied in different experiments. An approximate count of the diameter of the particles in these bulbs could be made by the application of Stokes' law to the falling particles.[10]

Several tubes of alternative designs, but based on the same principle, were devised and worked and thus many bulbs were prepared. The amount of propyl alcohol in each bulb was such that the bulbs were strongly diamagnetic.

The magnetic measurements were made with a Curie balance.[11] The retorsion method was employed to bring the bulb always to the same position with the field on. The deflection of the bulbs varied generally from 25 to 30 cm. A rough calculation showed that the deflections due to the propyl alcohol alone were about 35 to 45 cm.

After the magnetic experiments, the bulbs were carefully weighed, opened and immediately placed in a chamber that was then evacuated until the propyl alcohol evaporated completely. The bulbs were then rapidly weighed. The nickel was dissolved out by dilute nitric acid and the bulbs were cleaned, dried and weighed. They were then investigated magnetically. The deflections of the bulbs alone were only a few millimeters in each case. The nickel colloids weighed about 3 to 6 mg. Thus the masses of the bulbs, propyl alcohol and the colloids were separately determined in each case.

It was found that saturation in magnetization was obtained in all cases with a magnet current of about 6 amperes but the readings were taken at 8 amperes. The usual precautions to prevent heating of the samples were taken.

For comparison, tiny bits of the nickel crystal were produced by dissolving small pieces in dilute nitric acid to the required sizes, and after cleaning, immersed in propyl alcohol bulbs, which were investigated magnetically. The standard was taken to be water, the diamagnetic susceptibility of which was taken to be 0.72×10^{-6} at the laboratory temperature.

When there are small ferromagnetic impurities in a diamagnetic or paramagnetic body, then disregarding signs, Owen's equation gives[12]

$$\chi_i=\chi_p+\sigma m/H,$$

where the terms have the usual significance; if m is not minutely small, the equation can be written as

$$(1+m)\chi_i=\chi_p+\sigma m/H.$$

In the calculations, due allowances were made for the containers and air. The χ value of pure propyl alcohol (χ_p) was found to be 0.795×10^{-6}.

It is thus possible to calculate σ/H for the different colloidal specimens and for the bulk

[10] Burton, *The Physical Properties of Colloidal Solutions*, p. 125.

[11] For details see Ind. J. Phys. 6, 241 (1931).

[12] E. C. Stoner, reference 2, p. 137.

nickel. Remembering that all the measurements were taken with the same magnet current and hence in the same field, we could compare directly the specific intensities of the colloidal powders with the average value for the bulk metal.

III. Results

In Table I are given the results for ten samples. With due allowance for the various sources of error, it is found that the possible error of the values given in column 2 could not exceed 5 percent.

Table I. *Comparison of σ for colloid and bulk metal*

Range of diameters of the particles. μ		$\frac{\sigma \text{ colloid}}{\sigma \text{ bulk metal}} \times 100$	
0.8–1.0	1.1–1.5	70	82
0.8–1.1	1.2–1.7	72	85
0.8–1.2	1.5–3.0	70	95
0.9–1.4	2.0–4.0	72	98
1.0–1.5	2.5–5.0	77	97

A scrutiny of the table shows that the specific intensity of magnetization at particle sizes ranging from 0.8 to 5μ varies from 70 percent to almost the bulk value. It seems therefore quite likely that the decrease of the specific intensity is due to colloidalization. It is probable also that as the particles become finer the specific intensity of magnetization decreases also.

Montgomery[13] has worked with much finer colloidal suspensions of nickel in propyl alcohol and obtained specific intensities less than 15 percent of the mass value. He however attributes this to the low uncombined nickel content of the suspension, and suggests that probably some chemical action has taken place.

IV. Discussion

In these experiments there are three factors which might influence our magnetization values. First there is chemical action. By changing the sparking current from 2 to 10 milliamperes there does not seem to be any change in the values of the intensity of magnetization if the range of particle size remains the same. It seems therefore very doubtful whether chemical action could by itself account for the decrease noted. Secondly the presence of absorbed or adsorbed gases can give large variations. Under the conditions of the experiment, the gas content could not have been large. The gas molecules should either be loosely attached or place themselves in crystal array within the lattice. The first part may not produce any considerable change and so far as the present experimental evidence goes, the second part arises only when the crystal is heated sufficiently to moderately outgassing temperatures.[14] If the first state is responsible for so much decrease, even that would be an interesting result since that would make ferromagnetism distinctly an interatomic or cooperative[4] and not an atomic property.

Thirdly there is the possible influence of the subdivision on the intensity of magnetization. It is recognized that this report is preliminary in nature and that it may not be safe to theorize at this stage. More experimental evidence is necessary particularly with other metals. But it may not be out of place here to indicate that our results do not violate any of our ideas of ferromagnetism, but on the other hand, substantiate several of them. In this connection a general comment upon the work on nickel films is of interest. The investigations of Langmuir,[15] Steinberg,[16] Sorensen,[17] Wait,[18] Howey[19] and others show that if the films are prepared by depositing the nickel vapor on a cool surface the films consist of discontinuous minute crystal grains, which are too fine to distinguish in a microscope. The magnetic properties of these films were found to depend on the thermal treatment and on the nature of the backing medium. Ingersoll and De Vinney[20] obtained almost nonmagnetic films of nickel by depositing the nickel on a cold surface. But Ingersoll and Hanawalt[21]

[13] Reference 7. Sizes quoted are 300 mμ and 40 mμ.

[14] C. J. Davisson and L. H. Germer, Phys. Rev. **30**, 705 (1927).

[15] I. Langmuir, J. Am. Chem. Soc. **38**, 2221 (1916).

[16] J. C. Steinberg, Phys. Rev. **21**, 22 (1923).

[17] A. J. Sorensen, Phys. Rev. **24**, 658 (1924).

[18] G. R. Wait, Phys. Rev. **19**, 615 (1922).

[19] J. H. Howey, Phys. Rev. **34**, 1440 (1929).

[20] L. R. Ingersoll and S. S. De Vinney, Phys. Rev. **26**, 86 (1925).

[21] L. R. Ingersoll and J. D. Hanawalt, Phys. Rev. **34**, 972 (1929).

showed that by heating the deposited film, it attained its usual magnetic value. Since the heating facilitates outgassing and at the same time recrystallization, they admit that it is not easy to distinguish between the two causes.

In an interesting letter, Bitter[5] has proposed a model for a ferromagnetic body based on the block structure theory of Zwicky. According to his calculations for nickel, a microcrystal of this metal contains 10^5 atoms. If we assume for the sake of simplicity that the block is spherical, it can be seen that there should be nearly 2×10^5 such blocks in a particle of diameter 1μ. It is pertinent to ask why the intensity of magnetization decreases at such large particle diameters. However, it may be seen also that a large number of microcrystals may suffer disruption on the surface of the particles during the sparking, and the spherical particle may consist of full blocks and a number of broken ones, the latter not giving rise to any ferromagnetic intensity since the block is not complete for an internal field. It is easily seen also that on the spherical surface of the particle of diameter 1μ, we can draw sections of nearly 1.2×10^4 block spheres, which might be disrupted. In fact this number can easily be larger. The proportion of disrupted blocks increases with decreasing size of the particles and at less than certain diameters, this number becomes comparable with the number of full blocks in each particle. This might account for the observations noted. These approximate calculations are advanced as a possible explanation of the observed decrease of ferromagnetism at small particle sizes.

Attention may be drawn to the experiments of Tartakowsky and Kudrjawzewa[22] on the secondary electron emission in nickel. They found that as the temperature of a nickel target was increased, the total secondary electron emission at a given voltage showed a sudden decrease at a temperature which coincided very well with the Curie point of nickel. This means that the secondary electron emission and ferromagnetism are closely connected at least in the case of nickel. It seems therefore quite probable that the structure electrons, which Richardson[23] has postulated to explain secondary electron emission, may also be responsible for the existence of the Zwicky blocks in the crystal.

Further experiments from other points of view are being instituted in these directions.

---

[22] P. Tartakowsky and W. Kudrjawzewa, Zeits. f. Physik **75**, 137 (1932).

[23] O. W. Richardson, Proc. Roy. Soc. **A128**, 63 (1930).

LETTERS TO THE EDITOR

Prompt publication of brief reports of important discoveries in physics may be secured by addressing them to this department. Closing dates for this department are, for the first issue of the month, the twentieth of the preceding month; for the second issue, the fifth of the monih. The Board of Editors does not hold itself responsible for the opinions expressed by the correspondents.

Forbidden Lines in the Arc Spectrum of Lead

In the course of an experimental work on the "forbidden" radiations of various elements, I have obtained some results in the case of lead which are briefly reported below.

The five lowest energy states of the neutral lead atom $^3P_0$, $^3P_1$, $^3P_2$, $^1D_2$ and $^1S_0$ belong to the same electron configuration $6s^26p^2$. The last four of these states are metastable. Transition from any of them to a lower state with accompanying normal dipole radiation is forbidden by the Laporte selection rule.

Undamped high frequency discharges were excited in a mixture of a rarefied lead vapor and some noble gas, helium or argon. By a suitable choice of gas density and other discharge conditions only the lower energy states of Pb atoms were chiefly excited and collisions between metastable Pb atoms and those of the rare gas used were largely elastic, thus favoring the prolongation of the metastable states sufficiently for quadrupole radiation to become effective. The four lines given in Table I were observed.

The line λ7330 was observed in the arc spectrum of lead by Walters.[1] Also the line λ4618 has been observed by Gieseler and Grotrian[2] and by Sur.[3] The latter has suggested the origin of both these lines. However, in the spectra obtained by these authors the intensities of the mentioned two lines have not exceeded the intensities of the neighboring normal dipole Pb lines whereas in my experiments both these forbidden lines were comparatively much stronger. The lines λ5313 and λ4659, till now not observed, were much weaker than the other two.

TABLE I.

Notation	λ_{air} calculated from known term values	λ measured
$6s^26p^2$ $6s^26p^2$	A	A
$^3P_1 - {}^1S_0$	4617.9	4618.0
$^3P_2 - {}^1S_0$	5312.6	5312.7
$^3P_0 - {}^1D_2$	4659.4	4659.4
$^3P_1 - {}^1D_2$	7329.9	7330

The line λ4618 is forbidden by the selection rules for quadrupole radiation[4] because in the corresponding transition $J_1+J_2<2$. Therefore the appearance of this line cannot be explained as a quadrupole radiation but is due rather to the electrically disturbed dipole radiation. The other three lines may be as well quadrupole as perturbed dipole lines. Only by examining the Zeeman effect for these lines could their true nature be definitely determined.

A more detailed account of these experiments will appear elsewhere.

HENRYK NIEWODNICZANSKI

Physical Laboratory,
Stefan Batory University,
Wilno, Poland,
August 19, 1933.

[1] Walters, Bull. Bur. Stand. **17**, 161 (1921).
[2] Gieseler and Grotrian, Zeits. f. Physik **34**, 374 (1925).
[3] Sur, Phil. Mag. **2**, 633 (1926).
[4] Rubinowicz and Blaton (General report on quadrupole radiation), Ergeb. d. exak. Naturwiss. **XI**, 1932.

The Properties of Rochelle Salt

An extensive study of the dielectric, optical, electro-optical and pyroelectric properties of Rochelle salt in the temperature range from $-50°$ to $+50°$ leads to results which can be explained with the help of a theory which is a generalization of Weiss's theory of ferromagnetism. The new theory differs from Weiss's theory in two points, namely: (a) The polarization is not only due to the orientation of polar molecules, but part of it is due to polarization of nonpolar groups. (b) With decreasing temperature the polar molecules lose gradually their ability to orient themselves in the direction of the field. The latter assumption leads to the conclusion that the Curie point T_c is a function of temperature. There exist two temperatures T where $T_c=T$; they correspond to the two observed Curie points at 23.7° and $-18°$. Between these Curie points the dielectric properties of Rochelle salt are in every respect analogous to the magnetic properties of ferromagnetic materials. The theory is in agreement with all observations and leads to very reasonable values of all the physical quantities involved. The most important results of the experimental investigation can be summarized as follows:

(a) The dielectric behavior above the Curie point is analogous to the paramagnetic properties of nickel above the Curie point. There is a difference of 1.5° between the

ferro- and para- Curie point. The Lorentz factor L is 3 ± 0.2.

(b) Near the Curie point the susceptibility κ is a function of the applied field. The observed values of $\kappa(E)$ agree with the theory.

(c) Above 35° the Kerr effect approaches a quadratic dependence upon the applied field and gives a Kerr constant of the same order of magnitude as that of most liquids.

(d) Near the Curie point the Kerr effect is proportional to the 2/3 power of the applied field. This agrees with the assumption that the Kerr effect is proportional to the square of the inner field $F=E+LP$.

(e) The Kerr effect is different in the b and c axis of the crystal. There exists a longitudinal Kerr effect.

(f) The theory explains the observed size and shape of the hysteresis loops.

(g) Small crystals act as a single elementary Weiss region. They show a real pyroelectric effect. The pyroelectric moment is identical with the permanent moment calculated from the theory. It vanishes above the upper and below the lower Curie point.

(h) Large crystals consist of a limited number of Weiss regions. The Weiss regions in Rochelle salt have a cross section of about 2 cm². They can be made visible with electrified powder (analogy to Bitter's experiment).

(i) Large crystals have a very pronounced Barkhausen effect. This effect exists only on the steep part of the hysteresis loop. It disappears above the Curie point.

(j) Points (g) and (h) explain the asymmetries observed in small crystals.

(k) The Kerr effect below the Curie point shows a quadratic hysteresis loop and follows the theory even for large fields. For large fields the effect is nearly proportional to the absolute value of the applied field.

(l) The temperature variation of the natural birefringence shows a sharp discontinuity at both Curie points. This change of double refraction agrees quantitatively with the assumption that it is due to the Kerr effect of the permanent Weiss field. The Weiss field can be measured. It has a maximum value of 200 kv per cm at 0°.

(m) Measurements of the reversible susceptibility as a function of the applied field gives a curve which is the derivative of a hysteresis loop.

(n) The susceptibility for $E=0$ follows a Weiss law below the upper Curie point $1/\kappa_0=C(T_c-T)$.

(o) A similar Weiss law holds below and above the lower Curie point. All these results refer to fields in the a direction.

(p) The dielectric constants in the b and c direction increase with temperature. This is a consequence of the liberation of the dipoles at higher temperatures.

A complete account of the experiments and of the theory will appear soon.

HANS MÜLLER

Massachusetts Institute of Technology,
Cambridge, Massachusetts,
October 26, 1933.

Azimuthal Asymmetry of the Cosmic Radiation in Colorado

An investigation of the azimuthal asymmetry of the cosmic radiation near Fulford, Colorado, geomagnetic latitude 48°N, elevation 9500 feet, shows a difference between the west and east intensities of about two percent for angles of 30° and 40° from the vertical. The measurements were made with the same apparatus and in the same manner as at Swarthmore.[1] The results are summarized in Table I and are in accord with those found at Swarthmore.[1]

TABLE I.

Angle from vertical	Total time T (min.)	Total counts C	Counting rate C/T	Number of data n	Probable error from residuals R	Probable error from total counts R'	West-East difference (Counts/min.)
0°	1432	16,552	11.56	20	0.064	0.061	0
30° east	3951	30,463	7.71	25	0.031	0.026	0.17±0.045
west	4169	32,843	7.88	28	0.032	0.029	
45° east	4186	19,867	4.74	26	0.026	0.023	0.11±0.034
west	4801	23,295	4.85	25	0.022	0.022	

Also there is agreement with Korff[2] who set an upper limit of 3 percent for the west-east difference with an indication of a slightly greater west intensity. The dispersion of the points on the curves of Stearns and Bennett[3] indicates that their probable errors were too great to detect such a small asymmetry as exists at these latitudes.

This investigation was made possible by the invitation of Dr. A. J. Allen to spend a few weeks at his cabin in the mountains and use the facilities of his hydroelectric plant.

E. C. STEVENSON

Bartol Research Foundation
of The Franklin Institute,
October 23, 1933.

[1] Thomas H. Johnson and E. C. Stevenson, Phys. Rev. **44**, 125 (1933).

[2] S. A. Korff, Phys. Rev. **44**, 515 (1933). Phys. Rev. **44**, 130 (1933).

[3] J. C. Stearns and R. D. Bennett, Phys. Rev. **43**, 1039 (1933).

Scattering Processes Produced by Electrons in Negative Energy States

Recent calculations[1] of the changes in the absorption-coefficient of hard gamma-rays due to the formation of electron-positron pairs have lent strong support to Dirac's picture of holes of negative energy. Still, the almost insurmountable difficulties which the infinite charge-density without field offers to our physical understanding make it desirable to seek further tests of the theory. Here purely

[1] J. R. Oppenheimer and M. S. Plesset, Phys. Rev. **44**, 53 (1933).

radiation phenomena are of particular interest inasmuch as they might serve in an attempt to formulate observed effects as consequences of hitherto unknown properties of corrected electromagnetic equations. We are seeking, then, scattering properties of the "vacuum."

Two possible types of phenomena must be considered separately in connection with the foregoing: (1) All incident quanta have the same direction of propagation; (2) The incident quanta have different directions of propagation. Since we are only interested in purely radiation phenomena the frequencies in the second case should lie below mc^2/h so that no permanent formation of electron-positron pairs can occur.

When all incident quanta have the same direction of propagation, the principle of conservation of momentum excludes all scattering processes other than those in the direction of the incident radiation. These scattering processes would be observable if accompanied by a change in frequency. In the language of Dirac's theory of radiation such splitting of the incident quantum occurs in processes of the following type: An electron in a negative energy state passes by absorption of the incident quantum into a state of positive energy; the electron then returns in several steps under emission of $h\nu$ in toto to its original state. At each step total momentum should be conserved. A scattering process of this type can only *reduce* the frequency; the reduction, if small, would on the average be proportional to the distance travelled by the quantum through "vacuum." In this connection the hypothesis may be mentioned that Hubble's constant might be reducible to atomic constants without utilizing gravitational theories.

When the directions of propagation of the incident quanta do not coincide the additional case of simultaneous action of two quanta, of different frequencies in general, must be considered. This case can always be reduced by a Lorentz-transformation to the action of two equal and oppositely propagated quanta. In this "Pauli frame of reference" the scattering process would simply consist of a rotation of the line indicating the direction of propagation through a certain angle. In the original frame of reference we would of course encounter changes of both frequency and direction.

The writer will supply shortly the necessary quantitative considerations lacking at present.

O. HALPERN

New York University,
Department of Physics,
University Heights,
October 26, 1933.

On the Calculation of the Coefficient C in Frank's Formula for Change of Resistance

In Dr. Frank's formula,[1] $\Delta\rho/\rho = BH^2/(1+CH^2)$, for the relative increase in resistivity in a transverse magnetic field, the symbol ρ denotes the resistivity in the *presence* of the field.

On examining the tables in which $\rho(C)^{\frac{1}{2}}$ (calculated from Kapitza's measurements) is compared with accepted values of the Hall coefficients, I was struck by the fact that, for Sb and Bi, $\rho(C)^{\frac{1}{2}}$ is recorded as *less* than the Hall coefficient. For the other six metals the ratio is greater than 1. Mr. Norman A. Hedenberg and the writer therefore undertook to measure the resistivity and the Hall coefficient for two bismuth plates, at room temperature, in fields up to 13,000 gauss. The coefficient C turns out to have the same value, 13×10^{-9} gauss^{-2}, for each plate and $\rho(C)^{\frac{1}{2}}$ is more than twice as large as the Hall coefficient, even if one substitutes for ρ the value of the resistivity when H is zero.

In the writer's opinion, an error in calculating C from Kapitza's experimental results has made the recorded values of $\rho(C)^{\frac{1}{2}}$ too small for all the metals. The error is very large in the cases of Sb and Bi. The recorded values, it is true, agree very closely with those obtained by assuming that $\Delta\rho/\rho$ is equal to Kapitza's $\Delta R/R$. But in the latter's paper,[2] R denotes the resistance *before* the field is applied (otherwise $\Delta R/R$ could never be greater than 1 as it actually is for Sb, Bi and certain other metals). Accordingly, if Kapitza's $\Delta R/R$ be denoted by k, it follows that Frank's $\Delta\rho/\rho$ should be, not k, but $k/(k+1)$.

Using Kapitza's results and taking account of the discrepancy just mentioned, one finds that, for all the metals listed by Dr. Frank, the value of $\rho(C)^{\frac{1}{2}}$ is considerably increased. For Sb, the new values are 440×10^{-3} e.m.u. at 290°K, 390×10^{-3} at 193°K, and 370×10^{-3} at 90°K. Calculations have not yet been made for all the metals investigated by Kapitza, but so far the writer has found no exception to the rule that $\rho(C)^{\frac{1}{2}}$ is larger than the Hall coefficient at the same temperature.

I am very much indebted to Mr. Hedenberg for assistance in the calculations. We hope to publish soon the results of our experiments on bismuth.

K. K. SMITH

Northwestern University,
Evanston, Illinois,
October 29, 1933.

[1] Frank, Zeits. f. Physik **64**, 652 (1930). Sommerfeld and Frank, Rev. Mod. Phys. **3**, 18 (1931).

[2] Kapitza, Proc. Roy. Soc. (London) **A123**, 300 (1929).

Preliminary Report of the Results of Angular Distribution Measurements of the Cosmic Radiation in Equatorial Latitudes

A preliminary survey of the angular distribution of the cosmic radiation in equatorial latitudes has now been completed and measurements have been made in Mexico,[1, 2] geomagnetic latitude 29°, at elevations 10,000 ft., 7500 ft., and sea level; in Panama, geomagnetic latitude 20° at sea level; and in Peru, geomagnetic latitude 0°, at eleva-

[1] T. H. Johnson, Phys. Rev. **43**, 834 (1933).

[2] Confirmatory measurements were also made in Mexico by L. Alvarez and A. H. Compton, Phys. Rev. **43**, 835 (1933).

tions 14,000 ft., 11,000 ft. and sea level. As a part of the same program E. C. Stevenson has also completed measurements with similar apparatus at Swarthmore,[3] geomagnetic latitude 51° and sea level, and in Colorado,[4] geomagnetic latitude 49° and elevation 9500 ft. All measurements were made with a train of three Geiger-Mueller counters[5] arranged in line with a circuit for recording the coincident discharges. The counting rate was thus a measure of the intensity of that part of the radiation lying within the range of directions subtended by the outside counters. The principal measurements compared the intensities in the eastern and western azimuths at identical zenith distances and for this purpose frequent changes of orientation were made by rotation about a vertical axis. In the Peruvian and Panamanian measurements these changes were made automatically at thirty minute intervals and readings were taken photographically at fifteen minute intervals. The large amount of data, made possible by automatic operation, has reduced the probable error of the west-east differences in many cases to about five percent. In all latitudes the eastern intensity was less than the western, and the greatest differences were found on the magnetic equator. At the elevation of about ten thousand feet and zenith distance of forty-five degrees the east intensity in Peru was thirteen percent less than that of the west, in Mexico seven percent less, and in Colorado two percent less. The west-east differences for the three elevations in Peru satisfactorily fit the equation

$$\Delta(\theta) = \alpha x(\theta) e^{-\mu h \sec\theta}. \qquad (1)$$

This has been derived with the results of the Lemaitre-Vallarta theory for associating minimum energy with angle and assuming a corpuscular component uniformly distributed throughout the range of Lemaitre and Vallarta's energy parameter, x_0, from 0.35 to 0.75. $\Delta(\theta)$ is the west-east intensity difference at zenith distance θ expressed as a fraction of the average intensity at the same zenith distance, and $x(\theta)$ is the difference between the minimum energies (x_0) permitted at the same zenith distance from the east and from the west, respectively, as evaluated from Vallarta's curves.[6] μ is the difference between the absorption coefficients of the asymmetrical component and of the total radiation and h is the depth below the top of the atmosphere. The curves of Fig. 1 represent Eq. (1) with

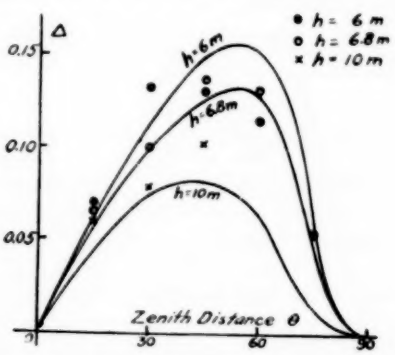

FIG. 1. Calculated and observed asymmetries for three elevations on the magnetic equator.

$\mu = 0.1$ per meter of water, $\alpha = 2.3$ and values of h corresponding to the three elevations at which measurements were made in Peru. The experimental values are also included and the agreement is satisfactorily within the probable errors, although the values of the constants may be slightly modified by a least-squares solution. The fact that μ is positive accords with the findings of Compton,[7] and of Bowen, Millikan and Neher[8] that the radiation which accounts for the latitude-intensity changes is softer than the total radiation.

In correlating the magnitude of the asymmetry with the latitude-intensity variations the following equation has been used:

$$D(\lambda, \theta) = \alpha\psi(\lambda, \theta) e^{-\mu h \sec\theta}. \qquad (2)$$

D is the fractional increase of intensity at a particular angle θ between latitudes 0° and λ, and ψ is the corresponding difference in minimum energies as evaluated from Vallarta's curves. The constant α in Eq. (1) represents the excess of positive over negative radiation, and in (2) α represents the sum of the positive and negative. If we assume that all of the radiation is positive, α has the same significance in both equations, and the latitude intensity change as it would be measured with an electroscope may be calculated by integrating D over all values of θ. For the latitude of Mexico the above stated values of the constants, determined from the asymmetry, predict an increase of intensity over that at the equator of 6.6 percent at sea level and 11.5 percent at 14,000 ft. These are almost exactly the values found by Compton. For Panama the predicted change is about one-third of that for Mexico. Since any admixture of negative radiation would diminish the asymmetry but would add to the latitude-intensity changes this comparison is a sensitive test of the assumption that the radiation within the effected range of energy is entirely positive.

Further evidence that there is no appreciable mixture of negative radiaton results from determinations in Mexico, Panama, and Peru of the dependence upon azimuth of the intensity of the radiation at a zenith distance of approximately forty-five degrees. Measurements were made in the west, southwest, south, southeast and east azimuths and at all stations a continuous increase of intensity was found from the east to the west with no indication of a second minimum in the west such as would be expected if an appreciable amount of negative radiation were also present.

If the conclusion is sustained that all of the corpuscular radiation is positive this would seem to restrict the Lemaitre theory of the radioactive origin of the corpuscular

---

[3] T. H. Johnson and E. C. Stevenson, Phys. Rev. **44**, 125 (1933).

[4] E. C. Stevenson, this issue.

[5] T. H. Johnson and J. C. Street, J. Frank. Inst. **215**, 239 (1933).

[6] M. S. Vallarta, Phys. Rev. **44**, 1 (1933).

[7] A. H. Compton, Phys. Rev. **43**, 387 (1933).

[8] I. S. Bowen, R. A. Millikan and H. V. Neher, Phys. Rev. **44**, 246 (1933).

cosmic radiation and would suggest the hypothesis that this component is generated in a cosmic or in a hitherto unknown terrestrial electric field. The cosmic radiation, therefore, may not be uniformly distributed throughout space and estimates of the fraction of the total energy in the universe based upon this assumption may be considerably in error.

The present measurements give no definite evidence concerning the character of the undeflected general radiation though it is perhaps significant that the four component analysis which Bowen, Millikan and Neher[8] have just given the intensity measurements, is nearly in accord with the angular distribution curves both at sea level and at 14,000 ft. This agreement would tend to support the underlying assumptions of their analysis that the radiation consists principally of photons. Their recent three component analysis and the earlier analyses of Millikan and Cameron[9] are not satisfactory from this point of view and this fact would suggest that angular distribution curves may be used in conjunction with intensity measurements in arriving at more definite solutions of the cosmic-ray energy bands.

A complete report of this work is in preparation and it will contain acknowledgments to the many who have cooperated to make these studies possible. Part of the funds used have been made available from the Carnegie Corporation of New York by the Carnegie Institution of Washington and part were supplied by the Bartol Research Foundation of the Franklin Institute. Generous aid in Mexico was also rendered by Sr. Jose de la Macorra.

THOMAS H. JOHNSON

The Bartol Research Foundation
of The Franklin Institute,
October 30, 1933.

[9] R. A. Millikan and G. H. Cameron, Phys. Rev. **37**, 247 (1931).

The Alpha-Particles from Radium C′

Lord Rutherford, Lewis and Bowden[1] have recently published very exact measurements of the energies of the α-rays from radium C′. I find that the energies of disintegration (corrected for recoil) may be arranged in pairs having sums equal to multiples of 3.85. This is shown in Table I. The unit is 10^5 electron-volts.

TABLE I.

Pairs of disintegration energies	Multiples of 3.85
78.29 + 91.12 = 169.41	3.85 × 44 = 169.40
78.29 + 94.93 = 173.22	3.85 × 45 = 173.25
78.29 + 102.69 = 180.98	3.85 × 47 = 180.95
91.12 + 105.26 = 196.38	3.85 × 51 = 196.35
92.41 + 0 = 92.41	3.85 × 24 = 92.40
94.93 + 105.26 = 200.19	3.85 × 52 = 200.20
96.73 + 99.68 = 196.41	3.85 × 51 = 196.35
96.73 + 103.42 = 200.15	3.85 × 52 = 200.20
100.97 + 107.09 = 208.06	3.85 × 54 = 207.90
102.69 + 105.26 = 207.95	3.85 × 54 = 207.90

The mean deviation of the sums from the multiples of 3.85 is 0.05 or about 1 part in 4000. The probable error of the energy measurements was estimated by Rutherford, Lewis and Bowden to be about 1 part in 5000. Table I includes all the observed α-rays, except one with disintegration energy 98.44.

These results show that the disintegration energies are equal to $3.85n \pm c$ where $n = 1, 2, 3 \cdots$ and c has a number of possible values. The writer has shown, in a paper not yet published, that the energies of the γ-ray quanta emitted by radium C′ can be represented by the same expression $3.85n \pm c$ with the same values of the c's. The values of the c's are found to be related in a simple way to the values of the K, L, M electronic energy levels which suggests that the c's represent energy exchanges with the electrons.

If this is so, it seems probable that the disintegration energies of the radium C′ nucleus are equal to $3.85n$. An excited nucleus with energy $3.85n$ may emit one or more γ-rays with total energy $3.85n'$ where $n' = 1, 2, 3, \cdots$, and then disintegrate with energy $3.85(n - n')$. The lowest value of $n - n'$ is 20. The simplest system which has such possible energies is a harmonic oscillator.

H. A. WILSON

Rice Institute,
Houston, Texas,
October 30, 1933.

[1] Rutherford, Lewis and Bowden, Proc. Roy. Soc. **A142**, 347 (1933).

The Disintegration Energies of Radioactive Nuclei

In two recent papers[1] by Lord Rutherford, Wynn-Williams, Lewis and Bowden very exact measurements of the energies of the α-rays emitted by radioactive atoms are described. In the first paper a list of the disintegration energies calculated from the α-ray energies is given and in the second paper similar results for the long range radium C′ α-rays.

It is shown by the writer, in a paper not yet published, that the energies of the γ-ray quanta emitted by radium C′ are equal to $3.89n \pm c$ where $n = 1, 2, 3 \cdots$ and c has one of the eight values 0, 0.38, 0.55, 0.89, 1.14, 1.30, 1.64, 1.89.

Table I shows this for some of the more intense γ-rays from radium C′. The unit is 10^5 electron-volts.

In a recent Letter to the Editor of *The Physical Review*

[1] Rutherford, Wynn-Williams, Lewis and Bowden, Proc. Roy. Soc. **A139**, 617 (1933); Rutherford, Lewis and Bowden, Proc. Roy. Soc. **A142**, 347 (1933).

TABLE I.

Gamma-ray energy	$3.89n+c$
22.19	$3.89\times6-1.14=22.20$
17.78	$3.89\times5-1.64=17.81$
14.26	$3.89\times4-1.30=14.26$
11.67	$3.89\times3\quad=11.67$
6.13	$3.89\times2-1.64=\ 6.14$
4.29	$3.89\times1+0.38=\ 4.27$

it is shown that the disintegration energies of the radium C′ atom can be represented by the expression $3.85n\pm c$. The constant 3.85 is used here instead of 3.89 because the more recent values of the γ-ray energies are slightly lower than those used in getting $3.89n\pm c$.

TABLE II.

Element	Disintegration energy	Mean c's
Radon	$55.80=14q+1.90$	
Actinium A	$75.08=20q-1.92$	
Actinium Cα	$67.39=18q-1.91$	1.91
Radium Cα	$56.15=15q-1.60$	
Radium Cα_1	$55.52=14q+1.62$	
Radium C′	$98.44=26q-1.66$	
Actinium Cα_1	$63.83=17q-1.62$	
Thoron	$63.94=17q-1.51$	1.63
Radium C′	$78.29=20q+1.29$	
Actinon α_1	$66.65=17q+1.20$	
Actinium C′	$75.81=20q-1.19$	
Radium C′	$91.12=24q-1.28$	
Radium C′	$94.93=25q-1.32$	
Radium C′	$102.69=27q-1.26$	
Radium C′	$105.26=27q+1.31$	1.27
Thorium C′	$89.47=23q+0.92$	
Radium C′	$100.97=26q+0.87$	0.89
Radium A	$61.09=16q-0.51$	
Radium C′	$103.42=27q-0.53$	
Radium C′	$107.09=28q-0.71$	
Radium C′	$96.73=25q+0.48$	0.55
Radium C′	$84.37=22q-0.33$	
Thorium A	$68.97=18q-0.33$	
Thorium Cα_1	$62.04=16q+0.44$	
Thorium C′	$96.61=25q+0.36$	
Thorium C′	$107.41=28q-0.39$	
Radium C′	$99.68=26q-0.42$	0.38
Polonium	$54.06=14q+0.16$	
Actinon α_2	$65.31=17q-0.14$	0.15
Radium C′	$92.41=24q+0.01$	
Thorium Cα	$61.64=16q+0.04$	
Actinon α	$69.37=18q+0.07$	0.04

I now find that all the disintegration energies can be represented by the same expression. This is shown in Table II where $q=3.85$. The mean values of the differences between the disintegration energies and the multiples of 3.85 agree nearly with the c's found for the γ-rays of radium C′. This is shown in Table III.

TABLE III.

c's from γ-rays of radium C′	c's from disintegration energies	Differences
1.89	1.91	+0.02
1.64	1.63	−0.01
1.30	1.27	−0.03
1.14	—	—
0.89	0.89	0.00
0.55	0.55	0.00
0.38	0.38	0.00
—	0.15	—
0.00	0.04	+0.04

The mean deviation corresponds to an error of about 1 part in 4000 in the values of the disintegration energies. The value $c=1.14$ does not appear among the disintegration c's and the value $c=0.15$ was not found for the γ-ray energies.

There seems to be little doubt that the expression $3.85n\pm c$ represents the disintegration energies of all the atoms and the γ-ray energies of radium C′ with the same values of the c's. It seems probable therefore that it will also represent the γ-ray energies of the other atoms but this question has not yet been examined.

It seems probable that there is some process which takes place in all the radioactive atoms which releases an amount of energy 3.85×10^6 electron-volts. The uranium nucleus contains 92 protons and 146 neutrons. We might suppose that the neutrons are not combined with the protons as closely as possible and that when a proton combines as closely as possible with a neutron energy 3.84×10^6 electron-volts is released. This would give $92\times3.85\times10^6=35.4\times10^6$ electron-volts for all the disintegrations of the uranium series. The total disintegration energy of the eight α-rays of the uranium series, however, is about 43×10^6 electron-volts which is about 20 percent greater than 35.4×10^6.

The c's probably represent energy exchanges with the electrons or some other secondary action between the γ-rays or α-rays emitted by the nucleus and the rest of the atom.

H. A. WILSON

Rice Institute,
Houston, Texas,
October 31, 1933.

Discrepancy Between Theory and Experiment in Cold Emission

Numerous writers on cold emission have mentioned that the electron currents drawn from cold cathodes by extremely high electric fields are much larger than is expected on the basis of the wave-mechanical calculation by Fowler and Nordheim. To explain this, the assumption is usually made that there are submicroscopic sharp points on the cathode at which the field is much more intense than the average value in that vicinity, and where the current density may be as high as 100,000 amperes per square centimeter. Some measurements at this laboratory show

that this is not the only factor to be considered, but that rather, if the emitted electrons can strike glass, substances removed from such a target can be ionized and move back along the electron stream. They are deposited on the cold cathode surface and reduce the work function of the cathode thus giving much larger currents than those calculated for a clean surface.

The apparatus was similar to that used in an investigation reported in this journal,[1] except that a glass disk was fastened on the anode with the center of the disk opposite the emitting point. The same kind of disk was used as is used for cover glasses on bacteriological slides. The emission was drawn from sharp copper cathodes held about 2 mm from the glass disk, while magnetic fields of about 5000 gauss were applied at right angles to the electric field, as before.

Although the magnetic field applied was several times stronger than sufficient to deflect the electrons away from the glass, a fluorescent spot appeared on the glass. As explained in the above-mentioned paper, this shows that there were positive ions in the stream. This spot did not gradually disappear as it did in the case of the metal anodes, so the material drawn from the glass is not nearly so exhaustible as it was in the case of the metal anodes.

The kinds of characteristics observed were very similar to those observed for a magnesium anode shown as Fig. 5, p. 420 of reference 1, except that with the glass disk, either kind of field-current characteristics could be produced at will. The characteristics were either like curve 1, or like curve 2, depending on whether the field was gradually decreased from the higher value, or suddenly dropped to zero. Although the effort was made by varying the field irregularly to get the cathode to give a characteristic lying between these two groups, this was unsuccessful. (The current is limited by space charge at current above 10^{-6} ampere with these cathodes.)

In the paper by Stern, Gossling and Fowler,[2] it is shown that if the logarithm of the current is plotted against the reciprocal of the field, the slope of the characteristic is proportional to the work function to the three-halves power and inversely proportional to the factor by which the measured field must be multiplied to give the true field at the tip of the emitting submicroscopic sharp point. Now if the characteristics were changed by repeated ruptures of the cathode surface, the sharpness of such points would have been quite accidental and continued observations would have yielded a quite random variety of slopes, instead of the two distinct groups typified by curves 1 and 2, respectively. (See Fig. 1.) The only explanation seems to be that continued operation did not rupture the cathode repeatedly, but that some of the time the surface had one work function, and the rest of the time it had another.

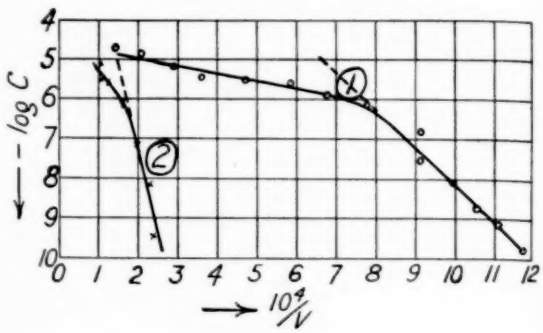

FIG. 1.

This observation leads to the conclusion that even when the best of vacuum conditions prevail, yet if electrons can readily miss the anode and strike glass, the emission is apt to be characteristic of a contaminated surface. This effect will probably explain the large discrepancies between theory and experiment found by previous observers, without the assumption of submicroscopic points impossibly small from space charge considerations. By taking particular care to keep the electrons from striking glass, we have been able to obtain characteristics near the theoretical value.

WILLARD H. BENNETT

Mendenhall Laboratory of Physics,
Ohio State University,
Columbus, Ohio,
November 1, 1933.

---

[1] W. H. Bennett, Phys. Rev. **40**, 416 (1932).

[2] Stern, Gossling and Fowler, Proc. Roy. Soc. **A124**, 699 (1929).